

## STATUS OF THESIS

Title of thesis EFFECTS OF MICROWAVE INCINERATED RICE HUSK ASH  
(MIRHA) ON HYDRATION CHARACTERISTIC AND  
MECHANICAL PROPERTIES OF FOAMED CONCRETE

I \_\_\_\_\_ RIDHO BAYUAJI \_\_\_\_\_

hereby allow my thesis to be placed at the Information Resource Center (IRC) of Universiti Teknologi PETRONAS (UTP) with the following conditions:

1. The thesis becomes the property of UTP
2. The IRC of UTP may make copies of the thesis for academic purposes only.
3. This thesis is classified as

Confidential

Non-confidential

If this thesis is confidential, please state the reason:

\_\_\_\_\_  
\_\_\_\_\_  
\_\_\_\_\_

The contents of the thesis will remain confidential for \_\_\_\_\_ years.

Remarks on disclosure:

\_\_\_\_\_  
\_\_\_\_\_  
\_\_\_\_\_

Endorsed by

\_\_\_\_\_  
Signature of Author

Permanent address:  
Jalan Raya Karang Pranti 232  
Pajajaran Probolinggo, East Java 67281  
Indonesia

Date : \_\_\_\_\_

\_\_\_\_\_  
Signature of Supervisor

Name of Supervisor  
Assoc. Prof. Ir. Dr. Muhd Fadhil Nuruddin

Date : \_\_\_\_\_

UNIVERSITI TEKNOLOGI PETRONAS

EFFECTS OF MICROWAVE INCINERATED RICE HUSK ASH (MIRHA)  
ON HYDRATION CHARACTERISTIC AND MECHANICAL PROPERTIES  
OF FOAMED CONCRETE

by

RIDHO BAYUAJI

The undersigned certify that they have read, and recommend to the Postgraduate Studies Programme for acceptance this thesis for the fulfillment of the requirements for the degree stated.

Signature:

\_\_\_\_\_

Main Supervisor:

Assoc. Prof. Ir. Dr. Muhd Fadhil Nuruddin

Signature:

\_\_\_\_\_

Co-Supervisor:

\_\_\_\_\_

Signature:

\_\_\_\_\_

Head of Department:

Assoc. Prof. Dr. Shamsul Rahman M. Kutty

Date:

\_\_\_\_\_

EFFECTS OF MICROWAVE INCINERATED RICE HUSK ASH (MIRHA)  
ON HYDRATION CHARACTERISTIC AND MECAHNICAL PROPERTIES  
OF FOAMED CONCRETE

by

RIDHO BAYUAJI

A Thesis

Submitted to the Postgraduate Studies Programme  
as a Requirement for Degree of

DOCTOR OF PHILOSOPHY  
CIVIL ENGINEERING DEPARTMENT  
UNIVERSITI TEKNOLOGI PETRONAS  
BANDAR SERI ISKANDAR  
PERAK

August 2010

## DECLARATION OF THESIS

Title of thesis

EFFECTS OF MICROWAVE INCINERATED RICE HUSK ASH  
(MIRHA) ON HYDRATION CHARACTERISTIC AND  
MECHANICAL PROPERTIES OF FOAMED CONCRETE

I RIDHO BAYUAJI

hereby declare that the thesis is based on my original work except for quotations and citations which have been duly acknowledged. I also declare that it has not been previously or concurrently submitted for any other degree at UTP or other institutions.

Witnessed by

\_\_\_\_\_  
Signature of Author

\_\_\_\_\_  
Signature of Supervisor

Permanent address:  
Jalan Raya Karang Pranti 232  
Pajarakan Probolinggo, East Java 67281  
Indonesia

Name of Supervisor  
Assoc. Prof. Ir. Dr. Muhd Fadhil Nuruddin

Date : \_\_\_\_\_

Date : \_\_\_\_\_

## **DEDICATION**

First of all the writer like to express his love and utmost gratitude to his Excellency BAPANDA GURU HAJI SYAIDI SYEKH DER MOGA BARITA RAJA MUHAMMAD SYUKUR MANGARAJA PARLINDUNGAN as WALI QUTB.

He is an affectionate remarkable man and devoted all His time to spread Islam as a rahmatan lil alamin religion.

He has been leading the people to communicate directly with Allah. He teaches this way to the people to heal and treat themselves from the serious illness including HIV-AIDS. With all His effort He has managed to bring back life to the affected patients to be good, devoted and loving Muslim.

Besides His involvement in preaching, He is also an entrepreneur planting trees in preventing Global Warming Issues.

## ACKNOWLEDGEMENTS

The writer would like to express his most sincere gratitude to his supervisor, Assoc. Prof. Ir. Dr. Muhd Fadhil Nuruddin for his precious guidance, advice, encouragement, aspiration and support from the initial to the final stage that enabled the writer to develop an understanding of the field. Appreciation is also due to Head of Department, Assoc. Prof. Dr. Shamsul Rahman M. Kutty for his encouragement and support. The writer also wishes to express his sincere appreciation to Universiti Teknologi PETRONAS for providing the facilities and financial grant in conducting the research.

The writer is thankful to Adhilah, Robeatul, Dyan and Azwan and fellow graduate students for their help with the experiments. Acknowledgements are also given to the Technical Staff for their assistance in the experimental program especially the crew of Civil Engineering Laboratory (Mr. Imtias @ Amir B Bahauddin, Mr. Johan Ariff Mohamed, Mr. Meor Asniwan Meo Ghazali, Mr Muhammad Hafiz, Mr. Mohd Khairul Anuar B Jamaludin, Mr. Mohd Idris B Mokhtar, Mr. Mohd Zaini Isman @ Hashim and Ms. Ima) and the crew of Petroleum Engineering and Mechanical Engineering Laboratory (Mr. Mohd Zairi B Zohaidi, Mr. Amirul Qhalis, Mr. Mohd Anuar B Abd Muin, Mr. Irwan B Othman, Mr. Mohd Faisal B Ismail, Mr. Mohd Riduan Bin Ahmad, Mr. Omar B Ramli and Mr. Mohd Shairul B Harun) for helping in conducting the experiment on of FC. My colleagues at Concrete Technology researcher cluster especially Andri Kusbiantoro, Salmiah Beddu Amang, and Nurliyana are very much appreciated.

The writer appreciates to the participation and support from his wife, Mrs. Dinda Irma Destari and family (his son “Addin”, his mother-in-law “Mama Wati”, his younger brother-in-law “Samgita and Edlin”, his younger brother “Yudi, Beni, Cak Tem, Mas Yon and Dito”) and dearest friend that has contributed ideas and encouragement.

## ABSTRACT

The better a material is understood, the better it can be utilized. With cement-based material such as foamed concrete (FC), knowledge of the fundamental cement hydration reactions and resultant product will facilitate design, behaviour prediction, and improved performance. Water is an integral part of all cement-based materials. It contributes to the mixing and placing ability of the material, enables the hydration process, and influences material property development. As such, it is worthy of comprehensive study, for one will never fully understand cement-based material if one does not have a good grasp of the role of water in them. The study of water in FC with Microwave Incinerated Rice Husk Ash (MIRHA) as pozzolanic material is particularly interesting, for which information about the water content can be used to understand the behaviours of the product. This study was mainly focused to investigate the role MIRHA on the non-evaporable water content in the FC

The mix proportion of the MIRHA FC was designed using the Taguchi method with  $L_{16}$  orthogonal array with five parameters, namely, MIRHA contents, water cementitious ratio (w/c), sand cement ratio (s/c), superplasticizer (SP) content, and foam content. The mixtures were tested, both in fresh and hardened states to meet technical requirement of FC. Analysis of the characteristics of concretes, namely its compressive strength, non-evaporable water ( $w_n$ ) by oven dry/furnace ignition (OD/FI), non-evaporable water ( $w_n$ ) by Thermogravimetry (TGA), dry density and porosity were conducted.

The results showed that MIRHA could facilitate enhancement in FC hydration with the evidence from  $w_n$  OD/FI and TGA, Calcium Hydroxide (CH) contents and change in non-evaporable water content. The degree of hydration of MIRHA FC was predicted using a model that employed non-evaporable water technique.

## ABSTRAK

Semakin sesuatu bahan itu lebih difahami, semakin ia boleh digunapakai. Dengan bahan berasaskan simen seperti Konkrit Berongga (KB), pengetahuan asas terhadap reaksi penghidratan simen dan produk yang dihasilkan akan memudahkan rekabentuk, ramalan perilaku, dan meningkatkan prestasi. Air adalah unsur utama dalam semua bahan berasaskan simen. Ia menyumbang kepada campuran dan kemampuan menempatkan, membolehkan proses penghidratan, dan mempengaruhi pembangunan bahan. Oleh itu, kajian menyeluruh adalah perlu, untuk satu yang tidak akan pernah memahami sepenuhnya tentang bahan berasaskan simen jika tidak mempunyai pemahaman yang baik mengenai peranan air di dalamnya. Kajian air bagi KB yang mengandungi Abu Sekam Padi Pembakaran Gelombang Mikro (ASPPGM) sebagai bahan pozzolana, adalah sesuatu yang menarik, yang mana maklumat tentang kadar air boleh digunakan untuk memahami perilaku produk tersebut. Tujuan utama kajian ini adalah untuk memastikan kesan ASPPGM terhadap kekuatan mampatan FC.

Nisbah campuran bagi ASPPGM KB ini direka dengan menggunakan kaedah Taguchi dengan  $L_{16}$  array ortogonal dengan lima lingkungan, iaitu, kandungan ASPPGM, nisbah air simen (w/c), nisbah simen pasir (s/c), kandungan superplasticizier (SP), dan kandungan buih. Campuran diuji, diperingkat fresh dan peringkat keras untuk memenuhi keperluan teknikal FC. Analisis ciri-ciri konkrit, iaitu kekuatan mampatan, air yang tidak tersejat ( $w_n$ ) dengan ketuhar kering/pembakaran relau (OD/FI),  $w_n$  dengan Termografimetri (TGA), ketumpatan kering dan keporosan dilakukan.

Keputusan kajian menunjukkan bahawa ASPPGM boleh memudahkan peningkatan dalam penghidratan FC dengan bukti dari  $w_n$  OD/FI dan TGA, Kandunga Kalsium Hidroksida (CH) dan perubahan  $w_n$ . Kadar hidrasi ASPPGM KB boleh dianggarkan dengan menggunakan model yang menggunakan teknik air yang tidak tersejat.



In compliance with the terms of the Copyright Act 1987 and the IP Policy of the university, the copyright of this thesis has been reassigned by the author to the legal entity of the university,

Institute of Technology PETRONAS Sdn Bhd.

Due acknowledgement shall always be made of the use of any material contained in, or derived from, this thesis.

© Ridho Bayuaji, 2010

Institute of Technology PETRONAS Sdn Bhd

All rights reserved.

## TABLE OF CONTENTS

STATUS OF THESIS	
APPROVAL PAGE	
TITLE PAGE	
DECLARATION .....	iv
DEDICATION.....	v
ACKNOWLEDGEMENTS.....	vi
ABSTRACT .....	vii
ABSTRAK.....	viii
COPYRIGHT PAGE .....	ix
TABLE OF CONTENTS .....	x
LIST OF TABLES .....	xiii
LIST OF FIGURES .....	xv
CHAPTER	
1. INTRODUCTION.....	1
1.1 Background .....	1
1.2 Problem Statement.....	4
1.3 Objectives and scopes of Study.....	5
1.4 Organization of thesis .....	6
2. LITERATURE REVIEW .....	8
2.1 General.....	8
2.2 Foamed Concrete (FC).....	8
2.3.1 Definition and Characteristic of FC .....	9
2.3.2 Advantage and Application of FC .....	9
2.3.3 Background and Basic Principle of FC, Approaches to Obtain FC and Possibilities of FC Lightweight as Structural Material.....	11
2.3.4 Material Aspects and Mixture Design for FC .....	13
2.3.5 Properties of Foamed Concrete.....	18
2.3.6 Strength Prediction Models .....	24
2.3 Rice Husk Ash.....	27
2.3.1 Definition, Composition and Its significance .....	27
2.3.2 Characteristic of Rice Husk Ash.....	28
2.3.3 Role of RHA in Concrete .....	31
a. Hydration Mechanism of Paste by RHA .....	33
b. Modification of Micro-pores Structure .....	34
c. Use in Lightweight Concrete .....	35
2.3.4 Characteristic of RHA by X-Ray Diffraction (XRD) and by X-Ray Fluorescence (XRF) .....	35
2.3.5 The Influence of RHA on Micro Properties .....	38
a. Porosity Properties .....	38
b. Autogenous Shrinkage.....	39
c. Non-Evaporable Water.....	40

d. Calcium Hydroxide .....	40
2.4 Chemically Bound Water .....	41
2.4.1 Cement Hydration Reactions.....	42
2.4.2 State of Water in Concrete .....	42
2.4.3 Measurement of Water.....	44
2.4.4 Change in Non-Evaporable Water Content Due to the Presence of A Cement Replacement Material (CRM) .....	54
2.4.5 The Model of the Degree of Hydration of Pastes with More Than One Cementing Material .....	55
2.5 Taguchi Method .....	56
2.5.1 Benefit .....	57
2.5.2 Application .....	57
2.5.3 The Procedure of Taguchi's method.....	57
2.5.4 Orthogonal Array.....	59
2.5.5 Analysis of Variance (ANOVA) .....	60
2.5.6 Determination level.....	63
2.6 Summary.....	65
3. EXPERIMENTAL PROGRAM.....	66
3.1 Overview.....	66
3.2 Material Properties .....	66
3.2.1. Microwave Incinerated Rice Husk Ash (MIRHA).....	66
3.2.2. Characteristic of Ordinary Portland Cement.....	70
3.2.3. Fine Aggregate .....	71
3.2.4. Water.....	73
3.2.5. Superplasticizier .....	73
3.2.6. Foam Agent .....	73
3.2.7. Experimental Design.....	74
3.3 Experimental Laboratory .....	77
3.4.1. Specimen Preparation .....	77
3.4.2. Mixing Process .....	77
3.4.3. Spread Measurement.....	80
3.4.4. Curing Regime.....	80
3.4.5. Hardened concrete test.....	81
3.4 Summary.....	88
4. RESULT, ANALYSIS AND DISCUSSION ON MECHANICAL PROPERTIES ..	90
4.1 Overview.....	90
4.2 Properties of MIRHA .....	90
4.2.1 X-Ray Diffraction Analysis.....	91
4.2.2 X-Ray Fluorescence Analysis .....	93
4.2.3 Particle Size Distribution and Surface Area.....	94
4.2.4 Accelerated Pozzolanic Strength Activity Index (APSAI) .....	95
4.2.5 Water Demand of Mix Constituent.....	96
4.3 Plastic Density and Cube Strength Repeatability of a Single Mix.....	97
4.4 Orthogonal Array .....	98
4.5.1. Workability of Foamed Concrete .....	98
4.5.2. Dry Density of FC .....	103
4.5.3. Compressive Strength of FC .....	108
4.5.4. Total Porosity of FC.....	116
4.5 Optimum FC Mix Proportion.....	120

4.6	Summary .....	122
5.	RESULT, ANALYSIS AND DISCUSSION ON HYDRATION	
	CHARACTERISTIC.....	124
5.1	Overview .....	124
5.2	The Non-Evaporable Water ( $w_n$ ) Analysis by OD/Fl.....	124
5.3	The Non-Evaporable Water ( $w_n$ ) Analysis by TGA.....	125
5.4	C-S-H and AFm Bound Water .....	128
5.5	CH Bound Water .....	129
5.6	Comparing C-S-H/AFm and CH Bound Water Content .....	131
5.7	Change in Non-Evaporable Water Content Due to the Presence of MIRHA..	133
5.8	Degree of Hydration of FC .....	135
5.9	Compressive Strength versus Non Evaporable Water Content Model.....	138
5.10	Compressive Strength versus porosity model.....	141
5.11	Compressive Strength versus gel-space ratio model .....	143
5.12	Comparison of Foamed Concrete Model of Porosity and Gel Space Ratio ....	144
5.13	Summary .....	145
6.	CONCLUSIONS AND FUTURE WORK.....	147
6.1	Conclusion .....	147
6.2	Recommendation for Future Study .....	148
	REFERENCE .....	150
	APPENDICES .....	160
	APPENDIX A: RAW DATA OF THIS STUDY .....	160
	APPENDIX B: MICROWAVE INCINERATOR.....	209
	APPENDIX C: TGA DATA PROCESSING.....	213
	APPENDIX D: PUBLICATION .....	224

## LIST OF TABLES

Table 2.1	Application of FC .....	10
Table 2.2	The study on possibility of FC as structural application.....	13
Table 2.3	Typical chemical oxide compositions of Portland cement [36].....	14
Table 2.4	The previous works on FC mixture proportion .....	17
Table 2.5	The investigation of fresh state property.....	19
Table 2.6	Classification of Foam Concrete Based on Spread Percent [25].....	19
Table 2.7	Empirical models for density determination [31].....	19
Table 2.8	A review of mixes used, compressive strengths and density ranges of FC [31].....	20
Table 2.9	Summary on strength prediction models on FC [72].....	25
Table 2.10	Chemical Composition of RHA under Different Burning Temperatures [9].....	28
Table 2.11	The Effect of Burning Conditions on the Crystal Structure and Surface Area of Rice Husk Ash [76] .....	29
Table 2.12	Physical properties of RHA [81] .....	30
Table 2.13	Typical chemical composition of rice husk ash [79] .....	31
Table 2.14	Summary of Drying/Ignition Procedures to quantify $w_n$ [102] .....	45
Table 2.15	Summary of TGA Experimental Variables [102].....	50
Table 2.16	Reported temperature ranges for C-S-H bound water removal.....	51
Table 2.17	Reported Temperature ranges for CH bound waster removal [102].....	51
Table 2.18	Reported temperature ranges for decomposition [102] .....	52
Table 2.19	The application Taguchi's method in concrete material.....	57
Table 2.20	Standard $L_{16} (4^5)$ orthogonal array [107] .....	59
Table 2.21	A review of mixes used, compressive strengths of mortar with RHA incorporation .....	63
Table 2.22	A review of mixes used, workability of FC with Superplasticizer .....	64
Table 2.23	A review of mixes used with foam content incorporation on FC.....	64
Table 2.24	Parameters and their variation levels .....	65
Table 3.1	MIRHA Chemical Composition.....	69
Table 3.2	Physical properties of MIRHA.....	70
Table 3.3	Physical and chemical properties of OPC type 1 adopted from Cement Industries of Malaysia Berhad (CIMA) .....	71
Table 3.4	Foam agent Chemical Composition.....	74
Table 3.5	Mix proportion with parameter and each level .....	75
Table 3.6	FC mixture proportion adopted .....	76
Table 3.7	Mix proportion with parameter and each level without foam.....	76
Table 3.8	Mortar mixture proportion adopted .....	77
Table 3.9	Hardened foamed concrete test .....	81

Table 3.10	OD/FI LOIs of component materials .....	86
Table 4.1	Chemical Composition.....	93
Table 4.2	Repeatability of mix FC-8 casting density and 50 cube compressive strengths .....	98
Table 4.3	Test results of spread test for MIRHA-FC .....	99
Table 4.4	Analysis of variance results of Workability of foamed concrete .....	100
Table 4.5	The summary of the effect of constituent on workability .....	103
Table 4.6	Classification of the effect constituent on workability .....	103
Table 4.7	Test results of dry density test for MIRHA-FC .....	104
Table 4.8	Analysis of variance results of 180 days dry density.....	105
Table 4.9	The summary of the effect of constituent on dry density.....	108
Table 4.10.	Classification of the effect constituent on dry density.....	108
Table 4.11	Test results of compressive strength for FC .....	109
Table 4.12	Analysis of variance results of compressive strength for FC.....	110
Table 4.13	The summary of the effect of constituent on compressive strength.....	115
Table 4.14	Classification of the effect constituent on compressive strength.....	116
Table 4.15	180 days test results of Porosity for FC .....	116
Table 4.16	Analysis of variance results of porosity of FC .....	117
Table 4.17	The summary of the effect of constituent on porosity .....	120
Table 4.18	Classification of the effect constituent on porosity .....	120
Table 4.19	Optimal mix-design proportions for properties of FC .....	121
Table 4.20	Optimum mix-design verification test results .....	122
Table 5.1	Non-evaporable water content ( $w_n$ ) by OD/FI .....	125
Table 5.2	TGA results for FC .....	126
Table 5.3	Change in non-evaporable water contents due to the presence of MIRHA by OD/FI.....	133
Table 5.4	Change in non-evaporable water contents due to the presence of MIRHA by TGA.....	134
Table 5.5	$a_1$ , $a_2$ and $a_3$ are fitting parameters for degree of hydration of FC.....	137
Table 5.6	$a_1$ , $a_2$ and $a_3$ are fitting parameters for degree of hydration of VCAS and SF (Neithalath's study [105]) .....	137
Table 5.7	The average data of 180 days Strength and porosity .....	141
Table 5.8	Summarizing Nambiar's study for porosity and gel-space ratio to strength.....	145
Table 5.9	Summarizing this study for porosity and gel-space ratio to strength.....	145

## LIST OF FIGURES

Figure 2.1	Determination on the saturation dosage for various types of superplasticizers [55].....	16
Figure 2.2	Double layer model of SP mechanism on action [56].....	17
Figure 2.3	Compressive strength as a function FC density [67].....	21
Figure 2.4	Foamed concrete model suggested by Hoff [70].....	22
Figure 2.5	The porosity as function of dry density [48].....	23
Figure 2.6	The porosity as function of strength [48].....	23
Figure 2.7	The Optimum Incineration Condition Curve for obtaining Reactive Cellular RHA [8].....	29
Figure 2.8	Micro-filling effect of RHA [87].....	32
Figure 2.9	Pozzolanic effect of RHA [87].....	33
Figure 2.10	Schematic Drawing of the Hydration of Cement Paste with RHA [88].....	34
Figure 2.11	Mechanism of void filling and transition zone strengthening effect of RHA [8] .....	35
Figure 2.12	Geometry of X-Ray Reflection [87].....	36
Figure 2.13	XRD Graphs from Various Samples of RHA [94].....	37
Figure 2.14	X-Ray Fluorescence Process [95] .....	38
Figure 2.15	Pore analysis of cement paste incorporating RHA [96]. .....	39
Figure 2.16	Autogenous deformation versus age of all pastes [97].....	39
Figure 2.17	Non-evaporable water content in paste [80]. .....	40
Figure 2.18	Amount of Ca(OH) <sub>2</sub> in hardened cement pastes [100] .....	41
Figure 2.19	The Charts of Terminology for state of water [102] .....	43
Figure 2.20	Schematic results from the OD/FI Procedure for Mortar with Pozzolanic [102].....	47
Figure 2.21	TG and DTG for a hydrated cement paste [71].....	49
Figure 2.22	CH normal values of VCAS ad SF [105].....	53
Figure 2.23	The procedure of Taguchi method .....	58
Figure 3.1	The process of MIRHA production.....	68
Figure 3.2	XRD Graph of MIRHA .....	69
Figure 3.3	Mechanical sieve used for this research .....	72
Figure 3.4	Fine aggregate obtained from sieving process.....	72
Figure 3.5	Superplasticizer type as used in this research .....	73
Figure 3.6	Schema of FC mix process.....	78
Figure 3.7	The preparation of mortar process as first process.....	79
Figure 3.8	Foam production and casting processes.....	79
Figure 3.9	Spread test .....	80
Figure 3.10	Water tank system for curing of FC sample .....	80
Figure 3.11	Compressive Testing Machine .....	82
Figure 3.12	Schematic diagram of Vacuum Saturation Apparatus [71] .....	83
Figure 3.13	Porosity equipment.....	83
Figure 3.14	OD/FI non-evaporable water measurement procedure.....	85
Figure 3.15	The crucible used in this experiment.....	86

Figure 3.16	The electrical furnace apparatus (Nabertherm 30-3000oC) used.....	87
Figure 3.17	The Thermogravimetry apparatus (Brand Perkin Elmer model Pyris 1 used in this investigation .....	87
Figure 3.18	The TGA monitor for viewing the temperature of process.....	88
Figure 4.1	XRD Graph of MIRHA.....	91
Figure 4.2	The X-Ray Diffraction of RHA under different burning conditions [9].....	92
Figure 4.3	Comparison of MIRHA gradation to cement, fly ash and silica fume .....	94
Figure 4.4	The accelerated pozzolanic strength activity index .....	95
Figure 4.5	Water demand of cement .....	96
Figure 4.6	Water demand of MIRHA.....	97
Figure 4.7	Main effect plot for Spread test .....	99
Figure 4.8	Main effect plot for 180 days dry density .....	104
Figure 4.9	Summary of main effect plot for compressive strength.....	109
Figure 4.10	Compressive strength versus age of FC with effect of MIRHA .....	112
Figure 4.11	Compressive strength versus age of FC with various w/c .....	113
Figure 4.12	Compressive strength versus age of FC with various level of s/c .....	113
Figure 4.13	Compressive strength versus Age of FC with various level of SP.....	114
Figure 4.14	Compressive strength versus age of FC with various foam content.....	115
Figure 4.15	Main effect plot for porosity .....	118
Figure 5.1	OD/FI Non-evaporable water content over time with MIRHA effect .....	125
Figure 5.2	TGA Non-evaporable water contents over time.....	126
Figure 5.3	C-S-H and AFm bound water over time .....	128
Figure 5.4	CH bound water over time .....	130
Figure 5.5	CH normal values of MIRHA .....	131
Figure 5.6	C-S-H/AFm versus CH bound water contents .....	132
Figure 5.7	C-S-H/AFm versus CH bound water contents with reference line.....	132
Figure 5.8	Change in wn due to the presence of MIRHA using OD/FI technique .....	134
Figure 5.9	Change in Non-evaporable water contents results of replacement material hydration for FC by TGA .....	135
Figure 5.10	Degree of hydration of FC from wn measured OD/FI.....	136
Figure 5.11	Compressive strength versus OD/FI Non-evaporable water content for FC.....	138
Figure 5.12	Compressive strength versus OD/FI Non-evaporable water content, with trend line for normal and MIRHA FC .....	139
Figure 5.13	Compressive strength versus TGA Non-evaporable water content for FC .....	139
Figure 5.14	Compressive strength versus TGA Non-evaporable water content, with trend line for normal and MIRHA FC.....	140
Figure 5.15	Strength versus porosity relation for normal FC (cement-sand) .....	141
Figure 5.16	Strength versus porosity relation for FC with MIRHA .....	142
Figure 5.17	Measure accessible Porosity versus Theoretical of Porosity .....	142
Figure 5.18	Relation between the strength of concrete and gel space ratio normal FC.....	144
Figure 5.19	Relation between the strength of concrete and gel space ratio MIRHA FC.....	144



# CHAPTER 1

## INTRODUCTION

### **1.1 Background**

Foamed concrete (FC) is one of the solutions in support of green building materials that were introduced several decades ago. The concept of green building associates with sustainability, which incorporates and integrates a variety of strategies during the design, construction, and operation of building projects. Sustainable design or building “green” is to use materials resourcefully while creating healthier buildings. It provides cost investments through enhanced productivity, lower cost building operations, and resource efficiency and it moves us closer to sustainable futures. The use of “green” building materials and products represents one significant move in the design of a building. Green building materials propose specific benefits to the building owner and building occupants: diminished maintenance/substitution costs over the life of the building, energy conservation, improved occupants’ health and productivity, lower costs associated with changing space configurations and greater design flexibility.

FC is a material with entrained air bubbles and mortar. The density of the material depends on the number and size of the bubbles. It is possible to achieve any desired density using special mixing equipment. FC of diverse densities is proper for structural and semi-structural applications as well as lightweight architectural details.

FC is a physically powerful material with excellent thermal and sound insulating characteristics. It can be produced at the project site like ordinary concrete. The main differing low feature of FC compared to normal concrete is that it is designed to the required light density by arranging air foam as an “aggregate” in concrete [1]. This

foam has no chemical action in concrete, it only serves as an impermanent wrapping material for the air foams till cement mortar develops its own final set and strength.

Rice husk that is burnt at properly controlled temperatures [2] produces an ash consisting almost of pure silica in the amorphous form. High silica content and porous structure of the ash lead to a very high pozzolanic activity comparable with that of silica fume [3]. RHA in some respects resembles silica fume, particularly in its large specific surface and huge content of amorphous silica. However, with regard to particle size, these two materials are significantly different. Silica fume particles are spherical with average diameter of 0.1  $\mu\text{m}$ . Its BET surface is about 20  $\text{m}^2/\text{g}$  [3]. Properly produced rice husk is very soft and can be easily ground to particle sizes less than 75  $\mu\text{m}$ . The resulting RHA particles are angular in shape and highly porous. Its BET surface is usually in the order of 40 to 100  $\text{m}^2/\text{g}$  [3]. Addition of RHA is reported to lead to a significant improvement of normal strength concretes [4]. It is reasonable to suppose that the use of RHA in combination with superplasticizers may also lead to increased strength and improved durability. RHA markedly diminishes the autogenous shrinkage as well as produces an autogenous relative humidity transform [5].

The use of rice husk ash (RHA) in FC research is very limited. RHA obtained by controlled burning of rice husks, which are agricultural wastes generated in the rice-milling industry. It has been found that RHA provides dramatic improvements in hardened properties and durability of concrete [6]. Similar effects might be observed when RHA is used in FC. Cement replacement materials (CRMs) are also essential for high strength and high durability FC. Moreover, the expense of some CRMs such as silica fume and high reactivity metakaolin increase the overall material cost of FC. Therefore, the use of less-expensive RHA is more desirable to decrease the overall production cost of FC. The usage of RHA also minimizes the environmental burden resolving vast waste disposal problems caused by rice milling industries.

More than 100 countries in the world cultivate rice with an annual production of 650.2 million tons [7]. During the milling process of paddy rice, more than 130 million tons of rice husk are obtained as by-product. On combustion, this amount of husk would yield about 26 million tons of ash. A huge amount of rice husk is

produced annually in Malaysia that is almost reaching 2.231 million tons. When burnt, about 20% of the rice husk would become RHA [8]. This means 0.1 million tons of RHA can potentially be produced annually in Malaysia.

Rice husk (RH) is a waste material that is in abundance in Malaysia. Burnt (open and/or controlled) RH needs costly disposal as it can create environmental issues. In fact, burning of RH can create air pollution to the environment. Proper burning method is important to obtain RHA with high reactive silica content. Modern incinerator is designed to avoid environmental problem as caused by open burning. Microwave incinerator as one of the modern incinerators is proposed to produce amorphous Microwave incinerated Rice Husk Ash (MIRHA) with high pozzolanic reactivity thus can significantly enhance concrete properties. This research also establishes the optimum replacement percentage of OPC by MIRHA that improves the quality of FC. In addition, the use of MIRHA lowers the demand for cement production and lessens the environmental pollution caused by cement production. Hence, MIRHA not only improves FC properties and durability, but also provides substantial economic and environmental benefits. Yet, no comprehensive research has been conducted to explore the potential of RHA by investigating its effects on fresh and hardened properties and durability of FC. This study attempted to develop FC utilizing MIRHA as a CRM. The key properties of FC and their binder mortar components are determined in this study. In particular, the effects of MIRHA on various properties of different binder foamed are examined. In addition, empirical models are developed for the filling ability and compressive strength and hydration process of FC. The outcome of this study has extended the scope of FC and thus generated new opportunities for the construction industry.

Due to high water absorption capacity and water retaining effect, RHA significantly increases cohesiveness of concrete mixtures, consequently reduces the risk of aggregate segregation. Since rice husk ash is highly pozzolanic, at a lower w/c RHA concrete has higher strength at early ages compared to the control concrete [9]. This positive effect of rice husk ash can be used to compensate for the reduction of early strength of concretes partly containing less reactive mineral admixtures such as fly ashes [3].

The better a material is understood, the better it can be utilized. With cement-based materials such as FC, knowledge of the fundamental cement hydration reactions and resultant product facilitate design, behaviour prediction, and improved performance. Water is an integral part of all cement-based material. It contributes to the mixing and placing ability of the material, enables the hydration process, and influences material property development. As such, it is worthy of comprehensive study, for one will never fully understand cement-based material if one does not have a good grasp of the role of water in them. The study of water in FC with rice husk ash as pozzolanic material is particularly interesting, for information about the water content can be used to follow the behaviour of pozzolanic materials.

## **1.2 Problem Statement**

Several kind of CRMs such as fly-ash [10-12], GGBS [13], bottom ash [14], sewage sludge ash [15], ultra fine granulated blast-furnace slag, and condensed silica fume [16] have proved effective application in since RHA has shown better effects in normal concrete, these fore it may add value in FC. However, there are some concerns regarding the use of RHA, which may complicate its applications. These problems are:

1. Very high water demand due to refined porous structure of RHA, the particle size ranges between 10 and 75  $\mu\text{m}$ . When added to a FC mixture, it absorbs water into the pores like a sponge. Hence, in order to obtain a workable FC mixture, it is necessary to use a considerable proper amount of mixing water. FC is more sensitive to water demand than normal concrete. If too little water is added to the mixture, the water will not be sufficient for initial reaction of the cementitious material and the cementitious material will withdraw water from foam, causing rapid degeneration of the foam. If too much water is added segregation takes place, causing a variation in density.
2. Introduction of superplasticizer into a FC mixture can offset the negative effect of RHA on workability. The combination of RHA and superplasticizer may reduce the water/binder ratio of the concrete mixture, while still retaining acceptable workability. However, the compactibility of RHA and

superplasticizers well as the effectiveness of their combination has not been investigated in detail yet.

3. While many researchers have discussed specific aspect of the role of water in cement-based materials (with and without pozzolanic materials), however the detailed study on role of water in FC is missing in the available research. Based on the gaps and issues derived from literature review, this study was mainly focused to investigate the role MIRHA on the non-evaporable water content in the FC.

### **1.3 Objectives and scopes of Study**

The effect of adding MIRHA in FC mixtures can be assessed through its influence on compressive strength and durability. This research is to evaluate the possibilities of using MIRHA for producing structural FC and to examine parameters influencing properties of the FC in both fresh and hardened state. In addition it is also to explore the behavior of the effect of MIRHA on the hydration process using non-evaporable water knowledge.

Hydration is one the key point, which is not captured specify on the effect of potential pozzolanic materials such as MIRHA in FC. Hydration has strong correlated with the hardening process in concrete is caused by chemical reaction taking place in the cement part of the mixture. The cumulative of these reactions is highly related to the non-evaporable water content in the reaction product, and determines hardened properties of the concrete mixture.

The main objectives of this research are:

1. To determine the composition of material proportion of foamed concrete for structural lightweight concrete (the minimum compressive strength of 17 MPa at 28 days).
2. To investigate the effects of MIRHA and other constituent on mechanical properties of foamed concrete using orthogonal array.

3. To identify the effects of MIRHA on hydration process using the non-evaporable water content OD/FI and TGA, Calcium Hydroxide (CH) contents and change in non-evaporable water content on MIRHA FC
4. To develop a correlation of non-evaporable water contents vs. compressive strength model for MIRHA-FC.

The investigation is based on criteria:

The source of rice husk was taken from rice milling plant, Bernas-Malaysia. Rice husk was then burnt in automatic microwave incinerator's Universiti Teknologi PETRONAS to produce MIRHA. Incorporation of MIRHA as CRM in FC was done at 5%, 10%, and 15%.

Portafoam Model Lightweight Concrete Method (LCM) was employed produce stable aqueous foam for the production of FC. The foaming agent used was LCM consisting of hydrolyzed proteins which was manufactured in Malaysia.

Analysis of the characteristics of concretes, namely their compressive strength at ages 3, 7, 28, 90, 180 days, non-evaporable water by oven dry/furnace ignition (OD/FI) at ages 3, 7, 28, 90, 180 days, non-evaporable water by Thermogravimetry (TGA) at ages 3, 28, 180 days, dry density at 180 days and porosity at 180 days.

#### **1.4 Organization of thesis**

Following this introduction chapter, Chapter 2 provides a review of available and related literature on invention and exploration in FC properties, material behavior (rice husk ash), non-evaporable water and Taguchi Method. Chapter 3 describes the research methodology that explains the procedure of all experiment, material selection, experimental design and experimental laboratories. Chapter 4 provides analysis and discusses that are MIRHA analysis, plastic density and cube strength, orthogonal array experimental, the non-evaporable analysis by OD/FI and TGA, Calcium Silicate Hydrate (C-S-H) bound water/AFm bound water, CH bound water, comparing C-S-H/AFm and CH bound, change in non-evaporable water content due

to the presence of MIRHA, degree of hydration of FC, compressive strength versus non-evaporable water model, compressive strength versus porosity model, compressive strength versus gel space ratio model, comparison of the model, optimum FC mix proportion. In chapter 5, conclusions resulting from the investigation are drawn and recommendations for future research and future work are put across.

## CHAPTER 2

### LITERATURE REVIEW

#### **2.1 General**

The density of concrete can be reduced by replacing some solid material in the mix by air void or by using lighter solid materials. There are three categories of lightweight concrete, namely, (i) lightweight aggregate concrete, (ii) no-fines concrete. (iii) foamed concrete (FC).

Foamed concrete is a potential material in the construction industry. This chapter presents a background and review of FC. It primarily gives the definition and briefly describes the characteristics, advantages, applications, and economic aspect of the use of FC. Then it provides the basic principles, production approaches, possibilities of FC as structural application that focuses on the performance criteria and material aspects of FC.

#### **2.2 Foamed Concrete (FC)**

This material was first patented in 1923 [1], at that time due to lack of specialized material and equipment limited its use to non structural application. The development phases of FC have gone through significantly. They change in the conceptual approach and construction methods for structural purpose, and opened new opportunities of design. The definition, characteristics, advantages, applications and economy of FC are briefly discussed in the following subsections.



### **2.3.1 Definition and Characteristic of FC**

FC is a porous concrete mixture containing no coarse aggregates. It contains only fine sand, cement, water and foam. The steady foams are formed by suitable foaming agent produce homogenous [1] void structure in FC mixes. According to ASTM-C796-97 [17], cementitious material can be used in mixes e.g. portland cement, cement-silica, cement-pozzolan, lime-pozzolan, or lime-silica pastes. In ACI-committee523 [18] it is stated that alternative aggregate may be added; for example, artificial lightweight aggregates such as expanded clay, shale, slate, sintered fly ash, perlite, and vermiculite as well as natural lightweight aggregates such as pumice, scoria, or tuff.

FC differs from ordinary concrete with respect to its specific characteristic strength and density. For ordinary concrete, the user would specify a certain compressive strength and the water/cement would be adjusted to meet the specification. When FC is specified, it is normally not only the strength, but also density. Compressive strength reduces exponentially with decreasing FC density, reflecting the greater quantity of air bubbles present in the cementations microstructure [11].

### **2.3.2 Advantage and Application of FC**

FC offers many advantages. Among them are:

- a. The basic contribution of FC to the field concrete technology is the ability to vary its density over a wide range. By suitable control in dosage of foam, a wide range of densities (400 to 1800 kg/m<sup>3</sup>) [19] of FC can be obtained for application to structural, partition, insulation and filling grades.
- b. Workability, compacting and leveling of FC show that it has good flow ability, self-compacting and self-leveling nature and may be pumped.
- c. Flows through and around reinforcing steel under self-weight and eliminates the need for vibration equipment or any other means of consolidation.
- d. Reduces noise and improves the construction environment in the absence of concrete vibrating equipment.

- e. Requires fewer laborers for transport and placement of concrete and thus becomes more economical.
- f. Eases concrete placement operations, and thus increases constructibility.
- g. Allows the formwork to last longer due to the elimination of vibration equipment.
- h. Reduces the heat temperature excellently and high fire resistance due to foam in mixes [59]
- i. Foamed concrete has good shock absorption and high impact resistance.
- j. Simplifies the construction of the structures of complicated design due to the easement in casting and molding of the complex architectural forms.

FC has been applied successfully in various applications as an alternative to granular fill because FC has the ability to flow easily under its own weight. Several application of FC are mentioned in Table 2.1

Table 2.1 Application of FC

Structure	Location
U.S. Army Engineer Waterways Experiment Station [20]	Vicksburg, Miss.
Void filling in Heathrow railway tunnel [10]	UK
Void filling in Coombe down mines [10, 21]	UK
Void filling in Harbour [10]	Netherlands
Smart Tunnel [19]	Kuala Lumpur
Kingstone Bridge widening and strengthening [21]	UK
Road construction, Canary Wharf [10]	London
Road base [10]	Boston, Holland, Washington DC, South Dakota
Road base in Logan International Airport [10]	Boston
Arches Housing application [10]	South Africa

FC is a porous lightweight concrete. The various economic benefits of FC as structural lightweight concrete are:

- a. Structural lightweight concrete has maximum density of two-third of normal concrete. This reduces the self weight of the structures and consequently imposes smaller loads to the substructure.
- b. One of the most common applications of structural lightweight concrete is in bridge redecking where lower dead load is achieved. This often means that

bridge widths, traffic lanes, and the thickness of structural slabs can be increased while utilizing existing piers, footings, and other structural members.

- c. Substantial cost savings can be realized when less dead load, smaller size structural members, less reinforcing steel are being introduced.

### **2.3.3 Background and Basic Principle of FC, Approaches to Obtain FC and Possibilities of FC Lightweight as Structural Material**

The future need for construction materials that are light, durable, simple to use, economic and more environmentally sustainable have been identified by foresight group around the world [22, 23]. There are plentiful applications where a lower density concrete may be proper, functional or enviable particularly when combined with other attributes such as improved processing, higher strength to weight ratio, enhanced insulation properties, and enhanced acoustic properties.

Foamed concrete has a surprisingly long history. It was first patented in 1923, mainly for use as an insulating material. Even though there is proof that the Romans used air entrainers to reduce density, this was not truly a true FC. However, the lack of specialized materials and equipment, limited its use to small-scale projects. Significant developments over the past 20 years in invention equipment and better quality surfactants (foaming agents) has facilitated the use of FC on larger scale.

The first review on cellular concrete was presented by Valore [1, 24] in 1954, he summarized the composition, properties and uses of cellular concrete, irrespective of the method of formation of the cell structure. Jones and McCarthy [10] have reported the history on use of FC, constituent materials used, its properties, and construction application including some projects carried out worldwide. The serviceable properties like fire resistance, thermal conductivity and acoustical properties are also incorporated in these reviews, while the data on fresh state properties [25], durability and air-void system of FC are rather limited. The construction of stable FC mix depends on many factors viz. choice of foaming agent, method of foam preparation and addition for unvarying air voids distribution, material section and mixture design strategies, production of FC, and performance with reverence to fresh and hardened.

When foam is added to the base mix, the consistency of FC is reduced, which depends on the foam volume added and for a given density on filler type. The values of consistency either lower (mixture is too stiff causing the foam to break) or higher (slurry becomes too thin to hold the foam resulting in segregation) than normal consistency lead to an increase in density.

The stability of FC is defined as the status of the mix at which the density ratio (the calculated density against cast density) is closer to unity, depends on the consistency of the base mix, and can be expressed in terms of the water–solids ratio, which varies with filler type.

Superplasticizers are sometimes employed to keep an appropriate workability even though it may diminish the stability of foam. Because of the complication of modern chemical admixtures, it is impossible to simplify their interactions with foam.

The preformed foam that is blended with the base material to produce FCs can be divided in two categories namely wet foam and dry foam:

- a. Wet foam is produced by spraying a solution of foaming agent (usually synthetic) and water over a fine mesh. The foam has large “loose” bubble structure and although relatively stable it is not recommended for the production of low density (below  $1100 \text{ kg/m}^3$ ) foamed material. It is not suitable for pumping long distances or pouring to any great depth.
- b. Dry foam [21] is produced by forcing a similar solution foaming agent and water through a series of high density restrictions whilst at the same time forcing compressed air into a mixing chamber. The bubble size is typically less than 1 mm in diameter and of an even size. This type of foam is extremely stable and these stable properties are passed onto foamed materials when the foam is blended with the base materials.

ASTM-C330 [26] point out that the criteria of structural lightweight concrete is that it has compressive strength and density of  $17 \text{ N/mm}^2$  and  $1680 \text{ kg/m}^3$  respectively. Additionally, ACI 213R-87 [27] classifies lightweight concrete for structural purpose has density between  $1350$  and  $1900 \text{ kg/m}^3$  and has minimum strength of  $17 \text{ N/mm}^2$  (BS EN 206-1/BS 8500).

The major contribution of structural lightweight is more into its density characteristic rather than the compressive strength performance. This subsequently could be used as the requirement for maximum limit of lightweight concrete density. However, because only fine aggregate water and foam tend to reduce the concrete strength greatly, the specifications require a minimum 28-day compressive strength to ensure that the concrete is of structural quality.

The potential of FC as structural application has been explored by Jones [22] and Kearsley [28]. The possibilities FC as structure purpose are mentioned in Table 2.2.

Table 2.2 The study on possibility of FC as structural application

Item	Kearsley	Jones
Special Material used	fly ash/cement of 1-4	fly ash/cement of 0.3-1
Density	Casting density : 700-1500 kg/m <sup>3</sup> , the correlation of dry density versus casting density such as $\gamma_{dry} = 0.868\gamma_{cast} - 55.07$	Casting density :1400-1800 kg/m <sup>3</sup>
Curing regime	The sample wrapped in plastic after demoulding and constantly placed in temperature room at 22°C	The sample wrapped in plastic after demoulding and constantly placed in temperature room at 22°C
Compressive Strength	2-25 MPa	8-42 MPa

### 2.3.4 Material Aspects and Mixture Design for FC

Foamed concrete mainly consists of cement, only fine aggregate, water, and foam. As a rule of thumb a FC is described as having an air content of more than 20% which distinguishes it from highly air entrained materials.

#### a. Portland cement

Portland cement is most widely used to produce various types of concrete. It is a hydraulic cement, which is produced by pulverizing clinker consisting of calcium silicates, and usually containing calcium sulfate as an interground addition [29]. Ordinary portland cement (OPC) is the most important cementitious component of FC. In addition to OPC, Rapid hardening Portland cement [11] and high alumina cement have been used for reducing the setting time and to improve the early strength

of FC. After reacting with water, Portland cement also reduces the porosity and results in a packed concrete mass leading to low transport properties and good durability [30].

## 1. Physical properties

The physical properties of cement significantly influence the performance of concrete. It is also valid for foamed concrete. The cement used for foamed concrete should have sound flow and setting properties [31]. It should enhance the fluidity of concrete and should be free from false setting due to premature stiffening within a few minutes of mixing with water. The cement should possess carefully controlled fineness, and should produce low or moderate heat of hydration to control the volume changes in concrete [32]. The ASTM [33-35] have specified the physical property requirements for various portland cements, which are also useful to choose the proper cement for FC.

## 2. Chemical composition

The chemical analysis of Portland cement has revealed that it mostly consists of various oxide compounds. The major oxide compounds are lime, silica, alumina, and iron. In addition, two minor oxides namely sodium and potassium oxides are of some importance, particularly with regard to alkali-aggregate reactions in concrete. In addition, magnesia and sulfuric anhydrite can be present, although they are not beneficial constituents of cement. The typical chemical composition of Portland cement is shown in Table 2.3. The ASTM [29] have specified the chemical requirements for different types of Portland cement. These requirements are also important to select the appropriate cement for FC.

Table 2.3 Typical chemical oxide compositions of Portland cement [36]

Chemical Name	Composition	Mass Content (%)
Calcium oxide (lime)	CaO	60-69
Silicon dioxide (silica)	SiO <sub>2</sub>	18-24
Aluminum oxide (Alumina)	Al <sub>2</sub> O <sub>3</sub>	4-8
Ferrous (iron oxides)	Fe <sub>2</sub> O <sub>3</sub>	1-8
Magnesium oxide (magnesia)	MgO	<5
Sulfur trioxide (sulfuric anhydrite)	SO <sub>3</sub>	<3
Alkaline oxides (alkalis)	Na <sub>2</sub> O and K <sub>2</sub> O	<2

## **b. Fine Aggregate**

The fine aggregate, a natural siliceous sand is additionally sieved to remove particles greater than 2.36 mm, to help improve the FC flow characteristics and stability [22]. Nambiar's study [37] showed that reduced particle size of sand caused an improvement in strength of FC.

## **c. Water**

The water content for a mix depends upon the material composition and use of admixtures and is managed by the consistency and stability of the mix [38]. With lower smaller water content, the mix may be too stiff causing foam to break while a high water content makes the mix too thin to hold the foam leading to separation of foam from the mix and thus segregation occurs [37]. Water cement ratio used ranges from 0.3 to 0.45 [10, 39] depending on the cement composition, consistency requirements and use of chemical admixtures, while ensuring foam stability.

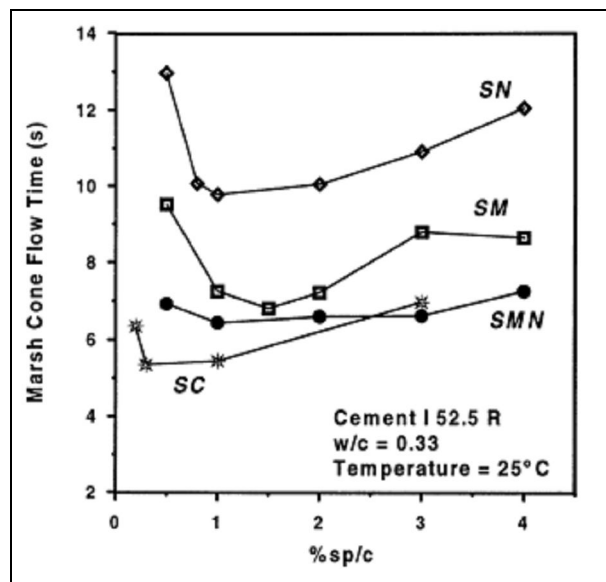
## **d. Foam Type**

Explanation on the generally used natural and synthetic foaming agents have been offered by Valore [1], Laukaitis et al [40], Park et al [41]. Most of the earlier investigations used proprietary foaming agents, viz. Neopar [42, 43], Mearlcrete [44], Elastizell [45, 46], and Foamtech [11, 12, 47, 48]. Foamed concrete is produced either by pre-foaming method or mixed foaming method. Pre-foaming method encompasses of producing base mix and stable preformed aqueous foam separately and then thoroughly blending foam into the base mix. In mixed foaming, the face active agent is mixed along with base mix ingredients and during the process of mixing, foam is formed resulting in cellular structure in concrete [49]. The foam must be dense and stable so that it stands firm to face the pressure of the mortar until the cement obtains its initial set and a strong skeleton of concrete is built up around the void filled with air [50]. Viscosity of liquid stage, surface effects such as Gibbs [the coefficient of surface elasticity in static condition was introduced as variable resistance to surface deformation during thinning] and Marangoni [the dynamic condition of coefficient of surface elasticity] effects, disjoining pressure between neighboring interfaces due to

adsorption of ionic and nonionic surfactants and polymers and concentration of foaming agents are some of the factors influencing foam steadiness as recognized by various researchers [51-53].

### e. Superplasticizer

To create workable FC, superplasticizers are also occasionally employed [10] but their use in FC can cause instability in the foam [54]. On the other hand, the incorporation of superplasticizer by changing influences the hydration process in cement paste clearly, especially achieving the rate of hydration [55]. Determination of the saturation dosage for various type of superplasticizer is shown in Figure 2.1.



SN= Naphthalene sulfonic acid based; SM=Melamine sulfonic acid based;; SC=Polycarboxylic acid based; SMN=Melamine– naphthalene based blend

Figure 2.1 Determination on the saturation dosage for various types of superplasticizers [55]

A double layer model [56] explains the SP mechanism of action. This model clarifies the electrical repulsion mechanism and helps to understand the definition of Zeta potential. Figure 2.2 depicts the detail of the double layer model.



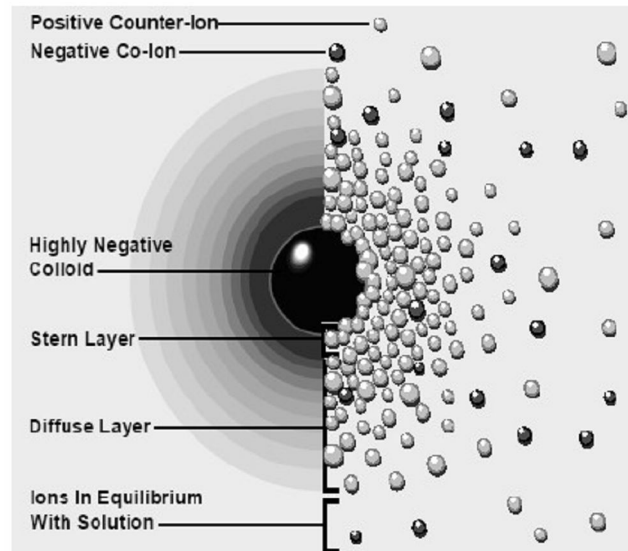


Figure 2.2 Double layer model of SP mechanism on action [56]

#### f. Design of Foam Concrete Mixes

Until today, there is no standard method for designing a FC mix. When designing FC, a target casting density, sand/cement, and water/cement are chosen and the water requirement determined. Using these values and the relative densities of materials, the mass of the ingredient and the volume of foam that should be added to obtain the required density can be determined. Several studies [18, 57] have been explored to accomplish mix design of lightweight FC. The density and the strength of FC have linear relationship; the strength can be decreased by changing the constituent materials. The principal of mixture design studies of foamed concret are listed in Table 2.4.

Table 2.4 The previous works on FC mixture proportion

Author	Method concept	Strength (N/mm <sup>2</sup> )	Density (kg/m <sup>3</sup> )
McCormick [44]	Based on solid volume calculations	0.1-26.82	960-1922 (casting density)
ACI-committee523 [18]	Based on target density calculation	1.8-24.7	800-1920 (casting density)
Kearsley &Mostert [39]	density and volume of FC	4-15 (7 days)	600-1100 (dry density)
Nambiar&Ramamurthy [58]	filler-cement ratio using respond surface analysis	1-18	550-1500 (dry density)

There are two equations proposed by Kearsley and Mostert in that study [39] and can be written as follows:

$$\rho_{LWFC} = C + C(w/c) + C(p/c) + C(s/c) + C(p/c)(w/p) + C(s/c)(w/s) + RD_f V_f \quad (2-1)$$

$$1000 = \frac{C}{RD_c} + C(w/c) + \frac{C(p/c)}{RD_p} + \frac{C(s/c)}{RD_s} + V_f \quad (2-2)$$

Where :

- $\rho_m$  = target casting density ( $\text{kg/m}^3$ )
- $C$  = cement content ( $\text{kg/m}^3$ )
- $w/c$  = water-cement ratio
- $p/c$  = pozzolan-cement ratio
- $s/c$  = sand-cement ratio
- $w/s$  = water-sand ratio
- $V_f$  = volume of foam (liter)
- $RD_f$  = relative density of foam
- $RD_c$  = relative density of cement
- $RD_p$  = relative density of pozzolan
- $RD_s$  = relative density of sand

Additionally ASTM C 796-97 [17] gives a technique of calculation of foam volume required to make cement slurry of known water-cement ratio and target density.

### 2.3.5 Properties of Foamed Concrete

#### a. Fresh State Properties

Fresh FC is only of temporal interest but the strength of foam concrete of given mix proportions is very seriously affected by the degree of its workability. Foamed concrete which cannot be subjected to compaction or vibration should have flow ability and self-compactibility. There were several studies to investigate the fresh state

properties of foamed concrete (Table 2.5). The classification of foamed concrete based on the spread test was shown in Table 2.6.

Table 2.5 The investigation of fresh state property

Author	Test	Result
Nambiar&Ramamurthy [25]	Flow time using marsh cone and flow cone spread tests	45% of the spread at which a foam concrete mix of good stability and consistency can be produced
Jones &McCarthy [22]	Repeatability of plastic density	Coefficient of variance values of less than 10%.
Kearsley &Mostert [39]	Water demand of mix constituent using ASTM flow table test [59]	Flow circle diameter in range 220 to 250 mm
Jones at all [60]	Spread test	It was found that the 200mm spread benchmark for flowing concrete.

Table 2.6 Classification of Foam Concrete Based on Spread Percent [25]

Class Designation	Flow values (%)	Description
VL	0-20	Very Low
L	20-40	Low
M	40-60	Medium
H	60-80	High
VH	80-120	Very High

## b. Density Properties

As the properties are articulated in terms of dry density, the relationships proposed in literature between dry and fresh density are summarized in Table 2.7.

Table 2.7 Empirical models for density determination [31]

Reference	Equation	Remark
ASTM C 796-97 [17]	$\text{Dry density} = (W_c + 0.2W_c)/V_{\text{batch}}$	$W_c$ and $V_{\text{batch}}$ are weight of cement and volume of batch respectively
ACI [18]	$\text{Dry density} = 1.2 C + A$	$C$ and $A$ are weight of cement and aggregate in kg per cubic meter of concrete
Kearsley [28]	$\gamma_{\text{dry}} = 0.868\gamma_{\text{cast}} - 55.07$	Casting density range of 700 kg/m <sup>3</sup> to 1500 kg/m <sup>3</sup> . Cement-fly ash mixture of varying Fly ash-cement ratio (F/C = 0 to 4)

### c. Compressive Strength

The overview of compressive strength of FC with various mixture composition and densities as reported in previous work is listed in Table 2.8.

Table 2.8 A review of mixes used, compressive strengths and density ranges of FC [31]

Author(s)	Proportion of cement kg/m <sup>3</sup> or composition	Ratios			Density range kg/m <sup>3</sup>	Comp. Strength N/mm <sup>2</sup> (28 days)
		S/C	W/C	F/C		
Mc Cormick [44]	335-446	0.79-2.8	0.35-0.57		800-1800	1.8-17.6
Tam et al. [61]	390	1.58-1.73	0.6-0.8		1300-1900	1.81-16.72
ACI 523 [62]	Neat cement paste				240-640 (DD)	0.9-1.72
	Cement-sand mix				400-560 (DD)	12.11
Hunaiti [42]	-	3	-	-	1667	12.11
Kearsley and Booyens [63]	Cement-fly ash replacement				1000-1500	2.8-19.9
Kearsley and wainright [11]	193-577		0.6-1.17			
Rahman [64]	362	1	0.6		799	0.82-1.04
Tikal'sky et al [65]	Neat cement				490-660	0.71-2.07
	149-420		0.4-0.45			
	Cement-sand/fly ash				1320-1500	0.23-1.1
	57-149		0.5-0.57			
Jones and McCarthy [66]	300		0.5		1000-1400	1.2
	300		1.11-1.56	1.22-2.11	1000-1400	3.9-7.36
Jones and McCarthy [22]	500		0.3		1400-1800	10-26
	500		0.65-0.83	1.15-1.77	1400-1800	20-43
Nambiar and Ramamurthy [58]	Cement-sand mix (coarse)	With filler cement ratio varied from 1 to 3 and fly ash replacement for sand varied from 0 to 100%			800-1350 (DD)	1-7
	Cement-sand mix (fine)				800-1350 (DD)	2-11
	Cement-sand-fly ash mix				650-1200(DD)	4-19

S/C: sand-cement ratio; F/C: Fly ash-cement ratio; W/C: water cement ratio; DD: dry density

Kearsley and Mostert's studies [67] showed that the compressive strength reduces exponentially with a decreasing in density of FC (Figure 2.3).

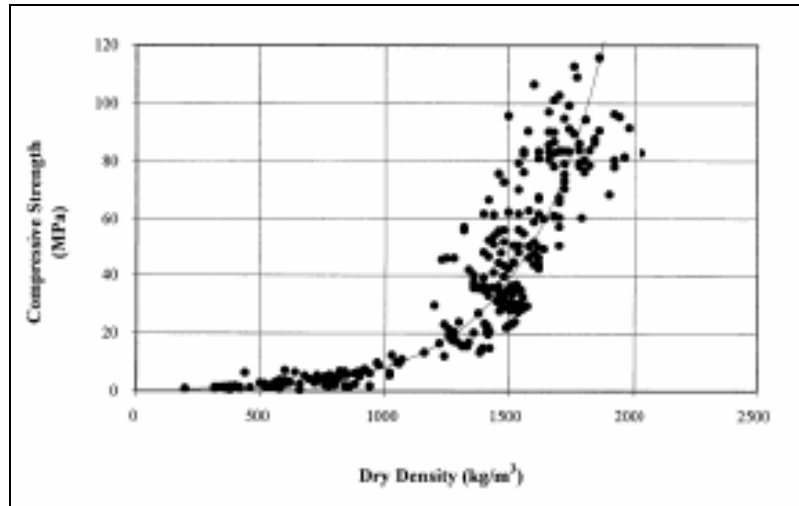


Figure 2.3 Compressive strength as a function FC density [67]

Investigation that was carried out by Hamidah et al. [68] concluded that other factors also affected the FC (e.g. cured FC in water gave higher strength than cured it in air; higher sand-cement ration resulted in lower strength of FC; added more cement content in the FC increased its strength). For densities higher than  $1000 \text{ kg/m}^3$ , the air-voids are too far apart to have an influence on the compressive strength, the composition of the paste determines the compressive strength [69]. It has been reported by Tam et al. [60] that i) the effect of water-cement ratio and air strongly affect the strength of FC and, ii) the combined effect should be considered when volumetric composition of air-voids approaches that of water voids. The study of replacing cement with fly ash [11] indicates that foamed concrete mixes with high fly ash content needed a longer time to reach their maximum strength which was observed to be higher than that achieved using only cement. When the cement is substituted with silica fume, higher compressive strength is obtained in the long term, due to their pozzolanic reaction and filler characteristics, with a more marked effect at high FC densities. For a given density, the fineness level of sand affects the strength and density, the mix proportion with finer size sand resulted in higher strength than the mix with coarse sand and the variation is higher at higher density. This higher strength to density ratio is recognized to the comparatively uniform distribution of pore in FC with fine sand, while the pores are larger and irregular for mixes with coarse sand [37, 44].

#### d. Porosity

Hoff [70] has defined the porosity of cellular concrete made of neat cement paste as the partial portion of the total volume equal to air void and evaporable water. The Figure 2.4 shows the porosity model of FC suggested by Hoff. This model can be constructed in a theoretical of porosity as shown in Equation (2-3).

$$n = 1 - \frac{dc(1+0.20\rho_c)}{(1+k)\rho_c\gamma_w} \quad (2-3)$$

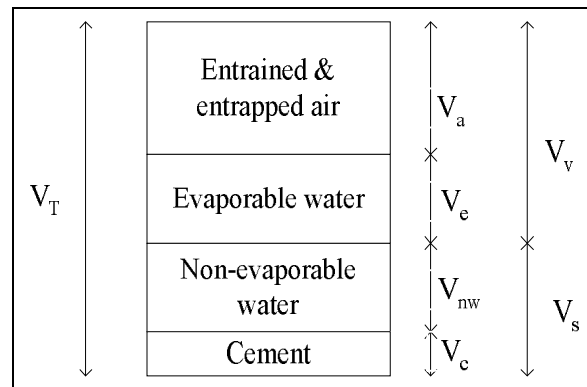


Figure 2.4 Foamed concrete model suggested by Hoff [70]

Where ;

- $n$  = theoretical porosity
- $dc$  = concrete density
- $\rho_c$  = specific gravity of the cement
- $\gamma_w$  = unit weight of water
- $k$  = water/cement ratio (by weight)
- $V_T$  = Volume of total
- $V_a$  = Volume of air
- $V_e$  = Volume of evaporable water
- $V_{nw}$  = Volume of non-evaporable water
- $V_c$  = Volume of cement
- $V_v$  = Volume of void
- $V_s$  = Volume of solid

An experimental study to investigate the porosity of foamed concrete, as determined using the Vacuum Saturation Apparatus, was carried out by Kearsley and Wainwright [48]. Then, the porosity was calculated using the following formula [71] (Equation (2-4)). Figure 2.5 shows the correlation between porosity and dry density where Figure 2.6 the correlation between compressive strength and porosity.

$$P = \frac{W_{SA} - W_d}{W_{SA} - W_{SW}} \times 100 \quad (2-4)$$

Where:

- P = Total porosity (%)
- $W_{SA}$  = Weight of saturated surface dry samples in air (g)
- $W_{SW}$  = Weight of saturated surface dry samples in water (g)
- $W_d$  = Weight of oven dry samples (g)

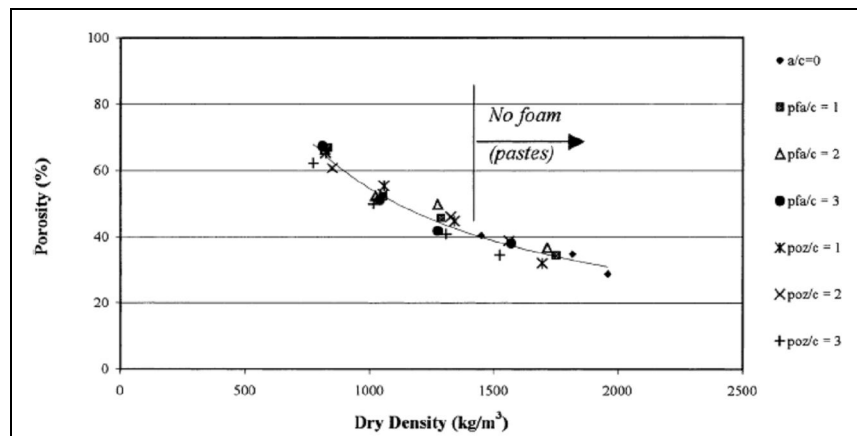


Figure 2.5 The porosity as function of dry density [48]

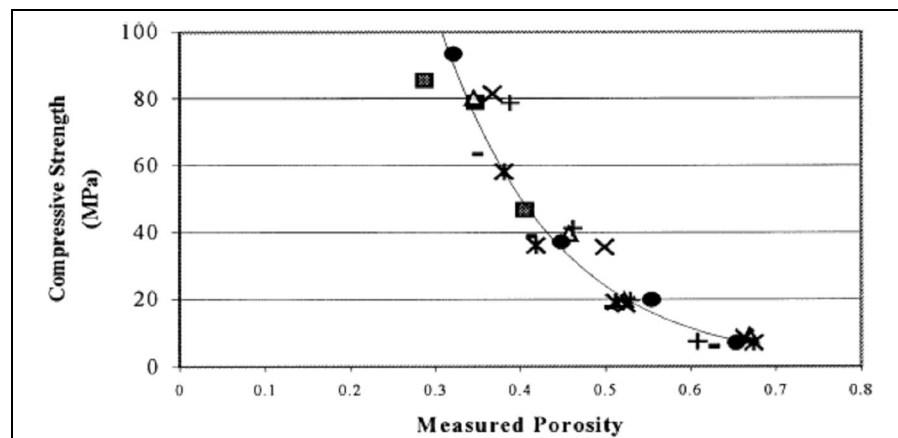


Figure 2.6 The porosity as function of strength [48]

Nambiar [72] has modified Hoff's model by including sand and fly ash as pozzolan and filler material to FC. The theoretical porosity proposed is shown in Equation (2-5)

$$n = 1 - \frac{d_c(1+0.20\rho_c + S_v)}{(1+k)(1+S_w)\rho_c\gamma_w} \quad (2-5)$$

Where;

- $n$  = theoretical porosity
- $d_c$  = concrete density
- $\rho_c$  = specific gravity of the cement
- $\gamma_w$  = unit weight of water
- $k$  = water/cement ratio (by weight)
- $S_v$  = filler cement ratio (volume)
- $S_w$  = Filler cement ratio (weight).

### 2.3.6 Strength Prediction Models

The strength of foamed concrete is significantly influenced by its pore structure characteristic, therefore the volume of all voids that exist in foamed concrete must be properly considered, i.e. entrapped air, capillary pores, gel pores, and entrained air. These significantly influence the strength of the foamed concrete [70]. There are several researchers who developed expressions for predicting strength of foamed concrete. The findings are summarized in Table 2.9.



Table 2.9 Summary on strength prediction models on FC [72]

Author	Ingredient	Strength Model
Hoff [70]	Cement paste	Based on Balshin's model, single strength-porosity relation is possible by combining space occupied by evaporable water and air void
Kearsley and Wainright [48]	Cement paste with and without fly ash	Based on Hoff's model (extension of Balshin's model), Hoff model can be effectively used to predict the compressive strength FC made of different fly ash replacement levels and densities at different ages
Tam et al [61]	Cement mortar	Based on Feret's and Power's equation, Feret's formula provides a good relationship with strength. The relationship is improved when degree of hydration is introduced through power's gel-space ratio
Nambiar [72]	Cement mortar with sand and fly ash as fine aggregate	Based on Power's gel-space ratio concept, For mixes with lower density ranges
Nehdi [20]	Cement mortar	Based on Neural Network model

#### a. Strength-porosity model

As already deliberated that the porosity have a considerable impact on compressive strength of foam concrete. In this study, Balshin's model was adopted to promote a strength-porosity model for foam concrete which can be expressed similar to the form.

$$\sigma_y = \sigma_0 (1-n)^b \quad (2-6)$$

Where ;

- $\sigma_y$  = strength of the material which has a given porosity.
- $\sigma_0$  = intrinsic strength at zero porosity
- $n$  = porosity
- $b$  = varied somewhat but was approximately equal to three

The combination of theoretical porosity equation between Equation (2-5) and Equation (2-6) can be written as:

$$\sigma_y = \sigma_0 \left[ \frac{dc(1 + 0.20\rho_c + S_v)}{(1+k)(1+S_w)\rho_c\gamma_w} \right]^b \quad (2-7)$$

Tam et al [62] has stated that hydration ratio of water to cement was vary from 0.18 to 0.23. In order to simplify the calculation, DoH of 0.2 was used throughout the study. It also satisfies the model of Hoff [70], Kearsley and Wainwright [47, 48] and Nambiar 's model [72], Kearsley and Wainwright [47, 48] and Nambiar 's model [72].

## b. Gel Space Ratio

One of the important factors that affects the strength depends on the degree of hydration of cement and its chemical and physical properties [30]. It is more correct, therefore, to correlate the strength to the percentage solid product of hydration of cement in the space available for these products. Gel-space ratio is defined as the ratio of volume of hydrated cement paste to the sum of volumes of the hydrated cement and of the capillary pores. The product of hydration of 1 ml of cement will be assumed to occupy 2.06 ml; not all the hydrated material is gel. As a result, the volume of gel is  $2.06\alpha V_c$ .

In the case of cement-sand pozzolan mix, the volume of products formed by the pozzolanic reaction is not considered. The space is the total volumes subtract the volume equal to solids that will not be hydrated (fillers) and unhydrated volume of cement.

$$\text{space} = 1 - V_{fi} - V_c (1 - \alpha) \quad (2-8)$$

$$\text{Gel-space ratio} = \frac{2.06\alpha V_c}{[1 - V_{fi} - V_c (1 - \alpha)]} \quad (2-9)$$

Where;

- $V_c$  = the volume of cement
- $V_{fi}$  = the volume of the fillers per  $m^3$  of FC
- $\alpha$  = the degree of hydration which is assumed as 0.80.

## 2.3 Rice Husk Ash

This section is focused on pozzolanic material in general, discussing the definition and material composition, reaction and reaction rates, and significance of use. There are many materials which can be substituted to cement material as mineral admixtures. The materials of interest in this work are pozzolanic materials, for through their interaction and reaction with the mixture components, they can enhance the final product.

### 2.3.1 Definition, Composition and Its significance

Pozzolanic materials are typically defined as cementitious materials that contain silica or alumina and silica, when they are ground finely will react chemically with Calcium hydroxide,  $\text{Ca}(\text{OH})_2$ , at normal temperature and in the presence of water to form insoluble product with cementitious properties [30]. Ramachandran's study [73] showed the general classification of mineral admixture with their chemical and mineralogical composition and particle characteristics.

Definition of pozzolanic reaction is the chemical reaction between a pozzolan (S) and calcium hydroxide (CH) in the presence of water (H). It can be generalized by the simplified equation shown in Equation (2-10) [74].



There are many benefits of using pozzolan material in cement and concrete amongst them are:

- a. Their ability to convert calcium hydroxide to calcium silicate hydrate, therefore, the capillary voids are either eliminated or reduced in size. This in turn improves cement-concrete material such as strength and durability of the hydrated paste.
- b. Pozzolans can also be used as cement replacement material (it is also economical since most pozzolans are cheaper than cement they replaced). This promotes the use of waste products and thus conserves energy and resource.

### 2.3.2 Characteristic of Rice Husk Ash

Rice husk ash is produced by incinerating the husks of rice paddy. Rice husk is a by-product of rice milling industry. Controlled incineration of rice husks between 500°C and 800°C produces non-crystalline amorphous RHA. RHA is whitish or gray in color. The particles of RHA occur in cellular structure with a very high surface fineness. They have 90% to 95% amorphous silica [75]. Due to high silica content, RHA possesses excellent pozzolanic activity.

#### a. Burning Procedure

The quality of RHA actually depends on the method of ash incineration and the degree of grinding. It also depends upon the preservation of cellular structure and the extent of amorphous material within the structure [8]. Burning temperature, time, and environment, have different effects on the RHA produced. Table 2.11 shows the chemical composition of RHA under different burning temperature.

Table 2.10 Chemical Composition of RHA under Different Burning Temperatures [9]

		Temperature (°C)				
		<300	400	600	700	1000
Element (%)	Si	81.90	80.43	81.25	86.71	92.73
	K	9.58	11.86	11.80	7.56	2.57
	Ca	4.08	3.19	2.75	2.62	1.97
	Na	0.96	0.92	1.33	1.21	0.91
	Mg	1.25	1.20	0.88	0.57	0.66
	S	1.81	1.32	1.30	1.34	0.16
	Ti	0.00	0.00	0.00	0.00	0.45
	Fe	0.43	1.81	0.68	0.00	0.68
Oxide (%)	SiO <sub>2</sub>	88.01	88.05	88.67	92.15	95.48
	MgO	1.17	1.13	0.84	0.51	0.59
	SO <sub>3</sub>	1.12	0.83	0.81	0.79	0.09
	CaO	2.56	2.02	1.73	1.60	1.16
	K <sub>2</sub> O	5.26	6.48	6.41	3.94	1.28
	Na <sub>2</sub> O	0.79	0.76	1.09	0.99	0.73
	Fe <sub>2</sub> O <sub>3</sub>	0.29	0.74	0.46	0.00	0.43

Burning the RHA with higher temperature will increase the SiO<sub>2</sub> content. But it is not suggested to burn rice husk above 800°C longer than one hour, because it tends to cause a sintering effect (coalescing of fine particles) and is indicated by a dramatic reduction in the specific surface [8].

Combustion environment also plays an important role. It should be noted the changing of the rate of oxidation from moderately oxidizing conditions (CO<sub>2</sub> environment) to highly oxidizing conditions (oxygen environment) is responsible for the steep drop in the micro porosity and surface area [8]. The effect of the combination of various conditions to RHA is shown in Table 2.11.

Table 2.11 The Effect of Burning Conditions on the Crystal Structure and Surface Area of Rice Husk Ash [76]

Burning Temperature	Hold Time	Environment	Properties of ash	
			Crystalline	Surface Area m <sup>2</sup> /g
500-600° C	1 min	Moderately oxidizing		122
	30 min		Non crystalline	97
	2 hours			76
700-800° C	15 min – 1 hr	Moderately oxidizing	Non crystalline	100
	> 1 hour	Highly oxidizing	Partially crystalline	6-10
> 800° C	> 1 hour	Highly oxidizing	Crystalline	< 5
*150° C (first stage)	1.5 hours	Flue Gas Filter	Amorphous and partially crystalline	
550° C (second stage)	2.5 hours			

\*The Burning procedure by MIRHA's Unversiti Teknologi PETRONAS [2]

At higher temperatures with longer burning times, a crystalline structure is formed with a sharp reduction in surface area. This lowers the pozzolanic activity. Figure 2.7 indicates the ideal time/temperature path to obtain optimum quality rice husk ash with a micro-porous and cellular structure which is highly reactive [8].

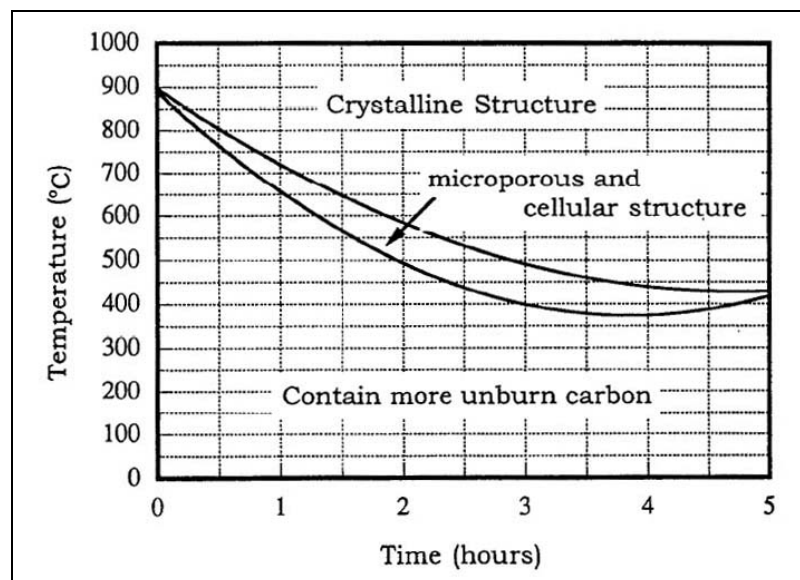


Figure 2.7 The Optimum Incineration Condition Curve for obtaining Reactive Cellular RHA [8]

## b. Physical properties

The physical properties of RHA largely depend on burning conditions. Particularly, the period and temperature of burning affect the microstructure and characteristics of RHA [8]. The partial burning of rice husks produces black RHA whereas the complete burning results in either white or grey RHA [77]. In addition, the uncontrolled burning at high temperature produces crystalline RHA, which possesses poor pozzolanic property. Conversely, the controlled burning at about 500oC to 800oC results in non-crystalline or amorphous silica, which shows very high pozzolanic activity [8]. The burning condition also affects the relative density of RHA. The relative density of grey RHA obtained from complete burning is generally 2.05 to 2.11 [77, 78]. The RHA particles are mostly in the size range of 4 to 75  $\mu\text{m}$  [79]. The majority of the particles pass 45- $\mu\text{m}$  (No. 325) sieve. The mean particle diameter typically ranges from 6 to 38  $\mu\text{m}$  [79], which is larger than that of silica fume. However, unlike silica fume, the RHA particles are porous and possess honeycomb microstructure [80]. Therefore, the specific surface area of RHA is extremely high. The specific surface area of silica fume is typically 20  $\text{m}^2/\text{g}$  whereas that of non-crystalline RHA can be in the range of 50 to 100  $\text{m}^2/\text{g}$  [6].

Table 2.12 Physical properties of RHA [81]

Property	Value			
	Mehta [6]	Zhang et al[80]	Feng et al (2004)	Bui et al [82]
Mean particle size ( $\mu\text{m}$ )	-	-	7.4	5
Specific gravity	2.06	2.06	2.1	2.1
Fineness: Passing 45 mm (%)	99	99	-	-

### c. Chemical Composition

Rice husk ash contains a high amount of amorphous silica, which originally comes from the surfaces of the husk [83]. This amorphous silica can be obtained by burning rice husk in moderately oxidizing environment at controlled temperature (500oC to 800oC) for a suitable time length (generally ranging from 15 minutes to 1 hour) [8]. The silica content (SiO<sub>2</sub>) of RHA is ranging between 90 to 95%, which is similar to that of silica fume [6]. The typical chemical composition of RHA is given in Table 2.13.

Table 2.13 Typical chemical composition of rice husk ash [79]

Chemical Name	Composition
Silicon dioxide (SiO <sub>2</sub> )	94.37
Aluminum oxide (Al <sub>2</sub> O <sub>3</sub> )	0.06
Ferric oxide (Fe <sub>2</sub> O <sub>3</sub> )	0.04
Magnesium oxide (MgO)	0.13
Sodium oxide (Na <sub>2</sub> O)	0.08
Potassium oxide (K <sub>2</sub> O)	1.97
Phosphorus oxide (P <sub>2</sub> O <sub>5</sub> )	1.19
Titanium oxide (TiO <sub>2</sub> )	0.02
Sulfur trioxide (SO <sub>3</sub> )	0.01
Igneous loss	1.18

For RHA to be used as pozzolan in cement and concrete, it should satisfy requirements for chemical composition of pozzolans as per ASTM-C618 [84]. The combined proportion of silicon dioxide (SiO<sub>2</sub>), aluminium oxide (Al<sub>2</sub>O<sub>3</sub>) and iron oxide (Fe<sub>2</sub>O<sub>3</sub>) in the ash should be not be less than 70%, and LOI should not exceed 12% as stipulated in ASTM-C618 [84] requirement.

#### 2.3.3 Role of RHA in Concrete

The role of RHA in FC is the same as that in any other concretes. In concrete, the RHA mainly serves as a microfiller, pozzolan, and viscosity modifier. The RHA particles can fill the voids between the larger cement grains because of their smaller size, as shown in Figure 2.8. However, the micro filling ability of RHA is not as effective as silica fume. The typical median particle size of RHA is about 7 µm, while that of the cement and silica fume is 13 µm and 0.1 µm, respectively [85, 86].

Although RHA is not very fine in particle size, it behaves as a very reactive pozzolanic material because of its extreme surface area and high silica content [6]. In the presence of water, the RHA actively reacts with  $\text{Ca(OH)}_2$  liberated during cement hydration (pozzolanic reaction) and produces additional calcium silicate hydrate (C-S-H), as shown in Equation (2-11) and Equation (2-12).

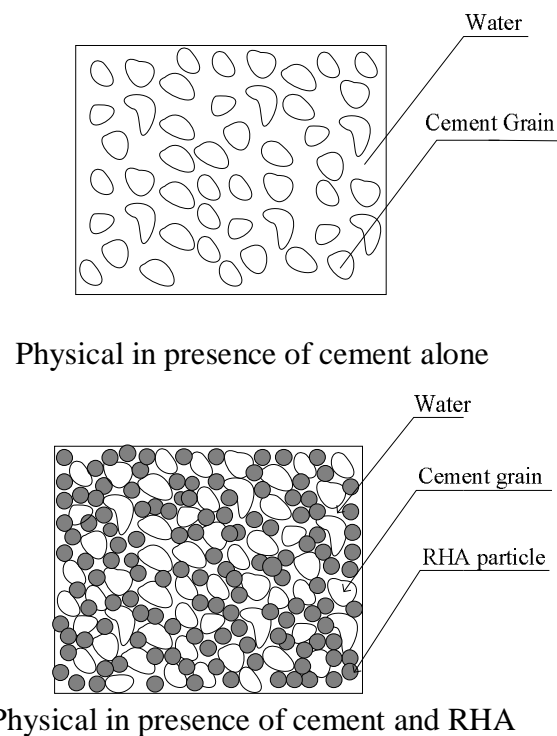
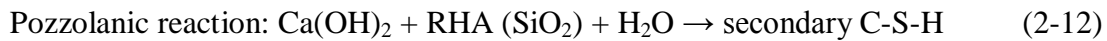
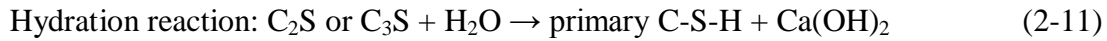


Figure 2.8 Micro-filling effect of RHA [87]

The pozzolanic reaction product fills the pores between hydrated cement grains and results in dense calcium silicate hydrate, as shown in Figure 2.9. Both micro-filling and pozzolanic effects of RHA play an important role to refine the pore structure in bulk paste matrix and interfacial transition zone of concrete. The pore refinement occurring due to the secondary reaction between RHA and  $\text{Ca(OH)}_2$  makes the microstructure of concrete denser and improves the interfacial bond between aggregates and binder paste. As a result, the strength, transport properties and durability of concrete are improved.



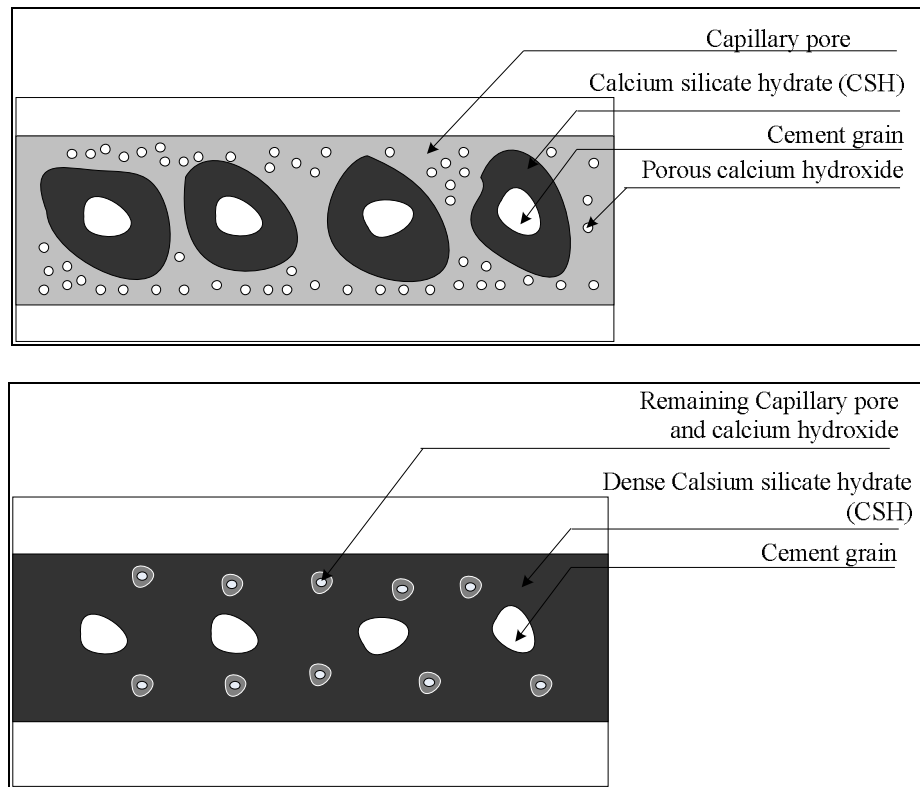


Figure 2.9 Pozzolanic effect of RHA [87]

Similar to silica fume, the RHA can also act as a viscosity modifier. Due to extreme surface fineness, it increases the water-retaining capacity, and thus enhances the viscosity of concrete mixture.

#### a. Hydration Mechanism of Paste by RHA

Clear understanding of RHA paste hydration is significant to explore its ability in improving the properties of cement paste, mortar and concrete. The first eight hours for hydration process in RHA+OPC paste is similar to the behavior of OPC paste with the growth of calcium hydroxide ( $\text{Ca}(\text{OH})_2$ ). Hwang and Chandra [8] mentioned that the penetration resistance during this period may be primarily due to the formation of  $\text{Ca}(\text{OH})_2$  crystals. The formation of  $\text{Ca}(\text{OH})_2$  at the surface of RHA may be due to its adsorption by cellular structure of RHA. In such case the bleeding water will significantly be reduced. The adsorbed water enhances the pozzolanic reaction inside the inner cellular spaces and the paste gains significant strength. After 40 hours, the pozzolanic reaction further binds Si in RHA with  $\text{Ca}(\text{OH})_2$  to form C-S-H gel and

solid structures (Figure 2.10). This means that RHA fills the finer pores and reduces the permeability, which is beneficial to the durability [8].

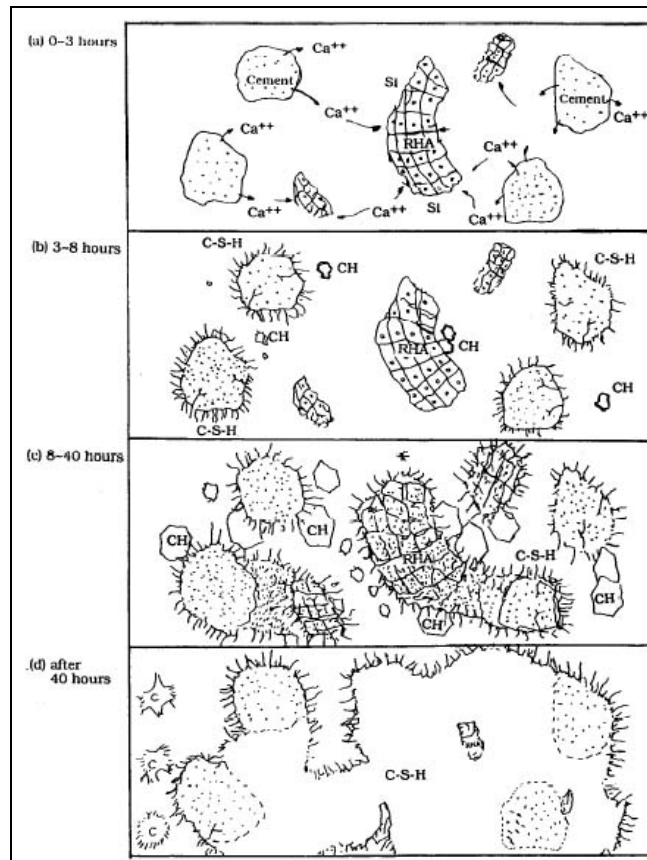


Figure 2.10 Schematic Drawing of the Hydration of Cement Paste with RHA [88]

### b. Modification of Micro-pores Structure

The addition of pozzolanic materials affects both strength and permeability of concrete by strengthening the aggregate-cement paste through pozzolanic reaction. This phenomenon is shown in Figure 2.11. It is drawn that the pozzolanic reaction modifies the micro pores structure. The products formed due to the pozzolanic reactions occupy the empty spaces in concrete which thus become densified. The porosity of cement paste is then reduced, and subsequently the pores are refined. Mehta [6] has shown significant reduction in the porosity of cement paste with RHA additions and refinement in the pore structure. Pozzolanic reaction is a slow process and proceeds with time [8].

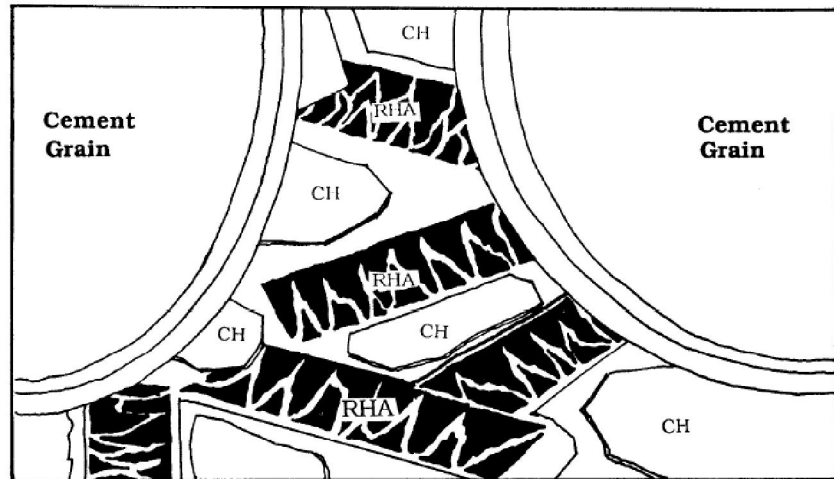


Figure 2.11 Mechanism of void filling and transition zone strengthening effect of RHA [8]

### c. Use in Lightweight Concrete

High strength lightweight concretes with compressive strength values up to 61 N/mm<sup>2</sup> at 90 days and a dry density lower than 1750 kg /cm<sup>3</sup> can be made using expanded clay lightweight aggregate, rice husk ash and superplasticizer in the mixture. These mixtures have high workability and no segregation [89].

The use of RHA in concrete was accelerated after Mehta's findings in 1973 [6]. Rice husk ash has the potential for making light weight aggregate [90] with low bulk density of 0.20–0.40 g/cm<sup>3</sup>. The properties of LWA concrete are improved with the increased fineness of RHA. The RHAs with 12% and 5% retained on sieve No. 325 give better LWA concrete than the as-received RHA. However, the use of RHA to produce foamed concrete has not been reported.

### 2.3.4 Characteristic of RHA by X-Ray Diffraction (XRD) and by X-Ray Fluorescence (XRF)

Routine XRD-mineralogy profiles can provide qualitative and semi quantitative records of shifts in the source of sedimentary components to a sequence. XRD mainly displays information on autochthonous and authigenic minerals, but can give some indication of the abundance of amorphous silica phases. Set up with routine data

collection, XRD is a rapid, accurate technique which can process 40 samples per day using an automated sample changer [91].

Each mineral is defined by a crystal lattice with characteristic diffraction properties resolved by x-rays. The Angstrom d-spacing of certain crystallographic lattice directions show up as relative peak (area) heights on the diffractogram (usually in mm) in a fixed relationship to the  $2\theta$  (two-theta) angle of the scintillator counter as defined by Bragg's law of diffraction [91]. Using calibrated peak area intensities of the major peak, the proportion of mineral species in a profile can be given with about + 5% at least for minerals which constitute more than 5% of the bulk sample. Generally, corundum is used as the reference mineral for intensity and for d-spacing [91].

Figure 2.12 shows that based on Bragg's law,  $n\lambda = 2d\sin\theta$ , by controlling the wavelength with vary and continuously measure the incident angle, it will leave only the lattice plane spacing as variable. So whenever a constructive interference is observed, at that point a fundamental spacing parameter for the mineral of interest can be calculated [92].

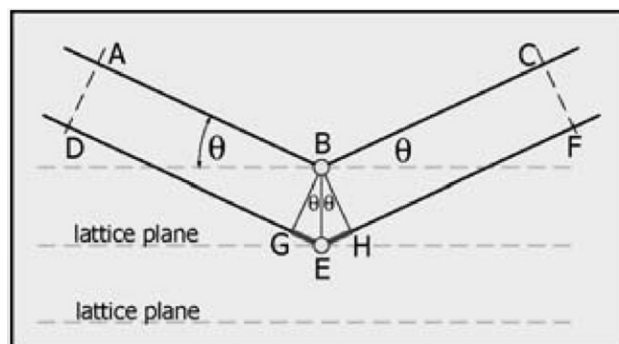


Figure 2.12 Geometry of X-Ray Reflection [87]

The amorphousness degree of material samples can be judged by the intensity or average height of the diffused band between  $15^\circ$  and  $26^\circ$  values of  $2\theta$ , using x-rays generated from a copper target and nickel filter [93]. Figure 2.13 shows the XRD result obtained from various samples of RHA. RHA A and RHA B show the amorphous characteristic of samples, whereas the maximal value of quartz could be recorded in the other samples. The presence of quartz shown by the XRD of RHA C

was probably due to the longer duration burning or could also be attributed to the contamination of sand particles from the pit of burning location [94].

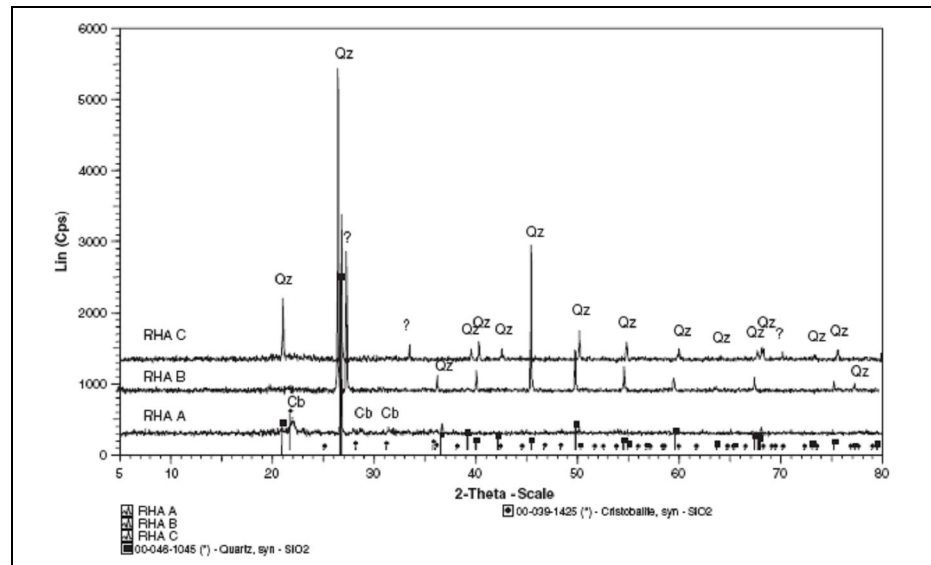


Figure 2.13 XRD Graphs from Various Samples of RHA [94]

X-Ray Fluorescence (XRF) is named as the process of emissions of characteristic x-rays. When a primary x-ray excitation source from an x-ray tube or a radioactive source strikes a sample, the x-ray can either be absorbed by the atom or scattered through the material. The process in which an x-ray is absorbed by the atom by transferring all of its energy to an innermost electron is called the "photoelectric effect." During this process, if the primary x-ray had sufficient energy, electrons are ejected from the inner shells, creating vacancies. These vacancies present an unstable condition for the atom. As the atom returns to its stable condition, electrons from the outer shells are transferred to the inner shells and in the process it gives off a characteristic x-ray whose energy is the difference between the two binding energies of the corresponding shells. Because each element has a unique set of energy levels, each element produces x-rays at a unique set of energies, allowing one to non-destructively measure the elemental composition of a sample. Analysis using x-ray fluorescence is called "X-ray Fluorescence Spectroscopy"[94].

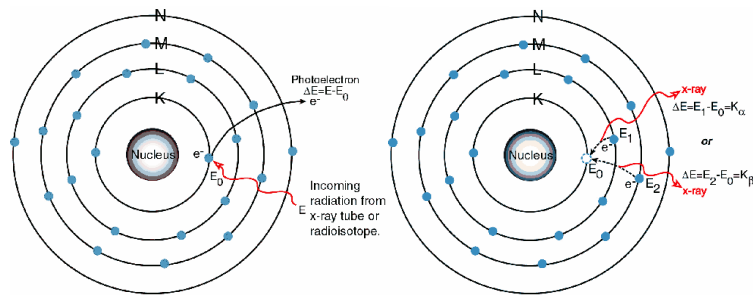


Figure 2.14 X-Ray Fluorescence Process [95]

Figure 2.14 reveals that when a radiation from x-ray tube or radioisotope coming, an electron in the K shell is ejected from the atom by an external primary excitation x-ray, creating a vacancy. An electron from the L or M shell fills the vacancy with movement like "jumps in". In the process, it radiates a characteristic x-ray unique to this element and in turn, produces a vacancy in the L or M shell. This process allows a measurement of elemental composition of a sample [95]. Table 2.10 shows the XRF analysis result of RHA with different burning temperature. From, it can be identified that the increment of burning temperature has an effect on to the amount of silica produced from rice husk. XRF analysis indicates that at lower burning temperature, the amount of  $\text{SiO}_2$  produced is smaller in amount compare to the higher temperature. However, as it has been described before, burning RHA with high temperature for a long period will result in a crystalline state of RHA.

### 2.3.5 The Influence of RHA on Micro Properties

RHA is an active Pozolan that will react with calcium hydroxide to form Calcium silicate hydrate (CSH). CSH products will give effect to micro properties in concrete. Effects of micro properties described as follows:

#### a. Porosity Properties

Figure 2.15 is evident that RHA decreases in the total porosity is caused the change occurring in the pore size distribution as a result of using RHA which could react with the calcium hydroxide to form C-S-H gel [96]. The other side, the effect of pozzolanicity of RHA has intensification mechanism on concrete confirmed that the average pore size of concrete incorporating RHA is decreased compared to that of

control concrete [96]. However, the percentage level of RHA more than 30% shown porosity increase due to more absorption water from pore structure of RHA and to make disordered void distribution enhancing porosity system.

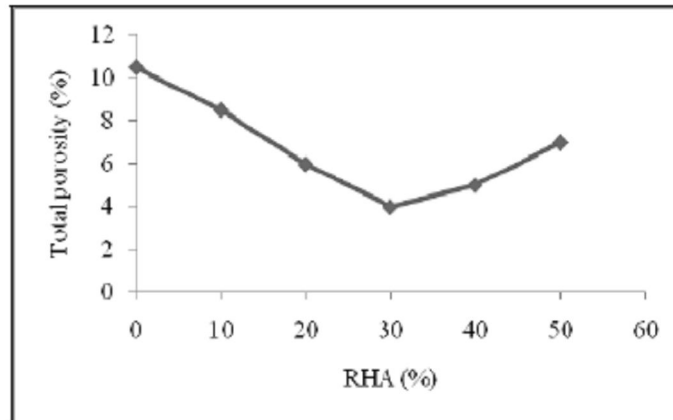


Figure 2.15 Pore analysis of cement paste incorporating RHA [96].

### b. Autogenous Shrinkage

GR de Sensale' study shows that with low water binder ratio RHA has significantly reduced autogenous deformation. The evident of this phenomenon is depicted in Figure 2.16

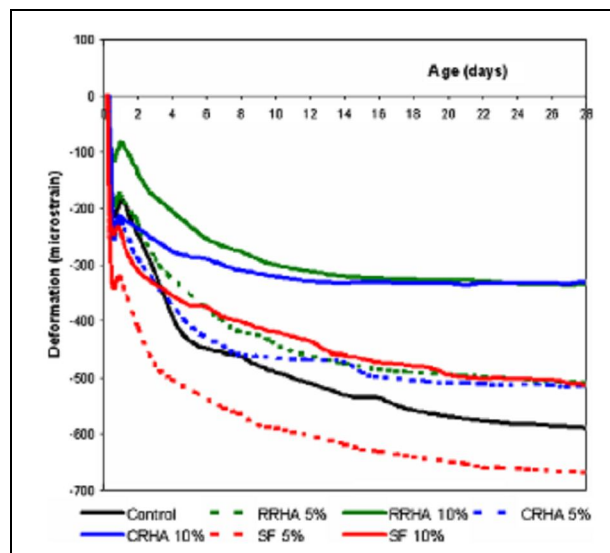


Figure 2.16 Autogenous deformation versus age of all pastes [97].

### c. Non-Evaporable Water

Determining the effect of RHA on non-evaporable water is a difficult task, since interpretation of non-evaporable water measurement result is complex. The information on the effect of RHA on non evaporable water is limited. Figure 2.17 should show that the incorporation of 10% RHA reduced the amount of non-evaporable water [80].

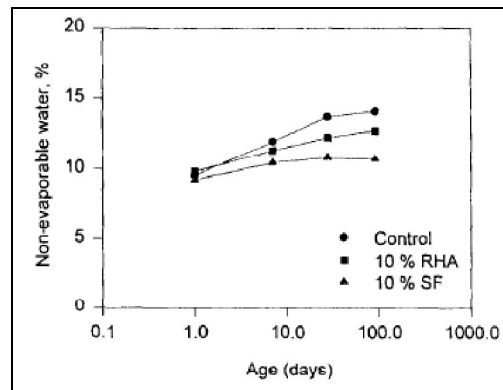


Figure 2.17 Non-evaporable water content in paste [80].

### d. Calcium Hydroxide

The RHA pozzolanic reaction is similar with all pozzolanic materials, in those pozzolanic materials the siliceous components in the RHA react with calcium hydroxide from the cement hydration to form calcium silicate hydrates. As a reference [98, 99], addition of RHA perhaps can be recognized to form C-S-H gel due to the reaction which occurs between RHA and  $\text{Ca}^{2+}$ ,  $\text{OH}^-$  ion or  $\text{Ca}(\text{OH})_2$  in hydrating cement. The decreasing of  $\text{Ca}(\text{OH})_2$  that is caused by increasing RHA level can be seen in Figure 2.18.



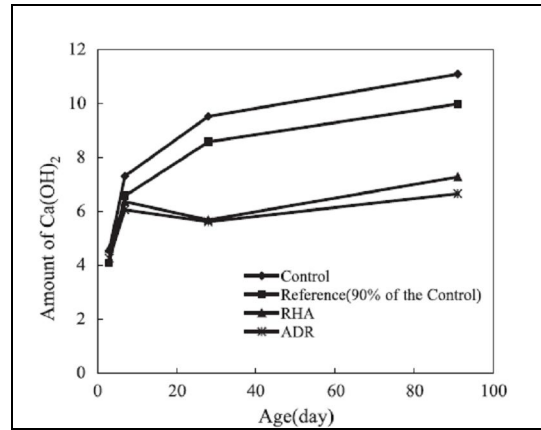


Figure 2.18 Amount of Ca(OH)<sub>2</sub> in hardened cement pastes [100]

## 2.4 Chemically Bound Water

The hardening process in concrete is caused by chemical reaction taking place in the cement part of the mixture. The cumulative of these reactions is highly related to the non-evaporable water content in the reaction product, and determines hardened properties of the concrete mixture. Structural lightweight FC often contain cementitious material in addition to OPC that enhances strength and durability. These cementitious materials can transform the rate of reaction and thus the development of mechanical properties.

This section provides a general overview and discussion of water contained FC, which is essentially cement-based material. The first main section provides a brief introduction to cement hydration, focusing on the structure of the hydrated products. The next section discusses the location of the water within these hydrated products and defines some commonly used terms for the different states of water in cement and FC.

### 2.4.1 Cement Hydration Reactions

Portland cement is an anhydrous mixture of oxides combined to form four primary compounds: tricalcium silicate ( $C_3S$ ), dicalcium silicate ( $C_2S$ ), tricalcium aluminate ( $C_3A$ ) and tetracalcium aluminoferrite ( $C_4AF$ ).

The general forms of the reactions are shown in Equation ((2-13) through (2-16) [30].



The main products of the hydration process are the calcium silicate hydrate (C-S-H) and calcium hydroxide ( $Ca(OH)_2$ ).

### 2.4.2 State of Water in Concrete

In conjunction with their original model of the structure of hardened cement paste, Powers and Brownyard [101] also proposed a classification system for the location of the water within the paste. Overall, they divided the water into three main categories; the chemically bound water, water bound by surface forces, and capillary water. The chemically bound water describes that water which has been chemically combined in the cement hydrates. In other words, the water is combined with one or more of the cement compounds to form an entirely new solid product. This water can be bound in hydroxides, held by covalent bonds, or bound by hydrogen bonds. The water bound by surface forces is that which is adsorbed onto the surfaces of the hydrates and held by Van der Waal's forces. The capillary pore network center as described by Powers and Brownyard [101] is the type of water that is in the space beyond the range of surface-forces of the solids [101].

For the purpose of clarity, the remainder of this thesis will adopt the three part water system described above. The term “capillary water” will encompass that water in both the micro and mega-capillary pores. An alternate phrasing for capillary water is “free water.” The terms “gel water” or adsorbed water” will be used as general terms to describe any water in/adsorbed to the gel, including the water within the interlayer spaces and that adsorbed on the surfaces of the gel layers. If further distinction is necessary, the two subtypes of adsorbed water will be referred to as “interlayer water” and “surface adsorbed water.” The phrase “chemically bound water” will imply the water that has participated in the hydration reaction and is chemically bound within the hydrates. Chemically bound water may also be referred to as “bound water or “chemically combined water”. A summary of these distinctions is presented in Figure 2.19.

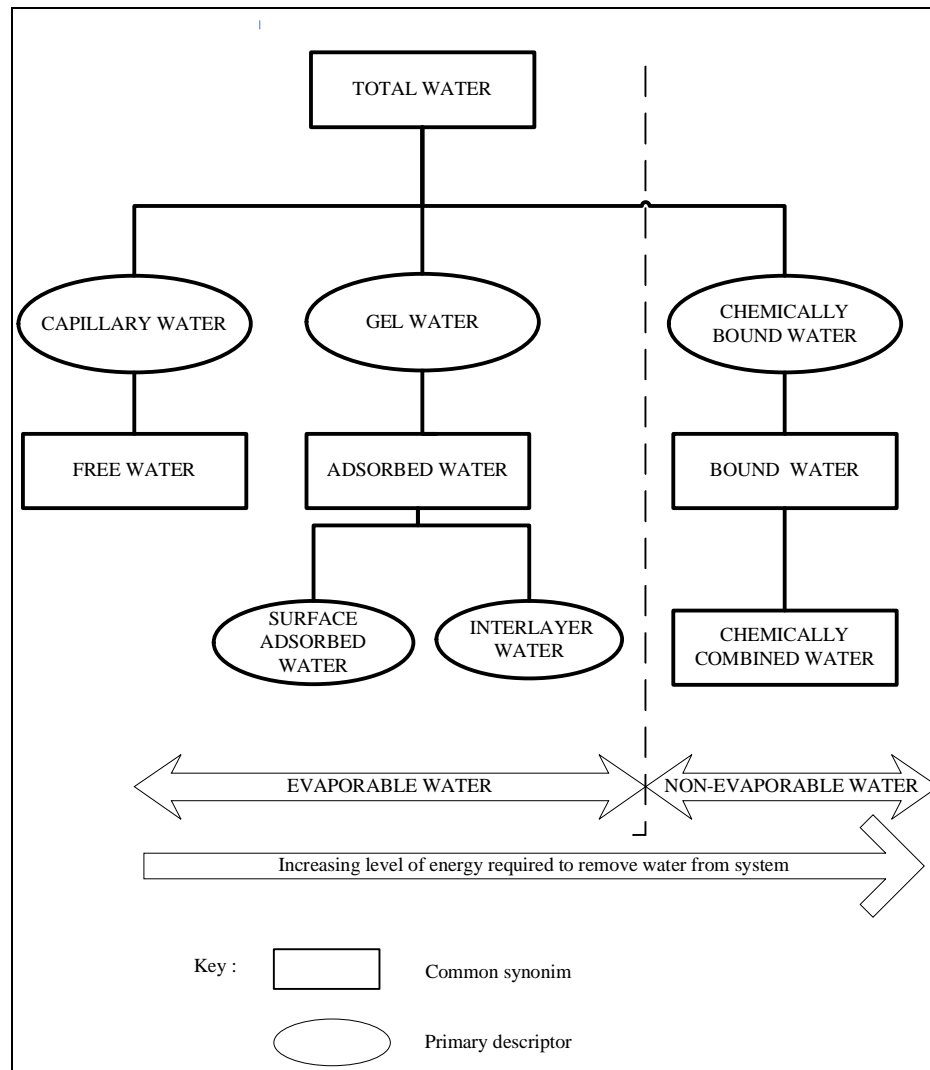


Figure 2.19 The Charts of Terminology for state of water [102]

### 2.4.3 Measurement of Water

The quantification of water is useful and relevant in the study of cement based materials. Since there are many different ways to calculate the water contents and numerous details requiring mention, this entire chapter is dedicated to describe methods to measure water in cement-based material.

#### a. Drying/Ignition Methods

The most common methods of establishing water contents in cement-based materials are based on drying followed by ignition. These methods first remove the targeted water type and then weight the mass loss upon removal of the balance. There are three methods to conduct the drying methods namely: P-Drying, D- Drying and Oven Drying. Each method has specific procedure, drying time, ignition temperature and time.

The term P-Drying is a shorthand notation for the drying method using magnesium perchlorate as desiccant, and to determine both evaporable water and non-evaporable water contents. The first researchers to explore this method were Power and Brownyard [102] in 1948. According to their procedure, a sample of cement paste is dried to constant mass at 23°C in vacuum desiccator with anhydrous perchlorate. The water removed during this process is identified as the evaporable water. To calculate the non-evaporable water content, the remaining material is heated, in one gram portions, at 1000°C for 15 minutes. The sample is then cooled before being weighed, and then heated again for five minutes to ensure the completeness of the ignition. The loss of mass during the ignition process is defined as the non-evaporable water content in material.

Copeland and Hayes [103] in 1953 continued the development method for determining evaporable and non evaporable water content, and thus subtly changed the definitions of the water classifications. “D-drying” is basically incorporating dry ice in the procedure. In accordance with Copeland and Hayes, [103] cement paste samples should be prepared for D-Drying in a CO<sub>2</sub>- free cabinet. The samples are therefore dried in air that is in equilibrium with ice at -79°C for five to-seven days or

until the mass loss is less than one mg per gram of sample in day. The mass loss until equilibrium is considered equal the evaporable water. The dried samples are then ignited in 1050°C furnace for 30 minutes, weighed, placed back in the furnace for 10 minutes and then weighed again. If the two ignited masses are equal the ignition process than it is considered completed. If not, the sample is reignited a third time.

Oven drying is used by Giertz-Hedtrsoom [102] in 1931 (as Cited in Danielsoon, 1974) [102]. In the oven drying procedure, the samples were placed in an oven in 100 to 110°C for duration of 3 to 20 hours and allowed to reach constant mass. After drying, they were weighed ignited in 1050°C furnace for one to two hours, cooled for an hour, and then weighed again.

The procedure of the various drying/ignition methods, as performed by different researches, is summarized in Table 2.14.

Table 2.14 Summary of Drying/Ignition Procedures to quantify  $w_n$  [102]

Source	Procedure	Drying Time	Ignition Temp, °C	Ignition Time	Comments
Powers et al	P-Drying	Constant mass	1000	20 mins	-5 gram sample size
Copeland et al)	D-Drying	5-7 days	1050	30 mins+10 check	- 5 to 6 gram sample size - CO <sub>2</sub> free drying
Helmuth et al	D-Drying	Constant mass	N/A	N/A	- dried slab samples - ignited 1 gram samples
Locher	D-Drying	N/A	1000	N/A	
Mills	Oven, 100°C	N/A	1000	N/A	70 gram samples
Danielson	Oven, 105°C	3+days to constant	1050	1 hour	- self-contained apparatus - 100L/hr air stream in oven
Taylor	Oven, 105°C	N/A	1100	N/A	- equilibrated over L <sub>i</sub> C <sub>i</sub> first - ignition in N <sub>2</sub>
Kjellsen	Oven, 105°C	20+hours	1000	1.25 hours	15 gram sample
Snyder et al	Oven, 110°C	overnight	950	3+hours	- methanol flushed sample
Pinto et al	Oven, 105°C	12+hours	1050	2+hours	- methanol flushed sample
Hobb	Oven, 105°C	12+hours	1050	3+hours	- 10 gram sample and methanol flushed sample

(An “N/A” entry in table means that the value was unreported)

For additional information, deservedly before the mix sample was investigated, the losses on ignition (LOIs) of the component materials (i.e. cement, fine aggregate, MIRHA) should be provided. Figure 2.20 shows a schematic illustration of the measurements from the OD/FI procedure.

In all cases, the average LOI of each component material (designated  $L_x$ , where the subscript  $x$  refers to the type of material) was calculated by averaging the individual LOIs of at least six separate samples of that material. Equation (2-17) shows the calculation for the average LOI of cement. (The LOIs for the other materials are calculated in the same manner, but with different lettered subscripts).

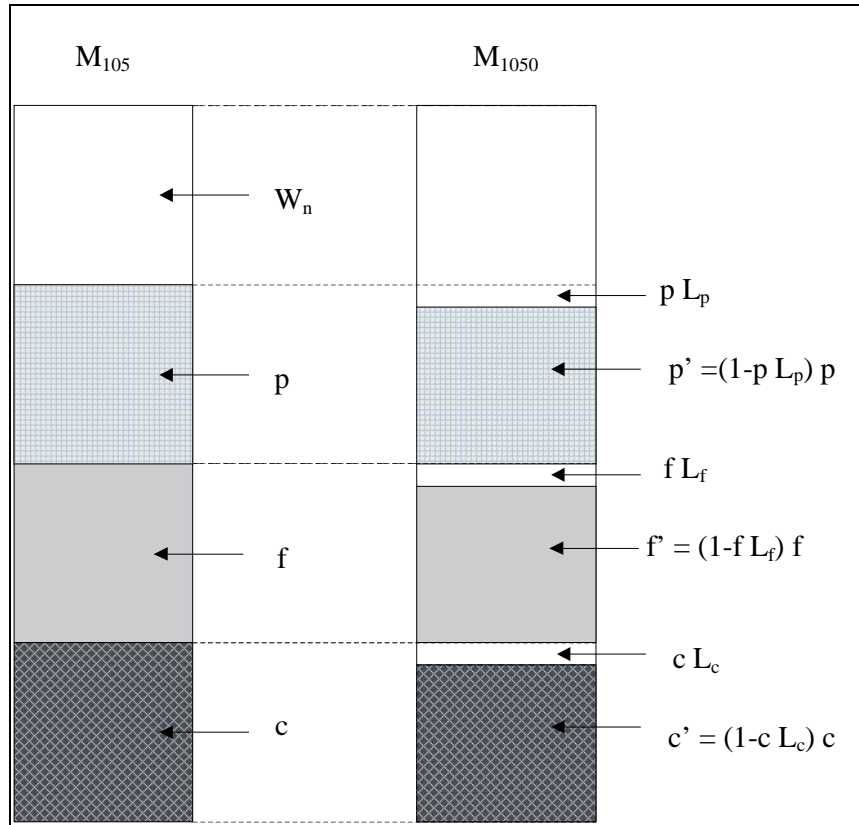
$$L_c = \sum_{i=1}^6 l_{c,i} = \sum_{i=1}^6 \frac{m_{c,105,i} - m_{c,1050,i}}{m_{c,105,i}} \quad (2-17)$$

Where

- $L_c$  = average LOI of cement
- $l_{c,i}$  = LOI of the  $i$ th cement sample
- $m_{c,105,i}$  = mass of the  $i$ th cement sample after oven drying
- $m_{c,1050,i}$  = mass of the  $i$ th cement sample after furnace ignition

The equation (as derived below) combined the data from the OD/FI procedure (i.e. the sample masses after drying and after ignition, and the LOIs of the component materials) with the aforementioned assumptions to yield a value for non evaporable water content.

As dictated by the OD/FI procedure, the sample is weight after the oven drying stage and after the furnace ignition stage. The result of FC measurements are shown schematically in Figure 2.20.



Where:

- $w_n$  = non-evaporable water content
- $p$  = initial pozzolan
- $f$  = initial fine aggregate
- $c$  = initial cement content
- $L_p$  = LOI of pozzolan
- $L_f$  = LOI of fine aggregate
- $L_c$  = LOI of cement

Figure 2.20 Schematic results from the OD/FI Procedure for Mortar with Pozzolanic [102]

Figure 2.20 can be represented in equation form as follows:

$$M_{105} = w_n + p + f + c \quad (2-18)$$

$$M_{1050} = p(1-L_p) + f(1-L_f) + c(1-L_c) \quad (2-19)$$

The division of equation (2-18) by equation (2-19) yields

$$\frac{m_{105}}{m_{1050}} = \frac{w_n + p + f + c}{p(1-L_p) + f(1-L_f) + c(1-L_c)} \quad (2-20)$$

which can be written in terms of  $w_n$  as

$$w_n = \left( \frac{m_{105}}{m_{1050}} \right) \left[ p(1-L_p) + f(1-L_f) + c(1-L_c) \right] - p - f - c \quad (2-21)$$

If equation (2-21) is then normalized by  $c$ , the result is

$$\frac{w_n}{c} = \left( \frac{m_{105}}{m_{1050}} \right) \left[ \left( \frac{p}{c} \right) (1-L_p) + \left( \frac{f}{c} \right) (1-L_f) + (1-L_c) \right] - \left( \frac{p}{c} \right) - \left( \frac{f}{c} \right) - 1 \quad (2-22)$$

This can also be written as

$$\frac{w_n}{c} = \left( \frac{m_{105}}{m_{1050}} \right) \left[ h(1-L_p) + g(1-L_f) + (1-L_c) \right] - h - g - 1 \quad (2-23)$$

Where

- $g = f/c$
- $h = p/c$

The corresponding equation for a FC mortar with pozzolanic materials is thus:

$$\frac{w_n}{c} = \left( \frac{m_{105}}{m_{1050}} \right) \left[ h(1-L_p) + (1-L_f) + (1-L_c) \right] - h - 1 \quad (2-24)$$

## b. Thermogravimetry methods (TGA)

Thermogravimetry method is another common method for calculating water content in cement-based material which has similar in concept to the drying/ignition methods presented TGA basically, in that removes water from the samples via heating. The difference of TGA with Drying method that the TGA continuous procedure, recording mass loss throughout the heating cycle rather than just at the end points of drying and ignition. The gain of the TGA method is that it accomplishes in a controlled environment (and not necessarily in air) to minimize carbonation, and it yields continuous mass change data. The main disadvantage of TGA is that it can only be



done on a very small sample size (approximately 5-10 mg), which may not necessary be representative of larger masses of the material. As a result, TGA is nearly always performed on cement paste or even just cement components, rather than on mortar or concrete.

## 1. TGA/DTG

Following the basic procedure, a small sample (on the order of mg size) is placed on a balance, and the balance is zeroed. The sample is then heated, most commonly at a linier rate less than 20°C/min, to the temperatures of 800-1000°C. During the heating process, the mass loss of the sample is recorded a set number of times each second or minute, to yield a (nearly) continuous mass loss curve (call the TG curve). These result are often expressed as a percentage of the mass of the original sample and it is a function of temperature. In addition, the mass loss results are often supplemented by differential mass loss data (known as DTG, for differential thermogravimetry) that more clearly depict the peaks of mass loss at specific temperatures. An example of the TG and DTG curves obtained from a hydrated is shown in Figure 2.21.

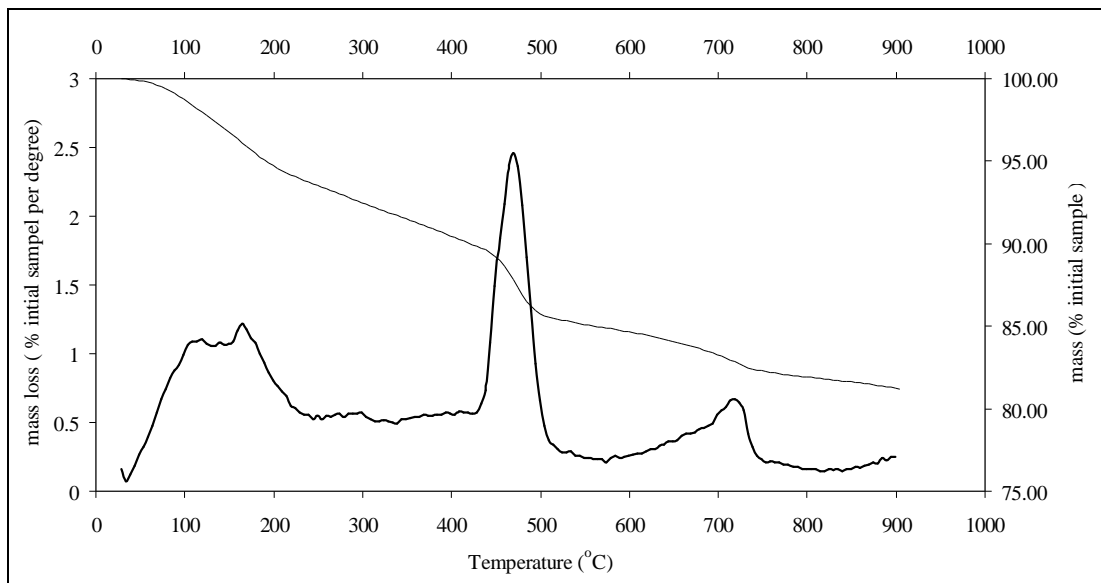


Figure 2.21 TG and DTG for a hydrated cement paste [71]

Table 2.15 lists a summary of TGA procedural parameters discussed above in this section. As before, a “N/A” entry in table means that the value was unreported.

Table 2.15 Summary of TGA Experimental Variables [102]

Source	Sample size (mg)	Start Temperature (°C)	Rate (°C/min)	End Temperature (°C)	Comments
El-Jazairi et al (1977, 1980)	N/A	21	15 (+30 min isothermis)	1007	First dried in 105°C oven
Halse et al (1984)	N/A	21	N/A	800	Heating in N <sub>2</sub>
Parrot et al (1984)	20	105	2	750 or 950	First dried in 33% RH Heating in N <sub>2</sub>
Feldman (1983)	20	100	20	1000	
Taylor (1985)	45	N/A	10	N/A	Heating in N <sub>2</sub>
Wei et al (1985)	N/A	100	10	950	First dried in 38°C oven
Berry et al (1989)	N/A	N/A	10	1000	First acetone ground, then dried ton constant mass at 60°C Everything in N <sub>2</sub>

(An “N/A” entry in table means that the value was unreported)

## 2. Temperature ranges for water removal

One the significant advantage of TGA procedure is that it enables continuous mass change measurements during heating. Since the various classifications of water are removed over different temperature ranges, TGA data can be used to classify and quantify the water in a hydrated sample. This section discusses some of water classifications and the temperatures ranges over which the water is considered to be removed. Differences in measurement technique may contribute to discrepancies the results found by different researchers.

### Evaporable water

Evaporable water is universally considered to be removed at temperature up to about 105°C [104]. As a result, most oven/furnace procedures conduct the drying stage in an oven at 100-105°C, so as to remove all the evaporable water.

### C-S-H bound water

The temperature range for the removal of C-S-H chemically bound water is highly questionable. In general, the majority of the C-S-H water is considered to have been about 100 and 400°C, but what happens after 400°C has not yet been resolved. The reported temperature ranges for C-S-H bound water removal is shown in Table 2.16.

Table 2.16 Reported temperature ranges for C-S-H bound water removal

Researcher (s)	Temperature range (°C)	Loss mass in temperature range (%)
El-Jazairi and Illston (1977)	105 and 398	N/A
Parrot, Patel, and Killoh (1984)	100 and 400	N/A
Smith (1994)	< 800°C, C-S-H water was removed gradually and was not complete until 800°C	N/A
Taylor (1997)	100 and 400°C, C-S-H water was removed gradually and was not complete until 900°C	80%

### CH bound water

The temperature range for the removal of CH bound water is far less controversial than that of the C-S-H bound water. Indeed, as is clear in Table 2.17. The results reported by different researchers are fairly comparable. The temperature range of CH bound water is much narrower than C-S-H water removal. In TGA data, this CH bound water loss is evident as a sharp drop in TG curve, starting after about 400°C. Such behavior is apparent in Figure 2.21.

Table 2.17 Reported Temperature ranges for CH bound waster removal [102]

Researcher (s)	Temperature range (°C)
El-Jazairi and Illston (1977)	440-580
Parrot, Patel, and Killoh (1984)	425
Wei, Grutzek, Roy (1985)	450-510
Taylor (1985)	425-500
Smith (1994)	> 400
Taylor (1997)	375- 500

## Calcium carbonate

When CO<sub>2</sub> dissolves in the pore water of hardened cement paste, the CO<sub>2</sub> will react with the CH to form calcium carbonate (CaCO<sub>3</sub>). Another mass loss evident in TGA data is result decomposition of calcium carbonate, and thus not of water removal at all. The reported temperature range for decomposition is shown in Table 2.18.

Table 2.18 Reported temperature ranges for decomposition [102]

Researcher (s)	Temperature range (°C)
El-Jazairi and Illston (1977)	580-1007
Taylor (1985)	650-750

## AFm bound water

AFm is the usual shorthand notation for hydrated aluminate, ferrite and monosulfate phase. As such, the AFm phases contain bound water, which is removed during the TGA heating process.

## Quantitative Analysis of Calcium Hydroxide Content Using TG results

The total amount of Ca(OH)<sub>2</sub> in the test specimen should be corrected [71, 105] due to the fact that the CO<sub>2</sub> reacts with the Ca(OH)<sub>2</sub> to form calcium carbonate (CaCO<sub>3</sub>) as follows:

$$\text{Ca(OH)}_2 = \left(\frac{74}{18}\right)(A) + \left(\frac{74}{44}\right)(B) \quad (2-25)$$

Where:

- A = Area under the DTG curve corresponding the total mass lost due to the dehydroxylation
- B = Area under the DTG curve total mass lost due the decarbonation reaction

The ratio (74/18) and (74/44) are the molar mass ratio CH to H<sub>2</sub>O and CH to CO<sub>2</sub> (decarbonation).

### Correction for Calcium Hydroxide Content in OPC/MIRHA Mixes

CH content replaced by pozzolanic could be lower because of lower cement content or the pozzolanic reaction that consumes CH of the enhancement in cement hydration in the presence of pozzolanic material. Hence, in this study, a normalized CH content (CH<sub>norm</sub>) is used, which defined below.

$$CH_{\text{normal}(t)} = \frac{CH_{(t)}}{CH_{\text{pure}(t)} \cdot m_c} \quad (2-26)$$

Where:

- CH<sub>pure(t)</sub> = the CH content of the pure pastes at any time (t)
- CH(t) = the CH measurement combining pozzolanic material
- m<sub>c</sub> = the mass fraction of the cement in the binder.

Neithalath's study [105] showed that comparing with pozzolanic material the CH<sub>normal</sub> values for the pastes with VCAS and SF. It can be seen in Figure 2.22.

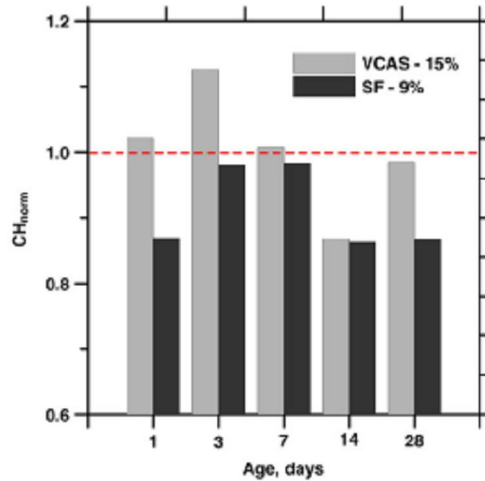


Figure 2.22 CH normal values of VCAS ad SF [105]

The degree of hydration (CH) is then calculated as follows:

$$\alpha_{\text{CH}} = \left[ \frac{\text{Ca(OH)}_{2(i)}}{\text{Ca(OH)}_{2(\text{FH})}} \right] * 100 \quad (2-27)$$

Where :

- i = Hydration at age (i)
- FH = Full Hydration

#### 2.4.4 Change in Non-Evaporable Water Content Due to the Presence of A Cement Replacement Material (CRM)

The definition of change in non-evaporable water content is an effect of adding cement replacement material (CRM) that causing non-evaporable water ( $w_n$ ) to increases or decreases because the special reaction of CRM. Determining the change in non-evaporable water content due to the addition of a cement replacement material is not easy to experimentally because associating of water with the reaction of the replacement material is complicated to separate from that of cement hydration.

In this section, a simple model is presented Nathan [106] to isolate the change in  $w_n$  due to the addition of a cement replacement material. The total non-evaporable water  $(w_n)_T$  of a cement paste incorporating cement replacement materials can be showed as:

$$(w_n)_T = (w_n)_c m_c + (w_n)_r m_r \quad (2-28)$$

Where  $(w_n)_c$  and  $(w_n)_r$  are the non evaporable water contents of the cement and replacement material respectively, and  $m_c$  and  $m_r$ , are their mass fraction. If the replacement material is purely a filler, then  $(w_n)_r=0$ . A cement replacement material in a paste system might make possible an enhancement in the hydration of the available cement grains in addition to its own hydration. According to a case, the non-evaporable water content of the cement can be explained as:

$$(w_n)_c = (w_n)_{c-0} + (w_n)_{c-r} \quad (2-29)$$

Where  $(w_n)_{c-0}$  is the non evaporable water content of a cement paste with no CRM and  $(w_n)_{c-r}$  is the non evaporable water content as result of the improvement in cement hydration due to the presence of the replacement material. If the equation  $(w_n)_c = (w_n)_{c-0}$ , when there is no replacement material present in the system. Substitution Equation (2-29) to Equation (2-28) can be stated as:

$$(w_n)_T = [(w_n)_{c-0} + (w_n)_{c-r}] m_c + (w_n)_r m_r \quad (2-30)$$

The above equation can be restated as:

$$(w_n)_T - (w_n)_{c-0} m_c = (w_n)_{c-r} m_c + (w_n)_r m_r \quad (2-31)$$

The right hand side of Eq. (2-29) gives an term for the change in non-evaporable water content in a modified paste  $(\Delta w_n)_r$  as a result of the hydration of the cement replacement material and the enhancement in hydration of the cement grains resulting from the presence of the replacement material.

$$(\Delta w_n)_r = (w_n)_{c-r} m_c + (w_n)_r m_r \quad (2-32)$$

$(\Delta w_n)_r$  provides an indication of the combined effects of enhancement in cement hydration due to increased effective w/c in a paste modified with a filler, and the secondary hydration in a paste modified with a pozzolanic material. Since all the terms in the left hand side of Eq. (2-31) are known, determination of  $(\Delta w_n)_r$  is straightforward. For a plain paste,  $(\Delta w_n)_r$  will always be zero. It should be noted here that  $(\Delta w_n)_r$  does not separate the individual effects of enhancement in hydration and secondary reaction.

#### 2.4.5 The Model of the Degree of Hydration of Pastes with More Than One Cementing Material

In pastes including one or more cement replacement materials; calculation of cement hydration and the replacement material reaction is made more complex by the same reason that was given in an earlier section that it is difficult to separate the chemically combined water contents fixed with both the reactions.

Nathan's work [106] has proposed the modeling of the degrees of hydration of cement and the replacement material. Using an equation of the form similar to Eq. (2-28) for the combined degree of hydration of the paste ( $\alpha_T$ ) incorporating the replacement material.

$$(\alpha)_T = \alpha_c m_c + \alpha_r m_r \quad (2-33)$$

Where,  $\alpha_c$  and  $\alpha_r$  are the degrees of hydration of the cement and the replacement material respectively. The degree of hydration of the non-evaporable water contents is presented as results in Eq. (2-33). It can be stated as:

$$\alpha_T = \left[ \frac{(w_n)_c}{(w_n)_{c-y}} \right] m_c + \left[ \frac{(w_n)_r}{(w_n)_{r-y}} \right] m_r \quad (2-34)$$

Where

$$\alpha_T = \left[ \frac{(w_n)_T}{(w_n)_{T-\infty}} \right] \quad (2-35)$$

$(w_n)_{T-\infty}$ ,  $(w_n)_{c-\infty}$ , and  $(w_n)_{r-\infty}$  are the ultimate non-evaporable water contents (at complete hydration) of the mixture, plain cement, and the replacement material respectively. Substituting Eq. (2-29) in Eq. (2-34) gives:

$$\alpha_T = \left[ \frac{(w_n)_{c-0} + (w_n)_{c-r}}{(w_n)_{c-\infty}} \right] m_c + \left[ \frac{(w_n)_r}{(w_n)_{r-\infty}} \right] m_r \quad (2-36)$$

From Eq. (2-31),  $(w_n)_{c-r}$  can be expressed as:

$$(w_n)_{c-r} = \frac{(w_n)_r}{m_c} - (w_n)_{c-0} - (w_n)_r \frac{m_r}{m_c} \quad (2-37)$$

Substituting Eq. (2-37) in Eq. (2-36) and rearranging the terms give  $\alpha_T$  as:

$$\alpha_T = \frac{(w_n)_T}{(w_n)_{c-\infty}} + (w_n)_r m_r \left[ \frac{1}{(w_n)_{r-\infty}} - \frac{1}{(w_n)_{c-\infty}} \right] \quad (2-38)$$

The above term is a summarizing means of representing the combined degree of hydration of pastes containing cement replacement materials. This equation accounts for the development in the degree of hydration, which may be the result of a higher effective w/c when non-reactive fillers are used, and the degree of hydration of the supplementary cementing material. This expression could be customized to account for more than one cement replacement material.

## 2.5 Taguchi Method

Taguchi method is a statistical method developed by Genichi Taguchi during the 1950s [107] as an optimization process technique. The parameter design in Taguchi's method design provides the design engineer with a systematic and efficient method for determining near optimum design parameters for performance and cost.



### 2.5.1 Benefit

There are number technical advantages of Taguchi method to help as design experimental i.e.: Reducing the number of experiment; Exploring the degree of influence of each factor and the optimum setting condition; its extra advantage is that the most advantageous working conditions determined from the laboratory work can also be reproduced in the real production environment.

### 2.5.2 Application

The Taguchi approach experimental design that is used to investigate the concrete is shown in Table 2.19. This method significantly helps to achieve the objective of this study.

Table 2.19 The application Taguchi's method in concrete material

Title of Study	Significance Finding
Investigating mix proportions of high strength self compacting concrete (SCC) by using Taguchi method [108]	Optimum mix-design high strength SCC
A Taguchi approach for investigation of some physical properties of concrete produced from mineral admixtures [109]	Applied to physical properties of high strength concrete to save energy, time, and material in experimental study
Performance of lightweight concrete with silica fume after high temperature [110]	The level of importance of these parameters on mechanical properties was determined.

### 2.5.3 The Procedure of Taguchi's method

There are several steps in a systematic approach to the use of Taguchi's parameter design methodology [111]. The first step is problem recognition and formulation, this step to acquire a good understanding of the problem and the objective of the experiment. Secondly, select quality characteristic that the appropriate quality characteristic(s) to measure the experimental results. Thirdly, select design or process parameters\, this step is to learn more the design or process parameters which are believed to influence the quality characteristic of interest. Fourthly, classify design parameters into control, noise and signal factors, control parameters are those which

can be controlled fairly easily under standard conditions, noise factors are those which cannot be controlled or are expensive to control during normal or standard conditions. Signal factors are those which are used for process tuning or adjustments. Fifthly, determine levels of design or process parameters determine the number of test levels for the design or process parameters (two or three levels are commonly used). Sixthly, choose appropriate orthogonal array (OA), select most suitable OA from standard OA designs and assign design parameters and their interactions to various columns of the chosen OA. Seventhly, conduct experiments; execute the experiment based on pre-prepared experimental layout showing all the experimental trial conditions. Eighthly, perform statistical analysis, determine the best design parameter settings, predict the optimal condition, and establish confidence interval for the predicted response or quality characteristic. Finally step is perform a confirmatory experiment and implement results, a confirmatory experiment is performed to verify the optimal settings of design parameters and to see whether or not the optimal condition derived by the experiment actually yields an improvement in product quality, yield or performance. If the results from the confirmatory experiment are confirmed, a specific action on the product or process must be taken for improvement. On the other hand, if unsatisfactory results are achieved, further investigation of the problem may be required. Summarizing of the procedure is shown Figure 2.23

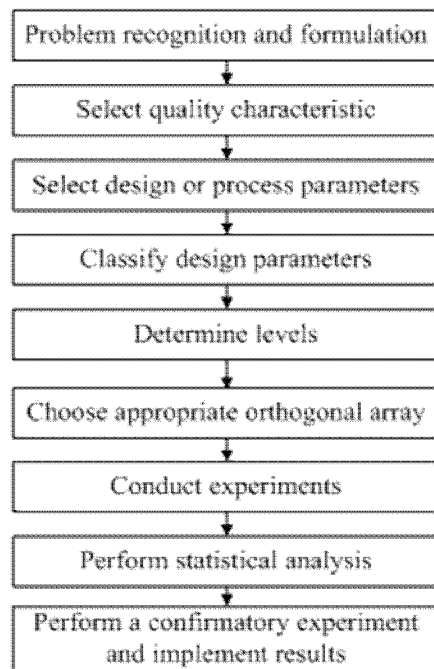


Figure 2.23 The procedure of Taguchi method

### 2.5.4 Orthogonal Array

Orthogonal Arrays signify a flexible matrix of combinational arrangements useful for conducting experiments to determine the optimum mix of a number of factors in a product to maximize or to minimize the yield, and in the construction of a variety of designs for various experiments. Orthogonally means that factors can be evaluated independently of one another; the effect of one factor does not bother the estimation of the effect of another factor.

The Orthogonal array (OA) experimental design method was selected to achieve the experimental plan,  $L_{16}(4^5)$ , which is one of the standard experimental plans improved by Taguchi [112] (see Table 2.20), the details of the method to obtain orthogonal array tables can be found in Taguchi's book titled "A primer on the Taguchi method"[107]. These ready-made orthogonal array tables have been successfully used in many areas.

In Table 2.20, the numbers to right of each row is called the experiment number or perform. parameter value with code FC, and ranges in value from 1 to 16; the vertical alignments that the parameter variable 1, 2, 3, 4 and 5 are termed the column of the orthogonal array, and each column consists of four numeral 1, 2, 3, and four.

Table 2.20 Standard  $L_{16}(4^5)$  orthogonal array [107]

Experiment number	Independent variables					Perform. parameter value
	Var. 1	Var. 2	Var. 3	Var. 4	Var. 5	
1	1	1	1	1	1	FC-1
2	1	2	2	2	2	FC-2
3	1	3	3	3	3	FC-3
4	1	4	4	4	4	FC-4
5	2	1	2	3	4	FC-5
6	2	2	1	4	3	FC-6
7	2	3	4	1	2	FC-7
8	2	4	3	2	1	FC-8
9	3	1	3	4	2	FC-9
10	3	2	4	3	1	FC-10
11	3	3	1	2	4	FC-11
12	3	4	2	1	3	FC-12
13	4	1	4	2	3	FC-13
14	4	2	3	1	4	FC-14
15	4	3	2	4	1	FC-15
16	4	4	1	3	2	FC-16

### 2.5.5 Analysis of Variance (ANOVA)

Taguchi introduced many methods for analyzing experimental results including novel applications of the analysis of variance and minute analysis. Analysis provides the variance of controllable and noise factors. In the analysis of variance many quantities such as degree of freedom, sums of squares, mean squares, etc., are computed and organized in standard tabular format. These quantities and their interrelationships are statistically defined below. The ANOVA tabular format in this study is adopted A Primer on the Taguchi method book [107] and explained below.

#### a. Total Number of Trial

For example in an experiment designed to establish the effect of factor A on response Y, factor A is to be tested at L levels. Assume  $n_1$  repetition of each trial that includes  $A_1$ . Similarly at level  $A_2$  the trial is to be repeated  $n_2$  times. The total number of trial is the sum of the number of trials at each level, i.e.

$$n = n_1 + n_2 + \dots + n_L \quad (2-39)$$

#### b. Degree of Freedom (DOF)

It is a quantify of the amount of information that can be uniquely determined from a given set of data. DOF for data concerning a factor equal one less than the number levels. The concept of DOF can be extended to the experiment. An experiment with n trial and r repetition of each trial has n x r trial runs. The total DOF becomes

$$f_T = n \times r - 1 \quad (2-40)$$

Similarly, the DOF for sum square term is equal to the number of terms used to compute the sum of square and the DOF of the error term  $f_e$  is given:

$$f_e = f_T - f_A - f_B - f_C \quad (2-41)$$

#### c. Sum of Squares

The sum of square is a measure of the deviation of the experimental data from for mean value of the data. Summing each squared deviation emphasize the total deviation. Thus

$$S_T = \sum_{n=1}^i (y_i - \bar{y})^2 \quad (2-42)$$

Where  $\bar{y}$  is the average value of  $y_i$

**d. Variance**

Variance measure the distribution of the data about the mean of data. Since data is representative of only a part of all possible data, DOF rather than the number of observations is used in the calculation.

$$V = \frac{ST}{f} = \frac{\text{Sum of squares}}{\text{degree of freedom}} \quad (2-43)$$

**e. Mean Sum (of Deviation) Squared**

Let  $T = \sum_{i=1}^n (y_i - y_o)$  the sum of all deviations from the target value. Then, the mean sum of square of the deviations is

$$S_m = \frac{T^2}{n} = \frac{\left[ \sum_{i=1}^n (y_i - y_o) \right]^2}{n} \quad (2-44)$$

**f. Variance Ratio**

Variance ratio, commonly is given term as the F statistic, is defined the ratio of variance due to the effect of a factor and variance due the error term. This ratio is employed to calculate the significance of the factor under investigation with reverence to variance of all the factors included the error term. The F value gained in the analysis is evaluated with a value from standard F-tables for given statistical level of significance. When an F table at the selected level of significance is lower than the computed F value, the factor contributes to the sum of the squares within the confidence level. The F value for A factor is calculated by:

$$F_A = \frac{V_A}{V_e} \quad (2-45)$$

**g. Pure Sum of Square**

The indecision due to the error in the testing, or error in a multiple regression, is accounted for using a metric called the pure sum of squares. The sum of squares terms are adjusted by the degrees of freedom and the mean square for error. The calculations reduce the sum of squares for the factors and increase the sum of squares

for the error term while keeping the total sum of squares constant. In so doing, this transform adds a measure of conservativeness to the decisions made based on the analysis of variance.

If factor A, B, and C, having DOF  $f_A$ ,  $f_B$  and  $f_C$  are included in an experiment, their pure sum of square are determined by:

$$\begin{aligned} S_A' &= S_A - f_A \times V_e \\ S_B' &= S_B - f_B \times V_e \end{aligned} \quad (2-46)$$

$$S_C' = S_C - f_C \times V_e$$

$$S_e' = S_e + (f_A + f_B + f_C) \times V_e \quad (2-47)$$

#### **h. Percent Contribution**

The percent contribution for any factor is obtained by dividing the pure sum of squares for that factor by  $S_T$  and multiplying the result by 100. The percent contribution is denoted by P for factor A and can be calculated using the following equation.

$$P_A = S_A \times 100/S_T \quad (2-48)$$

Where:

- V = mean squares (mean)
- S = sum of square
- S' = pure sum of square
- f = degree of freedom
- e = error (experimental)
- F = variance ratio
- P = percent contribution
- T = total of result
- N = number of experiment
- C.F. = correction factor
- N = Total degree of freedom

### 2.5.6 Determination level

Taguchi method is a powerful method for exploring the effect of parameter and its contribution. One of the key successes to determine the effects and contribution of a parameter is the exact determination of parameter level range. This step based on the literature that should be studied carefully.

#### a. Rice Husk Ash Level

The effect of RHA to improve the strength on cement paste research is depicted in Table 2.21.

Table 2.21 A review of mixes used, compressive strengths of mortar with RHA incorporation

Author(s)	Cement content (kg/m <sup>3</sup> )	Ratios			Ratio of Compressive Strength with control (28 day)
		S/C	W/C	RHA by weight cement (%)	
P. Chindapasirt [113]	-	2.75	0.53	0-40	0.97-1.03
Qingge Feng [100]	-	-	0.5	10	1.33
DD Bui [89]	-	-	0.34-0.48	0-30	0.90-1.12

#### b. Water Cement Ratio Level

Water content to achieve high strength FC was mentioned by Kearsley [39] for 0.35 because it prevents the value of cement to take water from the foam, but Jones et al [22] has succeeded in making foam concrete for the structure with w/c 0.3. The range level of water content is set at 0.35 and 0.5 with 0.05 increments.

#### c. Sand Cement Ratio Level

Sand cement ratio studied by Hamidah [68] showed that higher sand-cement ratio resulted in FC of lower compressive strength. The range level of sand cement ratio, which certainly causes the strength of FC, is high using level 0.25 to 1 with 0.25 incrementally.

#### d. Superplasticizier Content Level

In order to obtain high-strength concrete, the ratio of water to cement is generally kept low. However, the reduction of water/cement adversely affects the workability of the mortar. Therefore, in order to obtain high-strength FC, it is important to use a paste with good workability despite the low water/cement. The significant fresh state exclusivity of foam concrete is flowability and self-compactibility. Superplasticizers are sometimes used to keep up a suitable workability even though it may reduce the stability of foam. Table 2.22 shows the summary of FC that incorporating superplasticizier.

Table 2.22 A review of mixes used, workability of FC with Superplasticizer

Authors	Cement content (kg/m <sup>3</sup> )	F/C	W/C <sup>1</sup> or W/S <sup>2</sup>	FA by weight cement (%)	Foam volume (%)	SP by weight cement (%)	Flow cone (%)
EKK. Nambiar [113]	171-438	1-3	0.3-0.6 <sup>2</sup>	0-100	10-50	0.5-1.5	20-120

F/C: filler-cementitious ratio; W//C:water-cementitious ratio; W/S: water-solid ratio; FA: Fly ash; SP: Superplasticizier

#### e. Foam Content Level

Table 2.23 is summarized the mix proportion with a number foam content on FC.

Table 2.23 A review of mixes used with foam content incorporation on FC

Authors	Cement content (kg/m <sup>3</sup> )	F/C	W/C	FA by weight cement (%)	Foam volume (%)	Comp. Strength with control (28 days)
EKK. Nambiar [113]	171-438	1-3	0.3-0.6	0-100	10-50	20-120

The summing up of level determination above is adjusted to arrange level for this study that presented in Table 2.24.



Table 2.24 Parameters and their variation levels

Parameter	Unit	Level			
MIRHA	(%)	0	5	10	15
w/c	Ratio	0.35	0.4	0.45	0.5
s/c	Ratio	0.25	0.5	0.75	1
SP	(%)	0	0.5	1	1.5
FC	(%)	20	25	30	35

## 2.6 Summary

After detailed review of the available literature on foamed concrete, it is understood that most of the research was focused on developing the mix design for foamed concrete, to establish hydration and mechanical properties of foamed concrete. The literature showed some significant gaps in the area of research on foamed concrete. Some of prominent gaps are obtained as:

- a. Application of MIRHA in producing foamed concrete for structural lightweight concrete (the minimum compressive strength of 17 MPa at 28 days)
- b. The effect of MIRHA on hydration and mechanical properties of foamed concrete.

Some of the gaps derived from literature review were investigated in this research study.

## CHAPTER 3 EXPERIMENTAL PROGRAM

### **3.1 Overview**

Chapter 3 presents the details of the experimental program adopted in this work. It starts with a discussion of the experimental design of the primary experiments and the measurements they entailed. The next section describes the material, experimental procedures and test for all experiments. A strict measure of quality control is the most important criterion for the experimental investigation and forms part of any research programme. Therefore, the spurious result and false trend can be avoided by applying the prevailing code of standards and specifications for the selection of concrete making, materials and mix proportions.

### **3.2 Material Properties**

#### **3.2.1. Microwave Incinerated Rice Husk Ash (MIRHA)**

Rice husk used in this research was taken from rice milling plant of Bernas, Malaysia. Rice husk was dried under direct sunlight to reduce its moisture content so that when it was burnt, it would not produce large amount of smoke. Dried rice husk was then burnt in automatic microwave incinerator to produce amorphous ash called MIRHA.

**a. Microwave Incinerated Rice Husk Ash (MIRHA) Production**

High temperature microwave can penetrate the material for achieving the rapid internal heating, which may also improve the structural properties of the end product. Together with the environment of controlled heating, microwave incineration an efficient process that has the potential to reduce the burning time and use of energy.

The basic difference between the microwave heating and the conventional methods of heating is that the conventional heating relies on one or more heat transfer mechanisms namely convection, conduction, or radiation to transfer thermal energy into the material. In all three cases, the energy is deposited at the surface of the material and the resulting temperature gradient established in the material causes the transfer of heat into the core of the object. Thus, the temperature gradient is always transferred into the material with the highest temperature being at the surface.

In the microwave heating, the microwave energy does not only interact with the surface material but also penetrates the surface and interacts with the core of the materials. Energy is transferred from electromagnetic field into thermal energy throughout the entire volume of the material that is penetrated by the radiation. Microwave heating does not rely on conduction from the surface to bring heat into the core region. The Technical specifications [114] of the microwave incinerator is given in Appendix B.

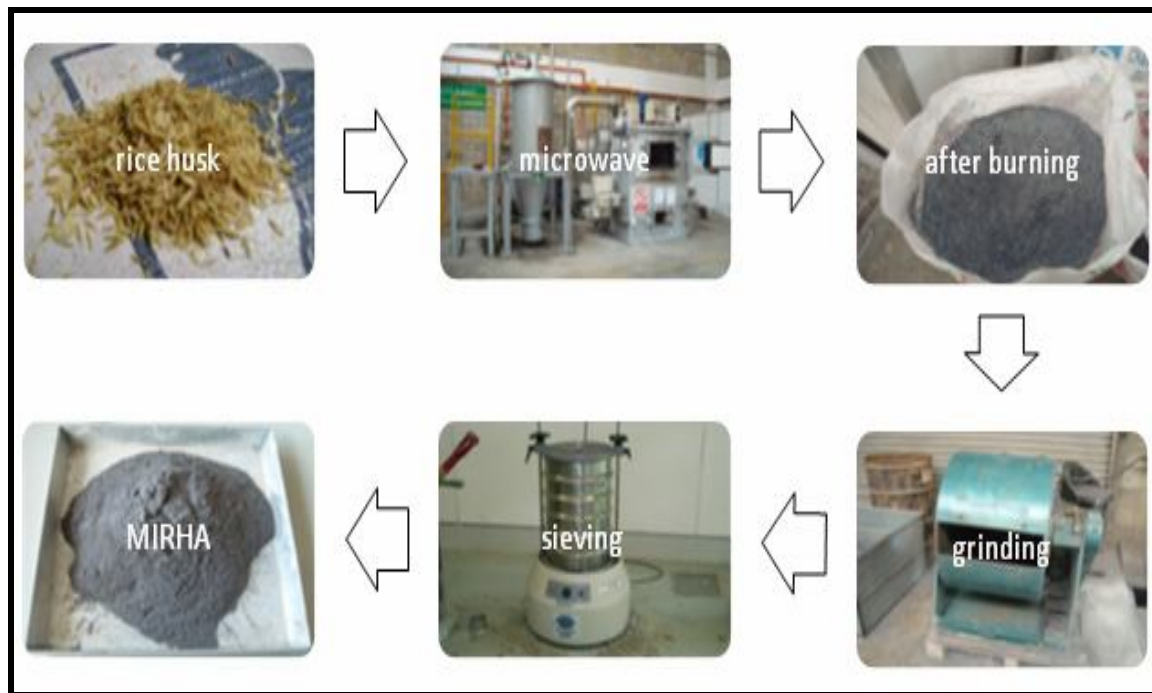


Figure 3.1 The process of MIRHA production

Figure 3.1 shows the process of MIRHA production the burning procedure was based on one-stage burning technique at a constant temperature of 500°C for 2 hours. The incinerated ash ground in a ball mill to achieve the require fineness. As cement replacement material (CRM), RHA should have particle size smaller than cement so it will able to function as micro structure filler in the Interfacial Transition Zone (ITZ). The particle size of Ordinary Portland Cement (OPC) is usually 100 micron, ground MIRHA was sieved to obtain particle size smaller than 100 micron. The amount of silica inside MIRHA was determined using X-Ray Diffraction (XRD) and X-Ray Fluorescence (XRF) techniques.

#### **b. Chemical Composition of MIRHA**

Chemical analysis MIRHA was preformed using X-Ray Fluorescence (XRF) technique. Chemical analysis indicated that the ash obtained essentially consisted of silica content of more than 90% by weight. The detail of the chemical composition is shown in Table 3.1.

Table 3.1 MIRHA Chemical Composition

Chemical Content	Mass content (%)
Silicon dioxide or silica (SiO <sub>2</sub> )	90.75
Aluminum oxide or alumina (Al <sub>2</sub> O <sub>3</sub> )	0.75
Iron oxide (Fe <sub>2</sub> O <sub>3</sub> )	0.28
Calcium oxide or lime (CaO)	0.87
Magnesium oxide or magnesia (MgO)	0.63
Sodium oxide (Na <sub>2</sub> O)	0.02
Potassium oxide (K <sub>2</sub> O)	3.77
Equivalent alkalis (Na <sub>2</sub> O + 0.658 K <sub>2</sub> O)	2.50
Titanium oxide (TiO <sub>2</sub> )	0.02
Phosphorous oxide (P <sub>2</sub> O <sub>5</sub> )	2.5
Manganese oxide (MnO)	0.08
Sulfur trioxide (SO <sub>3</sub> )	0.33
<b>Other</b>	
Sulfur (S)	< 0.01
Carbon (C)	0.15
Chloride (Cl):	110 g/t

**c. Grain size analysis of MIRHA**

X-Ray Diffraction (XRD) is used to analyze the grain size structural properties of material. Graph patterns of XRD analysis can show whether the material is in amorphous, partially crystalline, or crystalline state. Figure 3.2 describes the properties of MIRHA that was obtained from microwave combustion.

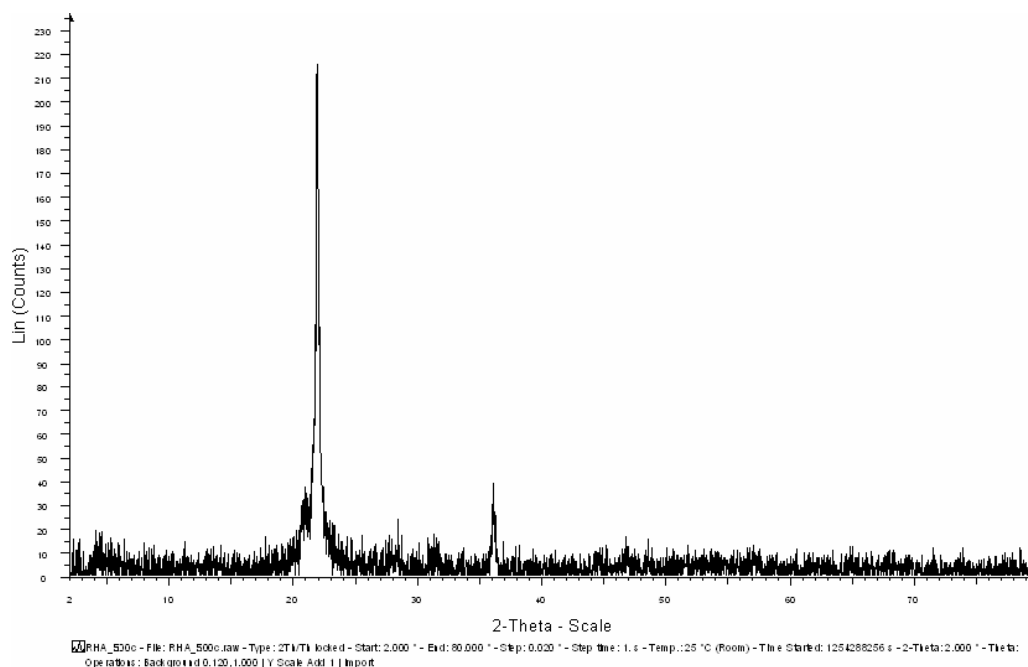


Figure 3.2 XRD Graph of MIRHA

#### d. Physical Properties

The results of physical properties of MIRHA are shown in Table 3.2. The relative density of MIRHA was 2.23 using ultracycnometer methods. It generally varies in the range of 2.05 to 2.30 for most sources of RHA [78].

Table 3.2 Physical properties of MIRHA

Properties	Value
Relative density	2.23
Accelerated pozzolanic activity (%)	92.3
Passing 45 $\mu$ m (%)	95.15
Specific surface area (m <sup>2</sup> /g)	7.81
The average particle ( $\mu$ m)	16.22
Loss on ignition (%)	5.02

#### 3.2.2. Characteristic of Ordinary Portland Cement

The Ordinary Portland Cement (OPC) Type 1 was used throughout this research. The physical and chemical properties as listed in Table 3.3. OPC Type 1 was chosen because of the observation on concrete properties could be done in normal hydration process without any addition of admixture to the concrete, hence the advantages of MIRHA usage in concrete can be maximally observed. The cement density and the surface area were found to be 3.15 and 450 m<sup>2</sup>/kg respectively.

The composition of the cement (in oxides) is presented in Table 3.3. This oxide information can be used to estimate the percentage of cement compounds via the Bogue equations [30]. For this cement, the resultant percentages were C<sub>3</sub>S = 59.1%, C<sub>2</sub>S= 13.1%, C<sub>3</sub>A= 8.2%, C<sub>4</sub>AF= 9.9%.

Table 3.3 Physical and chemical properties of OPC type 1 adopted from Cement Industries of Malaysia Berhad (CIMA)

Modulus	Lime Saturation Factor	0.96
	Silica Modulus	2.37
	Iron Modulus	1.58
Compressive Strength (N/mm <sup>2</sup> )	3 days	38
	7 days	46
	28 days	56
Chemical Ingredients (%)	SiO <sub>2</sub>	19.98
	Fe <sub>2</sub> O <sub>3</sub>	3.27
	Al <sub>2</sub> O <sub>3</sub>	5.17
	CaO	63.17
	MgO	0.79
	SO <sub>3</sub>	2.38
	Total Alkalis	0.90
	Insoluble Residue	0.2

### 3.2.3. Fine Aggregate

Natural quartzite sand as fine aggregate was used in this study; it was obtained from the deposit of Tronoh, Perak. The fine aggregate was recommended for use in foamed concrete which has the particle size up to 5 mm [115] and even distribution. The fine aggregate used was natural sand with 100% passing 425 mm sieve BS EN 12620 and its density was 2.65. Figure 3.3 and Figure 3.4 show the mechanical sieve used to sieve fine aggregate and fine aggregates obtained from sieving process, respectively. The absorption of sand obtained was 1.0%. The absorption of fine aggregate generally varies in the range of 0.2 to 3.0% [30]. The mass passing 75 mm sieve was obtained 1.38% that is lower than the value of ASTM-C33 standard 3 to 5% [116].



Figure 3.3 Mechanical sieve used for this research



Figure 3.4 Fine aggregate obtained from sieving process



### 3.2.4. Water

Water that is fit for drinking is generally regarded as acceptable for use in mixing concrete [117]. Water containing one thousand parts per million (ppm) of normally found minerals acids can be tolerated. However, small amount of sugar and chloride derivatives should not be used.

### 3.2.5. Superplasticizer

A chemical admixture was used in preparing MIRHA FC in order to decrease water content and to improve its workability. The superplasticizer incorporated in this research was in the form of liquid, known as Sulfonated Naphthalene Formaldehyde condensate (Figure 3.5).



Figure 3.5 Superplasticizer type as used in this research

### 3.2.6. Foam Agent

The surfactant used for the production of the preformed foam was by aerating palm oil based, this is typical of industry practice which has a ratio of 1:30 by volume and has aerated to a density of 110 kg/m<sup>3</sup> [17, 118]. The chemical composition of foam agent is listed in Table 3.4.

Table 3.4 Foam agent Chemical Composition

Chemical Content	Mass content
Oxide composition	(%)
Iron oxide (Fe <sub>2</sub> O <sub>3</sub> )	6.445
Calcium oxide or lime (CaO)	2.45
Magnesium oxide or magnesia (MgO)	4
Sodium oxide (Na <sub>2</sub> O)	15.368
Potassium oxide (K <sub>2</sub> O)	0.487
Phosphorous oxide (P <sub>2</sub> O <sub>5</sub> )	4.71
Sulfur oxide (SO <sub>3</sub> )	62.72
Cl	3.82

### 3.2.7. Experimental Design

For normal concrete, the user would specify a certain compressive strength and the water/cement would be adjusted to meet specification. Requirement of FC should not only be the strength, but also density. However, there is no standard method to carry out the mix design of FC. In order to understand the relationships between FC raw material mixtures and the resultant mechanical properties, many mixtures proportions should be studied or prepared.

In this research 5 design parameters have been identified, they are: Microwave Incinerated Rice Husk Ash Content (MIRHA); sand/cement (s/c); water/cementitious (w/c); Superplasticizer (SP) content; Foam content (fc). To have good quality of FC these parameters need to be carefully combined. It means that the experiments will have to study huge number of combinations. If each parameter has 4 levels therefore 4<sup>5</sup> numbers of experiments involving 1024 mix proportions.

An appropriate combination of parameters should be chosen to solve the problem of huge number of experiments. Taguchi's method [107] was used to solve the problem. Taguchi's method addresses the following issues: a) reduction of the number of experiment, b) determination of the degree of influence of each factor and the optimum setting condition, c) ability to reproduce real production environment from library experiment

In this research, the optimum composition of material proportion for FC according to BS EN 206-1/BS 8500 was determined. The criteria of structural lightweight concrete namely minimum 28 days cube compressive strength of 17 MPa and maximum dry density of 1800 kg/m<sup>3</sup> are observed. Spread test as workability measurement, dry density, compressive strength, porosity and non-evaporable water are the quality characteristics. Five design parameters, viz. MIRHA content, sand/cement, water/cementitious, *superplasticizier* (SP), Foam content (FC) were identified as design parameters.

Table 3.5 presented the schema of mix proportion with parameters and each level that is adopted from Table 2.20 and Table 2.24.

Table 3.5 Mix proportion with parameter and each level

Experiment No	RHA (%)	w/c (ratio)	s/c (ratio)	SP (%)	FC (%)
FC- 1	0	0.35	0.25	0	20
FC-2	0	0.4	0.5	0.5	25
FC-3	0	0.45	0.75	1	30
FC-4	0	0.5	1	1.5	35
FC-5	5	0.4	0.25	1	35
FC-6	5	0.35	0.5	1.5	30
FC-7	5	0.5	0.75	0	25
FC-8	5	0.45	1	0.5	20
FC-9	10	0.45	0.25	1.5	25
FC-10	10	0.5	0.5	1	20
FC-11	10	0.35	0.75	0.5	35
FC-12	10	0.4	1	0	30
FC-13	15	0.5	0.25	0.5	30
FC-14	15	0.45	0.5	0	35
FC-15	15	0.4	0.75	1.5	20
FC-16	15	0.35	1	1	25

When designing a foamed concrete mix, two variables, namely the cement content and the foam content should be established and therefore two equations have to be solved. To prepare 1 m<sup>3</sup> of foamed concrete, the sum of the material weights should be equal to the required casting density and the sum of the volume of the all the constituent materials should be one cubic meter (or 1000 liter).

Using spreadsheet in excel was used to calculate the measuring process and 16 FC mixtures were designed. The mix composition cast can be seen in Table 3.6.

Table 3.6 FC mixture proportion adopted

Code	Cement (kg/m <sup>3</sup> )	Sand (kg/m <sup>3</sup> )	Water (kg/m <sup>3</sup> )	MIRHA (kg/m <sup>3</sup> )	Foam Volume (liter/m <sup>3</sup> )	SP (kg/m <sup>3</sup> )
FC-1	1050	263	368	0	200	0
FC-2	828	414	331	0	250	4
FC-3	666	500	300	0	300	7
FC-4	544	544	272	0	350	8
FC-5	779	195	312	39	350	8
FC-6	797	398	279	40	300	12
FC-7	668	501	334	33	250	0
FC-8	685	685	308	34	200	3
FC-9	827	207	372	83	250	12
FC-10	761	381	381	76	200	8
FC-11	653	490	229	65	350	3
FC-12	614	614	246	61	300	0
FC-13	715	179	357	107	300	4
FC-14	635	318	286	95	350	0
FC-15	749	562	300	112	200	11
FC-16	674	674	236	101	250	7

Table 3.7 presented the schema of mix proportion with parameters and each level without foam that is adopted from Table 2.20 and Table 2.24.

Table 3.7 Mix proportion with parameter and each level without foam

Experiment No	RHA (%)	w/c (ratio)	s/c (ratio)	SP (%)
M-1	0	0.35	0.25	0
M-2	0	0.4	0.5	0.5
M-3	0	0.45	0.75	1
M-4	0	0.5	1	1.5
M-5	5	0.4	0.25	1
M-6	5	0.35	0.5	1.5
M-7	5	0.5	0.75	0
M-8	5	0.45	1	0.5
M-9	10	0.45	0.25	1.5
M-10	10	0.5	0.5	1
M-11	10	0.35	0.75	0.5
M-12	10	0.4	1	0
M-13	15	0.5	0.25	0.5
M-14	15	0.45	0.5	0
M-15	15	0.4	0.75	1.5
M-16	15	0.35	1	1

Using spreadsheet in excel was used to calculate the measuring process and 16 M mixtures were designed. The mix composition cast can be seen in Table 3.8.

Table 3.8 Mortar mixture proportion adopted

Code	Cement (kg/m <sup>3</sup> )	Sand (kg/m <sup>3</sup> )	Water (kg/m <sup>3</sup> )	MIRHA (kg/m <sup>3</sup> )	SP (kg/m <sup>3</sup> )
M-1	1313	328	459	0	17
M-2	1104	552	441	0	12
M-3	952	714	428	0	9
M-4	837	837	418	0	7
M-5	1199	300	479	60	14
M-6	1138	569	398	57	13
M-7	891	668	445	45	8
M-8	857	857	386	43	7
M-9	1103	276	496	110	12
M-10	951	476	476	95	9
M-11	1005	754	352	100	10
M-12	877	877	351	88	8
M-13	1021	255	511	153	10
M-14	977	489	440	147	10
M-15	937	702	375	140	9
M-16	899	899	315	135	8

### 3.3 Experimental Laboratory

Mix proportions resulting from the experimental design were then performed experimentally in concrete laboratory of civil department Universiti Teknologi PETRONAS. Testing procedures undertaken were as follows:

#### 3.4.1. Specimen Preparation

This section discusses the specimen preparation and curing methods used in this experimental program. Within each experiment, however, every attempt was made to be consistent for all mixtures, any exception are noted.

#### 3.4.2. Mixing Process

The preparation of concrete was divided into three stages. Figure 3.6 presents the schema of foamed concrete mix process.

For the mortar preparation, the aggregate was first mixed with half of water followed by the addition of OPC and MIRHA. The rest of the water was then poured in the mixes (see Figure 3.7)

In the preparation the of foam, foaming agent and water are mixed with a volume ratio of 1:30, the mixture was incorporated with the air pressure tank for 5 bar to produce foam with a density of 110 kg/m, this is typical of industry practice.

The appropriate volume of the foam was generated and added immediately to the base mix and it was mixed until no physical sign of the foam left on the surface and all foam was uniformly distributed and incorporated into the mix. Prior to the introduction of the foam, the density of the mortar was determined to ensure accurate amount of foam to be inserted. Six 50 mm cube samples were prepared for each age of 3, 7, 28, 90, and 180 days to monitor the compressive strength development, whilst 25.4 by 25.4 mm cylinders and 150 by 300 mm cylinders were used for determining the porosity and dry density level respectively. Figure 3.8 shows the process of foamed concrete production.

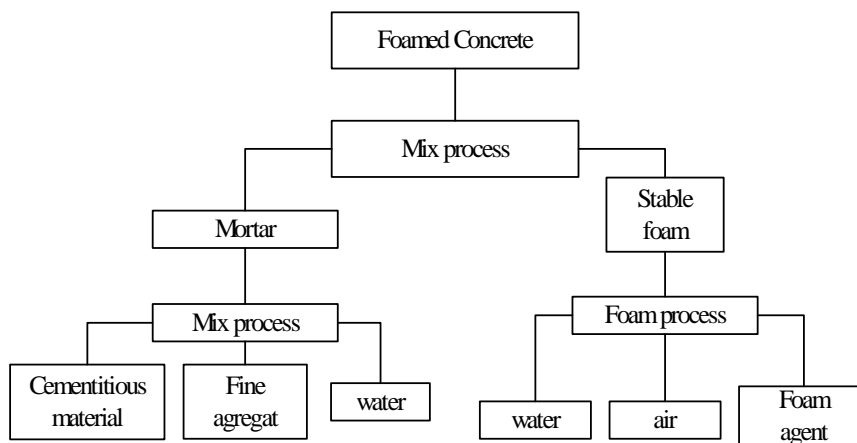


Figure 3.6 Schema of FC mix process



Figure 3.7 The preparation of mortar process as first process



Figure 3.8 Foam production and casting processes



### 3.4.3. Spread Measurement

The workability of the foamed concrete was evaluated through spread measurement in accordance with ASTM-230 [59]. The truncated cone mould was placed on a glass plate, filled with paste and lifted [119]. The diameters of the flow give indications of the workability of the mix. The spread test is shown in Figure 3.9.



Figure 3.9 Spread test

### 3.4.4. Curing Regime

24 hour after casting specimens were striped out of the molds and placed in water tank at  $23 \pm 2^\circ\text{C}$ . The curing is done in similarly accordance with BS EN 12390-2:2000. The curing system that was used in this research was shown Figure 3.10.



Figure 3.10 Water tank system for curing of FC sample



### 3.4.5. Hardened concrete test

Hardened foamed concrete specimens were tested in three modes called done in four conditions namely fresh stage test, destructive test, non-destructive test and loss on ignition test. The experimental details are shown in Table 3.9

Table 3.9 Hardened foamed concrete test

FC Type	Test Type	Standard	Equipment	Age	Sample Size	No. of Samples per Age	Unit
Non-destructive	Dry density	ASTM-567-00		180 days	150 by 300-mm cylinders	3/mix	kg/m <sup>3</sup>
	Porosity	ASTM 1220	Vacuum saturation	180 days	25.4 by 25.4-mm cylinders	3/mix	%
Destructive test	Compression Strength	BS 1881-116:1983	Compression Testing Machine	3,7,28, 90 and 180 days	50 mm <sup>3</sup> cube	6/mix	N/mm <sup>2</sup>
On loss ignition test	Oven Dry/Furnace Ignition (OD/FI)	RILEM	Oven and electrical furnace	3,7,28, 90 and 180 days	5 to 15 gram	3/mix	%
	TGA	-	TGA	3, 28 and 180 days	5 to 10 mg	3/mix	%

#### a. Compressive Strength

The compressive strength of foamed concrete was measured at different ages. Compressive strength development of the sample was measured using ELE International Digital Compressive Testing Machine (Figure 3.11). During the test, concrete cube was subjected 3 KN/s constant loading rate without any sudden shock loads. Compressive strength value was taken as ultimate load that can be sustained by the concrete cube divided by surface area of the contact surface on which the load is applied.

The calculations for compressive strength were conducted in accordance with BS 1881-116:1983 [120] in the mix proportion.



Figure 3.11 Compressive Testing Machine

**b. Porosity**

There are a number of methods that can be used to determine the total porosity of concrete and mortar, however, the technique of vacuum saturation is perhaps the simplest, cheapest and most direct. Although the vacuum saturation of concrete is not widely used, evidence shows that the method is gaining acceptance because of providing a closed approach to total or full saturation in a relatively short time period. Porosity was measured on three cylinders of 25.4 mm in diameter and 25.4 mm in height for each mix of foam concrete which had been moist-cured for 180 days. The vacuum saturation apparatus used in this investigation was similar to that developed by RILEM for measuring the total porosity. The diagram apparatus is shown in Figure 3.12 and Figure 3.13. The test concrete and mortar specimens conditioned to equilibrium at different RH were weighed in the air ( $W_i$ ). Then the specimens were vacuum saturated in water. At fully saturated condition; the specimens were weighed in the air ( $W_{SA}$ ) and in the water ( $W_{SW}$ ). Finally, they were dried in an oven at 105°C to constant weight ( $W_d$ ).

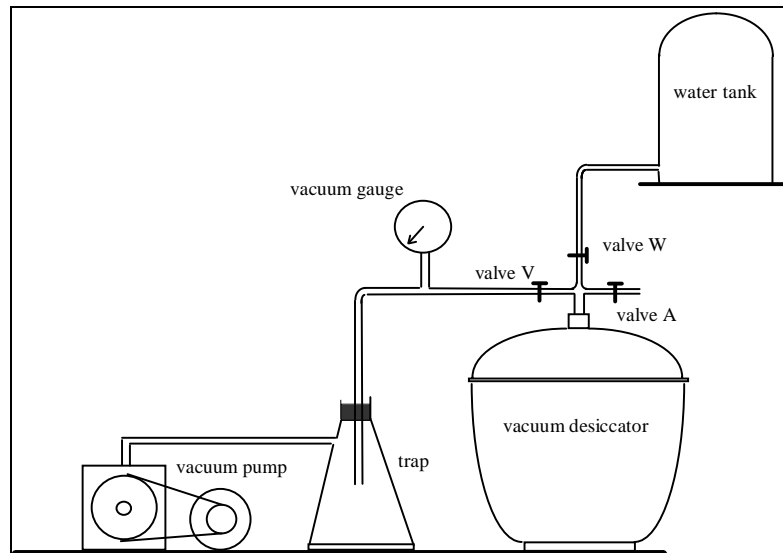


Figure 3.12 Schematic diagram of Vacuum Saturation Apparatus [71]

The total porosity (P) of FC was calculated using the following equations.

$$P = \frac{W_{SA} - W_d}{W_{SA} - W_{SW}} 100 \quad (3-1)$$

Where:

- P = Total porosity (%)
- $W_{SA}$  = Weight of saturated surface dry samples in air (g)
- $W_{SW}$  = Weight of saturated surface dry samples in water (g)
- $W_d$  = Weight of oven dry samples (g)



Figure 3.13 Porosity equipment

**c. Dry Density**

The method to calculate the dry density of FC was conducted in accordance to ASTM-567-00 [121]. After 24 hours but not to exceed 32 h, the 150 by 300-mm cylinders samples were removed from the mold. The apparent mass of the cylinders while suspended and completely submerged in water were measured and recorded as “G” the mass of the suspended-immersed cylinders. The cylinders were removed from the water and allowed to drain for 1 min by placing the cylinders on a 9.5-mm (3/8-in.) or coarser sieve cloth. Visible water was removed with a damp cloth and the mass was determined and recorded as “F,” the mass of the saturated surface-dry cylinders.

The cylinders were placed in the drying oven for 72 h or until constant mass was reached. Oven temperature was maintained at 110 +/- 5°C. The cylinders were allowed to cool at room temperature and the mass determined and recorded as “D,” the mass of the oven-dried cylinder. Oven-drying was repeated and the mass at 24-h intervals was measured until the mass of the specimen changes not more than 0.5% in successive weighing. The oven-dry density was determined from Equation:

$$O_d = D \times 997 / (F - G) \quad (3-2)$$

Where:

- $O_d$  = measured oven dry density (kg/m<sup>3</sup>)
- $D$  = mass of oven-dry density (kg)
- $F$  = of saturated surface-dry cylinder (kg)
- $G$  = apparent mass of suspended-immersed cylinder (kg)

**d. Non-Evaporable Water by Oven/Furnace**

The non-evaporable water content was obtained using a loss-on ignition procedure [102]. Samples for non-evaporable water content were desired from those cubes tested for compressive strength. After the maximum compressive load was achieved, each cube was further crushed to about half of its original height. Some of the semi crushed material was then collected to fill three-fourths of 15-ml crucible. This sample was then manually ground with mortar and pestle until all non-aggregate particles were less than about two mm in diameter, placed in a clean container, and covered with

acetone in 45 second [55] to halt the hydration process. The final ground sample in acetone was then heated in a drying oven at 105°C until constant mass. This drying procedure which required at least 12 hours, removed all the evaporable water from the sample. After oven drying the crucibles were weighed and then heated in a furnace for three hours at 1050°C, the crucibles were weighed again following ignition the furnace. Figure 3.14 shows a schematic illustration of the measurements from the OD/FI procedure.

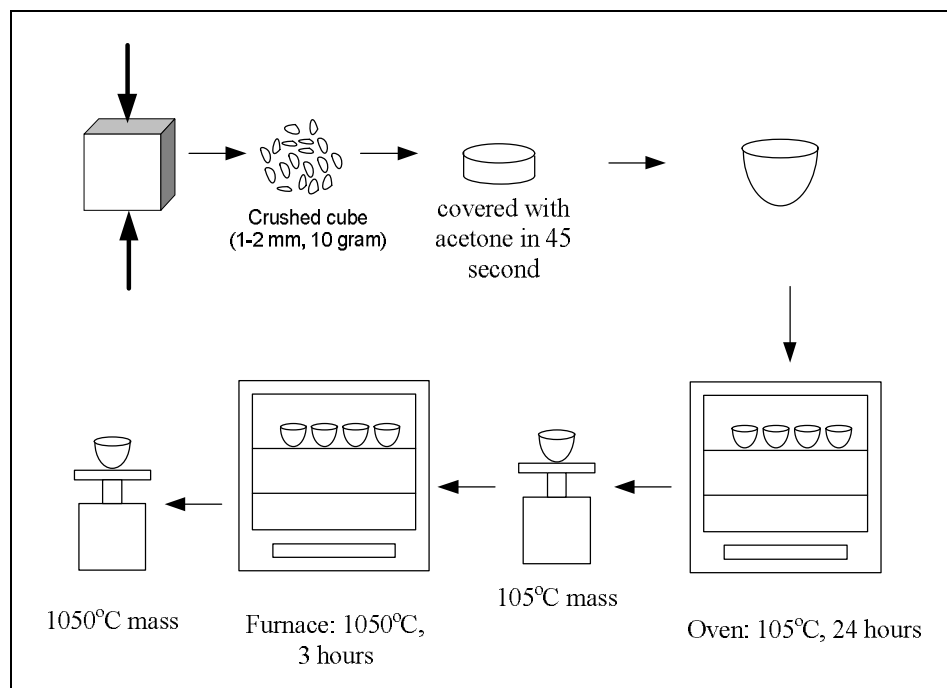


Figure 3.14 OD/FI non-evaporable water measurement procedure

According to the OD/FI procedure, the mass of the sample was measured after the oven drying stage and the furnace ignition stage. The sample was not weighed before being dried in the oven, however, since the sample was first flushed with acetone to stop hydration. In this process, the acetone was drawn through the samples removing some of the free capillary pore water, thus altering the original mass of the sample.

Although the initial sample mass was not known, the ratios of the component materials in the dry mix (i.e. fine aggregate/cement or MIRHA/cement) were known, since they were specified in the mix design and controlled in mixing. These ratios were assumed constant through the oven dry stage, such that the ratios in the 105°C

sample were the same as those in the original sample. Moreover, the mass of the component materials themselves (other than water) were assumed to remain unchanged during the oven dry. This assumption was reasonable since mass loss in these materials occurs during the high temperature furnace ignition and not during the low temperature oven drying.

As previously discussed in the section 2.4.3, the losses on ignition (LOIs) of the component materials (i.e. cement, fine aggregate, MIRHA) have to be determined prior to mix sample investigation. This was conducted to identify the characteristic of OD/FI LOIs of component materials. The result of OD/FI LOIs of component materials is tabulated in Table 3.10.

Table 3.10 OD/FI LOIs of component materials

Material	LOI from OD/FI (% of initial material)
Cement	1.66
Sand	0.71
MIRHA	5.02

The apparatus used for non-evaporable study by OD/FI is shown in Figure 3.15 and Figure 3.16.



Figure 3.15 The crucible used in this experiment



Figure 3.16 The electrical furnace apparatus (Nabertherm 30-3000°C) used in this study

**e. Non-Evaporable Water using TGA**

**Apparatus**

TGA may be defined as a technique whereby the weight of substance, in an environment is heated or cooled at a controlled rate and recorded as a function of time or temperature. The apparatus used in this was Brand Perkin Elmer model Pyris 1 as shown in Figure 3.17 and Figure 3.18.



Figure 3.17 The Thermogravimetry apparatus (Brand Perkin Elmer model Pyris 1) used in this investigation

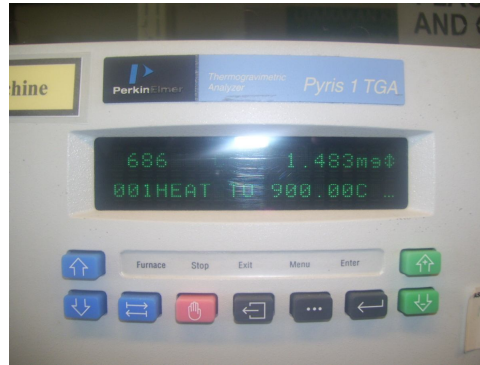


Figure 3.18 The TGA monitor for viewing the temperature of process

The instrument mainly consists of: a furnace capable of igniting the sample up to 900°C, an electro-microbalance for measuring the weight loss due the temperature rise, an operation programmer unit computer and plotter for analysis and plotting the results.

### Sample preparation

Sample preparation detail for non-evaporable water measurement is given in Table 3.6. At the time of every experiment, a sample was taken out of the curing chamber.

### 3.4 Summary

Summary of the methodology to achieve the objective of this study is explored as following:

- a. The mix proportions were performed efficiently by using  $L_{16}$  orthogonal array using five parameters.
- b. The workability test results were conducted according to water demand of mix constituent using ASTM flow table test with criteria from Kearsley's study [39] in the range of 220 mm to 250 mm as requirement consistency.
- c. The compressive strength results were calculated from the maximum load divided by the average cross-sectional area. This analysis method is standard and is documented in BS 1881-116[120]. The target minimum of compressive strength result is 17 MPa in 28 days.



- d. The vacuum saturation apparatus used in this investigation is similar to that developed by RILEM for measuring the total porosity.
- e. The method to calculate the dry density of foamed concrete was in accordance to ASTM-567-00.
- f. The OD/FI mass results, combined with information about the mixture proportions and the loss on ignition of the component materials, were converted to non-evaporable water contents based on mass-equilibrium equations.

## CHAPTER 4

### RESULT, ANALYSIS AND DISCUSSION ON MECHANICAL PROPERTIES

#### 4.1 Overview

This chapter discusses the result of experimental program namely (i) special CRM characteristic of MIRHA used in this experiment, (ii) plastic density and cube crushing strength repeatability of a single mix, (iii) orthogonal array experimental, (iv) confirmation of the optimum mix proportion by Taguchi method.

(iv) non-evaporable water by OD/FI and TGA experimental, (v) change in non-evaporable water content due to the presence of MIRHA, (vi) FC degree of hydration with and without MIRHA, (vii) compressive strength correlations to non-evaporable water, porosity and gel-space ratio characteristic, (viii) confirmation of the optimum mix proportion by Taguchi method.

#### 4.2 Properties of MIRHA

Assurance of the quality (chemical and mineralogical composition) is very important in order to use it as a potential CRM that can affect the quality of concrete. The capability of MIRHA to convert calcium hydrate to calcium silicate hydrate gels is influenced by the amorphous state of MIRHA, the amount of SiO<sub>2</sub> content, the pozzolanicity and the particles size distribution and specific surface area of MIRHA. The analysis on MIRHA was conducted by means of X-Ray Diffraction Test and X-Ray Fluorescence Test.

### 4.2.1 X-Ray Diffraction Analysis

The calibration standard materials used for the XRD analysis were tridymite (NIOSH TY-27) and cristobalite (NIST SRM 1879). The integrated intensities of the peaks at  $20.5^\circ$  ( $4.32\text{\AA}$ ) and  $21.8^\circ$  ( $4.06\text{\AA}$ ) were used for the determination of tridymite and cristobalite, respectively [125]. X-Ray Diffraction (XRD) technique is used to analyze the crystalline phases of a material. A representative XRD pattern of the MIRHA samples was shown in Figure 4.1.

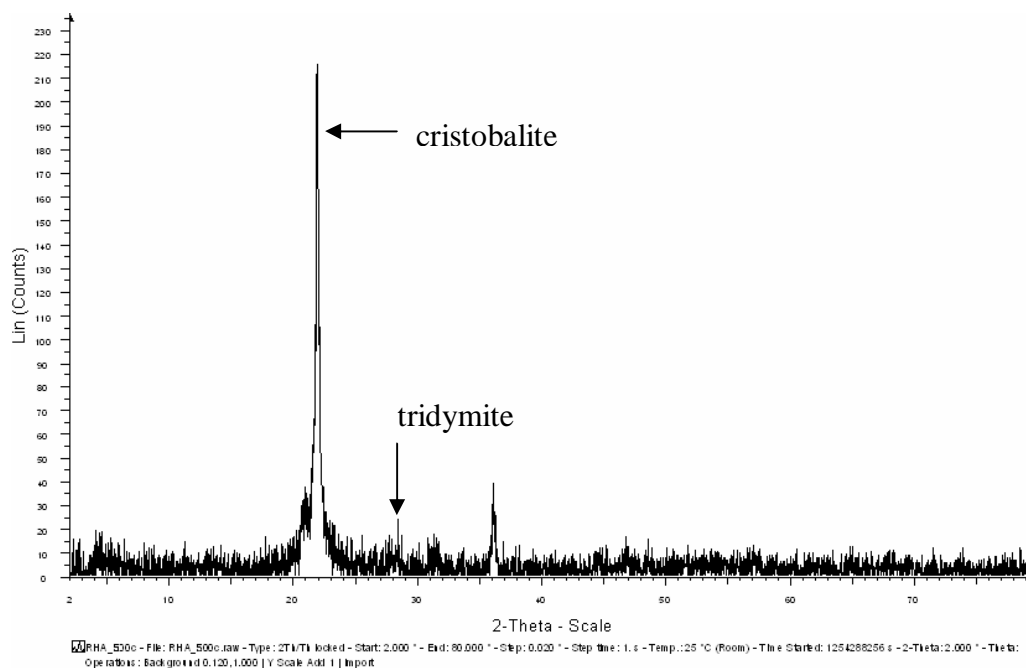


Figure 4.1 XRD Graph of MIRHA

In Figure 4.1, a strong peak at  $21.8^\circ$  indicated by arrows was identified a strong cristobalite peak and an additional weak peak at  $27.5^\circ$  was identified as tridymite. The gradual dense scatter of XRD graph was used to indicate the amorphous state of a material. The XRD pattern of cristobalite crystallized in MIRHA samples (Figure 4.1) has a feature in which the cristobalite peaks are broad compared with well-crystallized cristobalite. This type of cristobalite has been called disordered cristobalite and opal-C [125]. The XRD patterns of some opal-C and disordered cristobalite silicas are similar to each other, such as the peak position and peak width of the strongest peak. Some researchers considered that any forms of opal are not crystalline silica because opal-C is considered to be transformed from other forms of opaline silica at lower temperatures in nature, disordered cristobalite is an appropriate

term to describe this type of cristobalite in heated MIRHA samples. The MIRHA pozzolanic reactivity was observed to be high if utilized as CRM in FC. The verification of this observation will be explained in the next sub chapter of XRF analysis, compressive strength and non-evaporable water test.

As a reference, various crystalline properties of RHA are shown in Figure 4.2. Different burning temperatures that were used in burning rice husks give various properties in terms of their crystalline phase. Char obtained from 400° C combustion has amorphous phase according to the XRD pattern. This amorphous pattern was indicated by a blunt peak. However, using low temperature to burn rice husk will give low SiO<sub>2</sub> content in RHA, while burning rice husk with high temperature will give high SiO<sub>2</sub> content in RHA, but this high temperature will lead to a crystalline state of RHA [9]. The crystalline state is indicated by a sharp peak in the graph, as shown in 700°C and 900°C RHA XRD graphs.

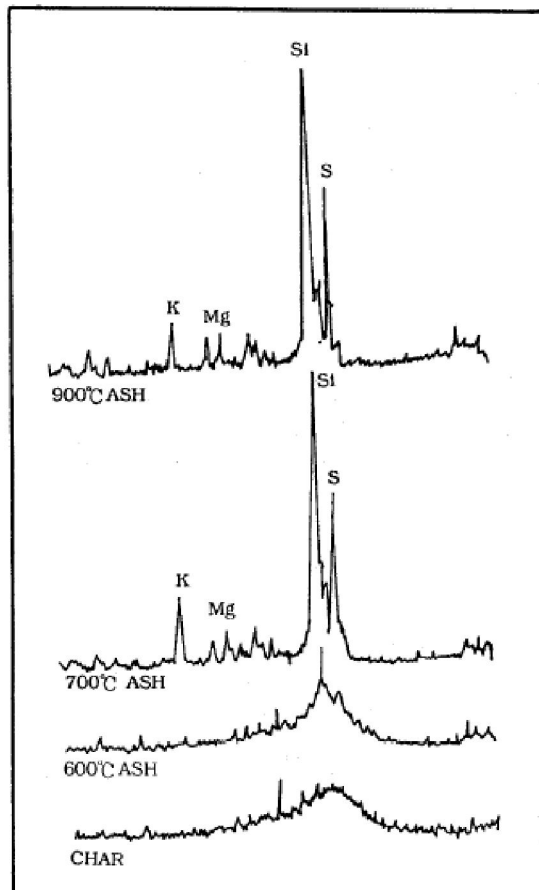


Figure 4.2 The X-Ray Diffraction of RHA under different burning conditions [9]

#### 4.2.2 X-Ray Fluorescence Analysis

The pozzolanic reactivity of MIRHA depends on the amorphous state of MIRHA particles and the high SiO<sub>2</sub> content. X-Ray Fluorescence (XRF) analysis was proficient in analyzing material contents inside MIRHA, hence the amount of SiO<sub>2</sub> can be observed. Table 4.1 shows various chemical oxide contents of MIRHA from XRF analysis.

Table 4.1 Chemical Composition

Chemical Content	MIRHA	SF	FA
	Mass Content (%)	Mass Content (%)	Mass content (%)
Silicon dioxide or silica (SiO <sub>2</sub> )	90.75	96.355	51.19
Aluminum oxide or alumina (Al <sub>2</sub> O <sub>3</sub> )	0.75	0.21	24.0
Iron oxide (Fe <sub>2</sub> O <sub>3</sub> )	0.28	0.77	6.6
Calcium oxide or lime (CaO)	0.87	0.24	5.57
Magnesium oxide or magnesia (MgO)	0.63	0.52	2.40
Sodium oxide (Na <sub>2</sub> O)	0.02	0.118	2.12
Potassium oxide (K <sub>2</sub> O)	3.77	1.01	1.14
Equivalent alkalis (Na <sub>2</sub> O + 0.658 K <sub>2</sub> O)	2.50	0.07	1.59
Titanium oxide (TiO <sub>2</sub> )	0.02	-	-
Phosphorous oxide (P <sub>2</sub> O <sub>5</sub> )	2.5	0.13	-
Manganese oxide (MnO)	0.08	-	-
Sulfur trioxide (SO <sub>3</sub> )	0.33	0.55	0.88
Others			
Sulfur (S)	< 0.01		
Carbon (C)	0.15		
Chloride (Cl):	110 g/t		

As a comparison Table 2.10 illustrates chemical contents of RHA with different burning temperatures. Higher loss on ignition (LOI) is related to lower silica content. MIRHA LOI was found to be less than 12%, which is in accordance with the ASTM requirement [84]. Hwang, Lung, and Chandra [8] noted that the oxide content of SiO<sub>2</sub> and K<sub>2</sub>O are able to lower the heat evolution in concrete gives lower hydration process. The use of pozzolanic material in concrete strength development in early days but higher in later days, compared to normal concrete [8]. The chemical composition of MIRHA in this research is also positioned within the result trends obtained by Hwang and Wu [9], as shown in Table 2.10. As far as SiO<sub>2</sub> is concerned MIRHA has the highest content compared to the different types of RHA [9] and Fly ash.

### 4.2.3 Particle Size Distribution and Surface Area

In this study, MIRHA particle sizes were found less than these of cement. Therefore, it was able to fill voids between cement particles that effectively produce calcium silicate hydrate in the hardened state. Comparison of MIRHA gradation and cement can be seen in Figure 4.3.

The specific surface area of MIRHA (Table 3.2) was 7,810 m<sup>2</sup>/kg, about 17.3 times that of OPC. The specific surface area of cementing material or binder influences the strength of FC. The finer the binder, the higher is the strength of concrete. Hence, the higher specific surface area of MIRHA indicates that it would produce a good development of compressive strength in FC. In contrast, the incorporation of MIRHA would cause a reduction in the flowing ability of FC. This was because the increase in specific surface area results in a greater water demand and reduces the amount of free water available in concrete mixture. Particle size distribution of MIRHA as seen in Figure 4.3 was not similar to the other binder namely OPC, silica fume and fly ash

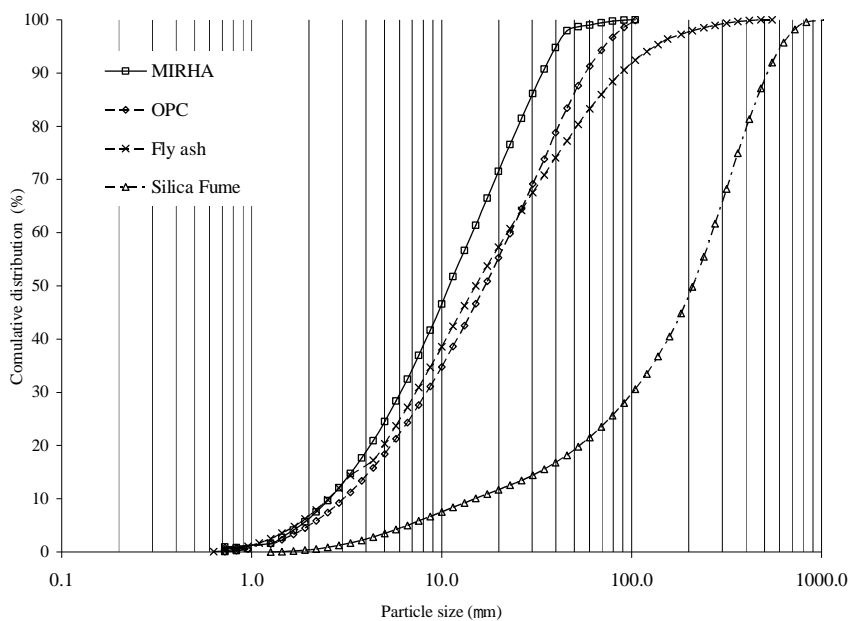


Figure 4.3 Comparison of MIRHA gradation to cement, fly ash and silica fume

#### 4.2.4 Accelerated Pozzolanic Strength Activity Index (APSAI)

The accelerated pozzolanic strength activity index of MIRHA with OPC was obtained according to the procedure, as given in ASTM C 1240 (2004). Figure 4.4 shows that the APSAI of MIRHA was 92.3%, which was much higher than 85%, the minimum requirement for silica fume [35]. This was due to extremely high specific surface area of MIRHA. The APSAI of MIRHA was lower than the control but higher than silica fume and fly ash, it indicated that it gave slightly bigger effect in the strength development at the early ages of concrete than silica fume and fly ash.

The APSAI of RHA was generally greater than that of other supplementary cementing materials such as silica fume [78]. It was due to the specific surface area of RHA which was much higher than that of fly ash and ground granulated blast-furnace slag, and even silica fume.

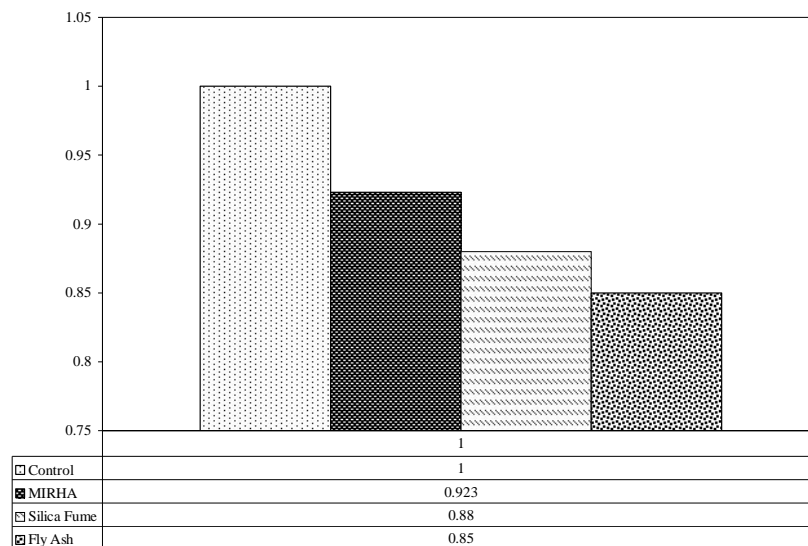


Figure 4.4 The accelerated pozzolanic strength activity index

It could be concluded that MIRHA had the ability to accelerate the early strength reaction compared to silica fume and fly ash. The APSAI of MIRHA obtained was 4.89% and 8.59% higher than silica fume and fly ash respectively. These were caused by the amorphousness, silica content and the large surface area of MIRHA which was highly effective to react with CH and produce large amount of C-S-H. This C-S-H latter will promote the acceleration of concrete strength development.

#### 4.2.5 Water Demand of Mix Constituent

In order to maintain stability of foam in the mixture, proper water demand calculation need to be established before the experimental works. Since OPC and MIRHA were two different materials utilized in the mixture, the calculation on water demand adopted need to differentiate between for OPC and MIRHA.

The spread test for cement was illustrated in Figure 4.5. The water demand of cement used in this investigation was taken to be 35% of cement weight, which means the minimum water cement ratio of 0.35 was required to prevent the water absorption from mixture by cement. The reference line was shown in Figure 4.5 and Figure 4.6.; this line was adopted from the Kearsley's study [39] to obtain the water demand of cement.

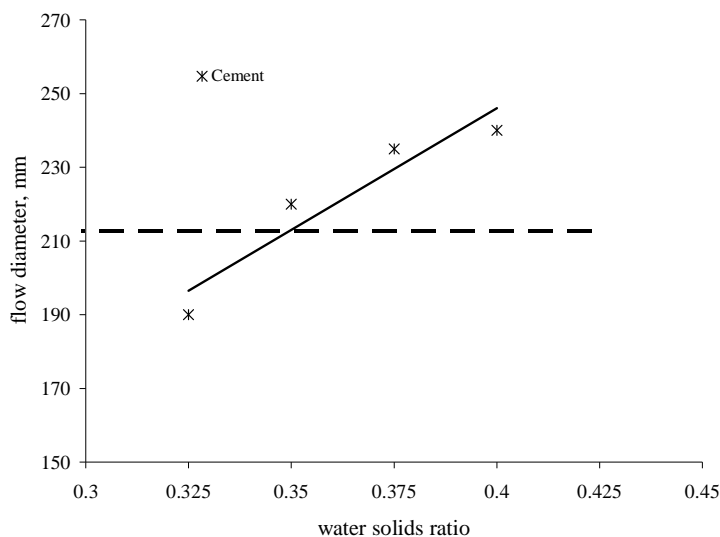


Figure 4.5 Water demand of cement

Meanwhile, as described in Figure 4.6, the water demand of MIRHA was observed to be 34.5% of MIRHA weight. It means that 0.345 liter of water will be needed for one kg of MIRHA used in the mixture.



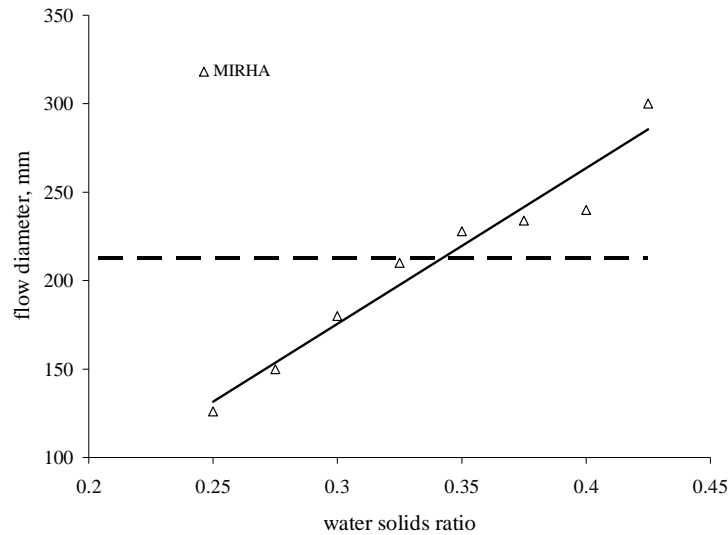


Figure 4.6 Water demand of MIRHA

From the two figures on the analysis of water demand by MIRHA and cement, it was found that 0.345 water cement ratio gave the minimum flow diameter spread for FC; that is 200 mm. Therefore in this research a water cement ratio of 0.35 was adopted as the min w/c for the mixes.

#### 4.3 Plastic Density and Cube Strength Repeatability of a Single Mix

To ensure the reliability of the plastic density, 6 sample measurements were taken based ASTM standard [122]. The FC-8 was adopted as it demonstrated the highest dry density amongst all mixes. Table 4.2 shows the statistical analysis of the reliability by of FC-8 mix.

It can be seen that the casting densities obtained ranged from 1693 to 1753 kg/m<sup>3</sup>. The standard deviation and coefficient of variation of FC casting density were 28.24 kg/ m<sup>3</sup> and 1.64% respectively. Similarly, the 3, 7, 28, 90 and 180 days measurements of 50 mm cube compressive strengths of the six cubes exhibited standard deviations and coefficients of variance between 0.7 and 1.01 N/mm<sup>2</sup> and between 1.55 and 15.47% respectively. Therefore, the repeatability strength test was satisfactory, with coefficient of variance values of less than 10% [22] (except at 3 days). This analysis confirmed that the repeatability for laboratory-produced normal weight concrete was within the stipulated requirements.

Table 4.2 Repeatability of mix FC-8 casting density and 50 cube compressive strengths

Mix no	Actual casting density (kg/cm <sup>3</sup> )	Compressive strength (N/mm <sup>2</sup> ) at different ages (days)				
		3	7	28	90	180
FC8-1	1736	6.7	13.1	25.8	39.8	51.9
FC8-2	1705	4.6	10.8	24.0	38.6	50.8
FC8-3	1752	6.5	12.5	25.4	40.1	51.8
FC8-4	1694	4.9	11.8	24.3	38.3	50.0
FC8-5	1753	6.3	13.4	25.1	39.1	51.7
FC8-6	1693	5.6	11.4	24.4	38.2	50.6
Mean	1722	5.8	12.2	24.8	39.0	51.1
Standard Deviation	28.24	0.89	1.01	0.70	0.80	0.79
Coefficient of Variation %	1.64	15.47	8.32	2.82	2.06	1.55

#### 4.4 Orthogonal Array

The orthogonal array approach is a tool used to achieve the objective of this study that is explained in detail in section 2.5.4.

##### 4.5.1. Workability of Foamed Concrete

Table 4.3 shows the spread test results of the various mixes with the mean spread measurement diameter ranging between 13.7 cm and 31.8 cm.

The main effect plot by each factor for spread test of FC is shown in Figure 4.7. The degree of contribution of each factor was clearly calculated by analysis of variance (ANOVA). This is to understand the influence of there factors to the spread test of FC (Table 4.4). The critical value of F at 95% probability level (3.411) is much lower than the observed value of F-statistic 325.86, 1573.70, 657.01, 96.51 and 50.88 for MIRHA content, w/c, s/c, SP and foam respectively. This means that the factor which contributes to the sum of the squares is within the confidence level.

Table 4.3 Test results of spread test for MIRHA-FC

Mixes	Spread test (cm)
FC- 1	26.3
FC-2	25.0
FC-3	24.4
FC-4	24.3
FC-5	26.9
FC-6	24.4
FC-7	25.8
FC-8	19.5
FC-9	31.3
FC-10	29.2
FC-11	17.1
FC-12	17.2
FC-13	31.8
FC-14	23.6
FC-15	18.0
FC-16	13.7

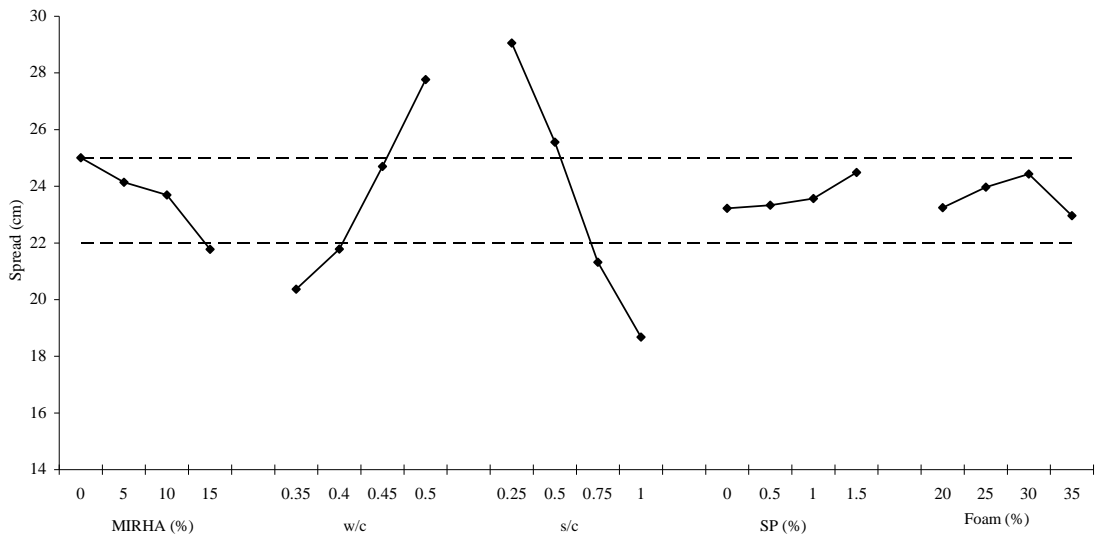


Figure 4.7 Main effect plot for Spread test

Table 4.4 Analysis of variance results of Workability of foamed concrete

Parameter	statistical parameters	Workability
MIRHA	Degree of freedom (DoF)	3
	Sequential sum of square (SSS)	175.47
	Adjusted sum of square (ASS)	175.47
	Mean square /variance (MS)	58.49
	<i>F-statistic</i> ; $F_{0.5} (3,13)$	325.86
	Contribution (%)	12.06%
w/c	DoF	3.00
	SSS	847.41
	ASS	847.41
	MS	282.47
	<i>F-statistic</i> ; $F_{0.5} (3,13)$	1573.70
	Contribution	58.03%
s/c	DoF	3.00
	SSS	353.79
	ASS	353.79
	MS	117.93
	<i>F-statistic</i> ; $F_{0.5} (3,13)$	657.01
	Contribution (%)	24.07%
SP	DoF	3.00
	SSS	51.97
	ASS	51.97
	MS	17.32
	<i>F-statistic</i> ; $F_{0.5} (3,13)$	96.51
	Contribution (%)	3.96%
foam	DoF	3.00
	SSS	27.40
	ASS	27.40
	MS	9.13
	<i>F-statistic</i> ; $F_{0.5} (3,13)$	50.88
	Contribution (%)	1.88%

Table 4.4 explains the component statistical of each parameter which consists of degree of freedom (DoF), sequential sum of square (SSS), adjusted sum of square (ASS), mean square variance (MS), F-statistic and Contribution. The SSS and ASS has same value for orthogonal design. The MS value equal to the SS divided by the DoF. The F statistic, is defined the ratio of variance due to the effect of a factor and variance due the error term. The percent contribution for any factor is obtained by dividing the pure sum of squares for that factor by total of sum of square total and

multiplying the result by 100. For example, The SSS and ASS value on the parameter w/c was almost five times higher than MIRHA. This value explains the influence of the contribution of w/c greater than MIRHA to the workability of FC.

Figure 4.7 shows the lower (220 mm) and upper (250 mm) values of the spread workability test values. All the critical values attached to MIRHA, w/c, s/c, SP and foam were within the stipulated ranges.

#### **a. Effect of MIRHA Content**

In Figure 4.7 FC incorporating MIRHA shows lower spread result than normal FC. The spread measurement decreased with the increase of MIRHA percentage, at was due to the high specific surface area of MIRHA, which increased the water demand. This was mainly due to the adsorptive character of MIRHA cellular particles, thus FC containing MIRHA required more water for a given consistency. However, for FC with high water cement ratio, addition of MIRHA could improve the concrete stability since it absorbed water and was able to reduce the tendency towards bleeding and segregation. The addition of MIRHA truly absorbs large amount of water in the mixture, and it also needed superplasticizer (SP) with specific amount to increase the workability and reached the similar slump as control concrete. The increment in percentage of MIRHA added was followed with the increment in percentage of SP used. The contribution of MIRHA parameter to achieve the required consistency of FC was 12.06%. A stabled and consistent FC can be achieved with 5 to 15% of MIRHA because there percentage inclusions were in the spread rest range proposed.

#### **b. Effect of water cement ratio**

Workability of FC was significantly affected by water cement ratio factor as shown by F-test value 1573.30 that was more than F-test criteria 3.411. Moreover, w/c parameter's contribution to create the consistency of FC was the highest compared to the other parameters i.e. 58.03% (Table 4.4) and Table 4.6 shows that w/c has medium level in the classification of the effect constituent on workability.

Increasing water cement ratio would affect the enhancement of mixture consistency. According to the criteria of good stability and consistency, the range of

water cement ratio for FC was obtained to be between 0.4 and 0.45 with 220 to 250 mm spread range (see Figure 4.7). This range was classified as medium level in spread percent range based on the classification of FC study by Nambiar [25]. The other comparison shows that this range was higher than the required value for flowing properties, which is 200-mm in spread range [60].

#### **c. Effect of sand cement ratio**

According to literature [68], the workability of FC was affected by the sand cement ratio (s/c). This was supported by sand cement ratio contribution on FC workability i.e. 24.07%. Figure 4.7 depicts that increasing of sand cement ratio would decreasing the workability. This was because the amount of solid volume increased in the same water cement ratio. In consequence, the water solid ratio was reduced and it decreased the consistency. The result also show that the effects of higher sand cement ratio can be either eliminated or reduce the paste volume of mortars. This is consistent with the results from FC workability tests.

#### **d. Effect of superplasticizer**

As shown in Figure 4.7, the adding of SP increases the workability of FC. Due to the mechanism of action of SP [56], the surface potential of all cement phases becomes negative that they start repelling each other. Generally, there are four main clinker phases of cement namely  $C_2S$ ,  $C_3S$ ,  $C_3A$ , and  $C_4AF$ . The chemical compounds of these SP's get grafted on them.  $C_2S$  and  $C_3S$  have a negative zeta-potential while  $C_3A$  and  $C_4AF$  have a positive zeta-potential in the fresh stage. This leads faster coagulation of the cement grains. In principle, SP directly adsorb to the surface and changes its characteristics. It was discussed in detail in section 2.2.4. The value range of SP to have stable and consistent FC was 0.5 to 1.5 (220-250 mm spread). 3.96% was the contribution of SP value to improve workability of FC.

#### **e. Effect of Foam Content**

As shown in Figure 4.7, all foam content percentages fulfilled the workability requirement. Above the level of 30%, it indicates the workability decreased because the mechanism of the adhesion between the bubbles and solid particles in the mixture.

If the amount of foam is increased, it reduces the spread-ability. However, below the level of 30% shows the workability increases as the percentage foam content increases where the foam was assumed as “aggregate” in mortar. Large amount of foam will reduce the friction between particles in FC. Foam has minimum contribution to create the workability of FC as shown in ANOVA analysis.

Overall view of the effects of constituent of MIRHA-FC on workability is summarized in Table 4.5. Based on this table, MIRHA-FC workability is strongly influenced by the w/c, because of any of the following reasons: (i) the key factor to overcome the friction between solid particles and bubbles (ii) to maintain the MIRHA had adsorptive characters.

Table 4.5 The summary of the effect of constituent on workability

The Criteria	Effect of MIRHA	Effect of w/c	Effect of s/c	Effect of SP	Effect of foam
Desired level	5-15%	0.4-0.45	0.5-0.75	0.5-1.5%	20-35%
Characteristic	Incorporating MIRHA showed lower result than normal FC	Increases in water cement ratio affected for enhancing the consistency of the mix	The consistency to be low with enlarging s/c	Adding SP gave a little development on workability	30% was optimum level consistency of FC
Contribution (%)	12.06	58.03	24.07	3.96	1.88
Explanation	The MIRHA had adsorptive character as cellular particles, thus FC containing MIRHA required more water for a given consistency	The key factor that overcome the friction between solid particles with bubbles in FC.	The value of s/c determined the water solid ratio in FC	The mechanism of action of SP overcome the surface potential of all cement phases becomes negative that they start repelling each other	Above the level of 30%, it indicated the workability occurs because of the adhesion between the bubbles and solid particles. However, below the level of 30% shows dominate mortar workability..

Table 4.6 Classification of the effect constituent on workability

Constituent	Class designation	Contribution values (%)	Description
MIRHA, SP and foam	VL	0-20	Very Low
s/c	L	21-40	Low
w/c	M	41- 60	Medium
-	H	61-80	High
-	VH	81-100	Very High

#### 4.5.2. Dry Density of FC

The results from this experiment are shown in tabular form in Table 4.7. A statistical analysis was performed using the response data to find out the statistically significant factors. The data analyses are presented in Table 4.8, and plotted in Figure 4.8.

Table 4.7 Test results of dry density test for MIRHA-FC

Experiment number.	Density(kg/m <sup>3</sup> )
FC- 1	1604
FC-2	1502
FC-3	1397
FC-4	1295
FC-5	1261
FC-6	1442
FC-7	1467
FC-8	1636
FC-9	1413
FC-10	1443
FC-11	1354
FC-12	1468
FC-13	1256
FC-14	1239
FC-15	1476
FC-16	1565

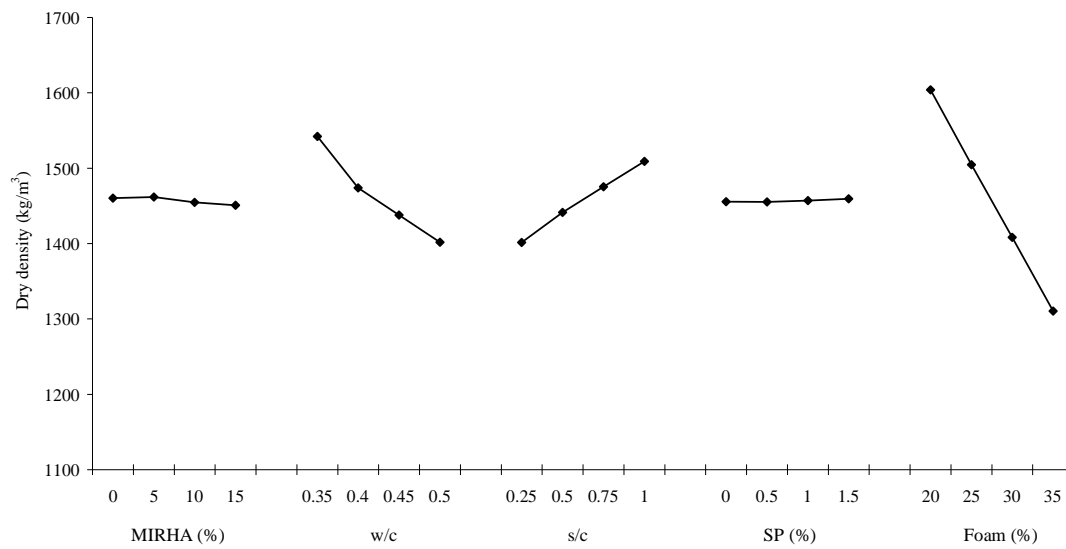


Figure 4.8 Main effect plot for 180 days dry density



Table 4.8 Analysis of variance results of 180 days dry density

Parameter	statistical parameters	Dry Density
MIRHA	Degree of freedom (DoF)	3
	Sequential sum of square (SSS)	1829
	Adjusted sum of square (ASS)	1829
	Mean square /variance (MS)	610
	<i>F-statistic</i> ; $F_{0.5} (3,13)$	0.29
	Contribution (%)	0.12%
w/c	DoF	3
	SSS	153429
	ASS	153429
	MS	51143
	<i>F-statistic</i> ; $F_{0.5} (3,13)$	24
	Contribution	9.81%
s/c	DF	3
	SSS	263657
	ASS	263657
	MS	87886
	<i>F-statistic</i> ; $F_{0.5} (3,13)$	42
	Contribution (%)	16.85%
SP	DF	3
	SSS	248
	ASS	248
	MS	83
	<i>F-statistic</i> ; $F_{0.5} (3,13)$	0.04
	Contribution (%)	0.02%
Foam	DF	3
	SSS	1145138
	ASS	1145138
	MS	381713
	<i>F-statistic</i> ; $F_{0.5} (3,13)$	181
	Contribution (%)	73.20%

#### **a. Effect of MIRHA Content**

It can be seen from Figure 4.8, that increase in MIRHA content did not significantly decrease the dry density. This was due the fact that the amount of MIRHA as cement substitution was too small. A closer look at the data of Figure 4.8, the MIRHA FC dry density was slightly decreased in all percentages composed to that of the normal FC. Absorptive character of MIRHA, which was absorbing water during mixing process, had interrupted the cement hydration process to produce  $\text{Ca(OH)}_2$ . With insufficient amount of  $\text{Ca(OH)}_2$ , pozzolanic reaction could not occur properly and resulted in lower calcium silicate hydrate (C-S-H) gels being produced. FC pores and water-filled spaces that were expected to be filled with C-S-H gels existed in large number and it explained the lower dry density result of MIRHA FC concrete compared to normal FC concrete. The ineffective hydration process also had an effect on the irregular pores distribution. The contribution of MIRHA is similarly no effect to reduce the density, as can be seen in Table 4.8 (0.12% only).

#### **b. Effect of water cement ratio**

The study of effects of water cement ratio (w/c) with four levels was performed in Figure 4.8. In this figure, the density of FC decreased on the water cement ratio increased. This was due to space left after access water has been removed. The volume of space depends primarily on the water cement ratio.

#### **c. Effect of sand cement ratio**

Aggregate has several advantages for concrete e.g. higher volume stability; more durable than hydrated cement paste alone. The effect of sand cement ratio on the density of FC has contradictive impact compared to with MIRHA and w/c. Adding greater the amount of aggregate, the density will be increased [44, 68]. These results can be explained very clearly that high sand cement ratio produces a low ratio water to solid. Low water/solid significantly increases the solid in concrete.

#### **d. Effect of Superplasticizer**

In this study SP had little contribution to the FC density. It is because of the small amount of SP in mix proportion than other ingredient. In addition, SP was used to improve workability i.e. to facilitate the ease of placement and not directly correspond to the density of FC.

#### **e. Effect of Foam Content**

FC with higher foam content tends to produce larger air voids. Because of the closeness of the air voids, this yielded the higher incidence of void coalescing and forming larger air voids. The coalescence of void in FC may be due to the difference of surface tensions in different size of foam that creates different of pressure. The presence of water that surrounds the foam will affect the foam pressure. This gave the effect of diffusion changes in foam which was initially small to be big. This diffusion seems to be more dominant in lower density mixtures that contain lower solid mix content. Figure 4.8 shows the summary of these effects on dry density. The effective way to decrease the density was inserting more foam in mixes. As a result, Table 4.8 shows foam content has highest contribution (73.20%) for density of FC. Foam content is categorized high level in the classification of the effect constituent on dry density (see.

Table **4.10**).

Table 4.9 presents the general view of the effects of parameters of MIRHA FC on dry density. It can be summarized that foam content was the significant parameter to attain a low dry density MIRHA FC. It has a very obvious reason that by entering the amount of air through the foam in the mix is going to affect the density of concrete.

Table 4.9 The summary of the effect of constituent on dry density

The Criteria	Effect of MIRHA	Effect of w/c	Effect of s/c	Effect of SP	Effect of foam
Desired level	15%	0.5	0.25	1%	35%
Characteristic	Increasing MIRHA level does not significantly decrease the dry density	The decreasing density is influenced by water cement ratio increase	The effect of sand cement ratio has contradictive effect with MIRHA and w/c	SP performs little contribution best possible value to build the lightest density	FC with higher foam content tends to construct in larger air voids.
Contribution (%)	0.12	9.81	16.85	0.02	73.20
Explanation	Absorptive character of MIRHA, which was absorbing water during mixing process, had interrupted the cement hydration process to produce Ca(OH) <sub>2</sub> .	This is due to space left after access water has been removed. The volume of space depends primarily on the water cement ratio	These results can be explained very clearly that high sand cement ratio produces a low ratio of solid water.	it may be SP is only workable admixture to facilitate the ease of placement and the resistance and not directly construct the density of FC	The closeness of the air voids, which yields to higher interconnectivity of void coalescing and forming larger air voids

Table 4.10. Classification of the effect constituent on dry density

Constituent	Class designation	Contribution values (%)	Description
MIRHA, s/c, w/c and SP	VL	0-20	Very Low
-	L	21-40	Low
-	M	41- 60	Medium
Foam	H	61-80	High
-	VH	81-100	Very High

### 4.5.3. Compressive Strength of FC

Compressive strength was determined at the age of 3, 7, 28, 90 and 180 days. Table 4.11 presents the compressive strength results in N/mm<sup>2</sup> of the 16 trial mixture proportions. The results show that 3, 7, 28, 90 and 180 days strength were obtained in the range of 1.2-6.9, 2.3-12.6, 5.5-28.1, 13.9-47.3 and 12-57.9 N/mm<sup>2</sup> respectively.

The highest and the lowest compressive strength were obtained from FC-4 and FC-10 respectively. The summary of main effect plot for 3 to 180 days compressive strength of FC is shown in Figure 4.9. The degree of contribution for each factor for 3, 7, 28, 90 and 180 days compressive strength of FC was statically calculated and shown in Table 4.12.

Table 4.11 Test results of compressive strength for FC

Experiment Number	Compressive strength (N/mm <sup>2</sup> ) at different ages (days)				
	3	7	28	90	180
FC- 1	3.2	8.3	17.1	27.7	34.7
FC-2	6.4	12.2	26.8	43.6	52.2
FC-3	3.1	5.9	13.4	31.1	27.5
FC-4	1.2	2.3	5.5	13.9	12.0
FC-5	4.2	7.5	17.4	27.8	36.7
FC-6	4.6	11.0	20.3	33.8	42.4
FC-7	4.1	7.2	17.3	26.3	34.4
FC-8	5.8	12.2	24.8	39.0	51.1
FC-9	6.0	11.2	25.5	44.2	55.8
FC-10	6.9	12.6	28.1	47.3	57.9
FC-11	3.1	7.4	14.5	25.6	33.0
FC-12	4.5	8.3	19.1	37.9	42.6
FC-13	3.0	5.8	13.2	21.3	26.5
FC-14	4.0	7.6	16.8	26.6	31.9
FC-15	5.1	9.7	21.4	34.7	41.8
FC-16	3.6	9.2	17.3	32.5	35.5

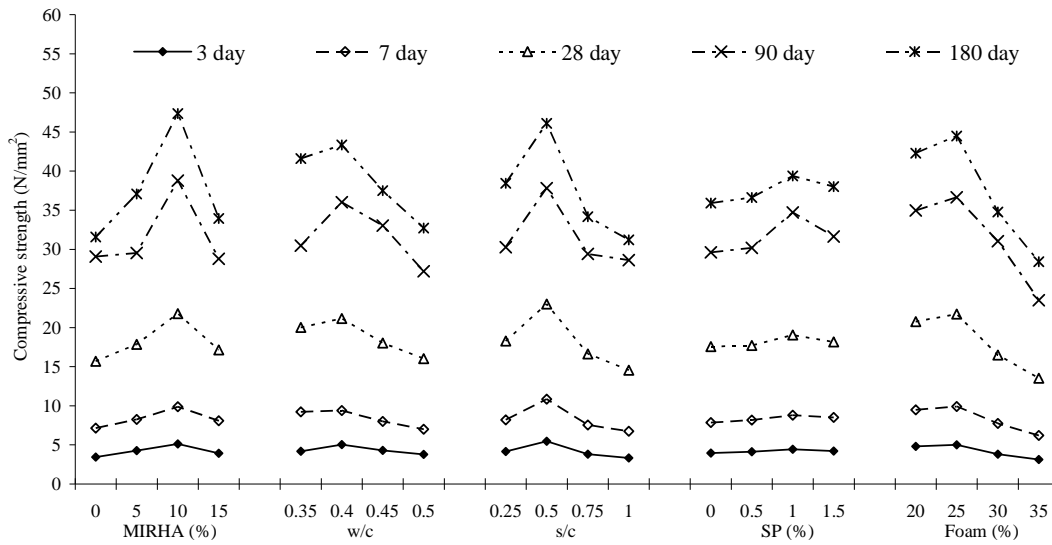


Figure 4.9 Summary of main effect plot for compressive strength

Table 4.12 Analysis of variance results of compressive strength for FC

Parameter	statistical parameters	Compressive strength at different ages (days)				
		3	7	28	90	180
MIRHA	DoF	3.0	3.0	3.0	3.0	3
	SSS	35.6	91.7	490.9	1682.9	3479
	ASS	35.6	91.7	490.9	1682.9	3479
	MS	11.9	30.6	163.6	561.0	1160
	<i>F</i> -statistic; $F_{0.5}(3,411)$	3.48	17.6	11.8	9.0	19
	Contribution	20%	15%	17%	25%	28%
w/c	DoF	3.0	3.0	3.0	3.0	3
	SSS	60.4	227.6	931.0	1294.3	3006
	ASS	60.4	227.6	931.0	1294.3	3006
	MS	20.1	75.9	310.3	431.4	1002
	<i>F</i> -statistic; $F_{0.5}(3,411)$	5.9	43.7	22.4	6.9	17
	Contribution	34%	36%	32%	19%	24%
s/c	DF	3.0	3.0	3.0	3.0	3
	SSS	21.4	91.8	413.0	1014.1	1770
	ASS	21.4	91.8	413.0	1014.1	1770
	MS	7.1	30.6	137.7	338.0	590
	<i>F</i> -statistic; $F_{0.5}(3,411)$	2.1	17.6	9.9	5.4	10
	Contribution (%)	12%	15%	14%	15%	14%
SP	DF	3.0	3.0	3.0	3.0	3
	SSS	2.9	12.0	32.2	371.8	171
	ASS	2.9	12.0	32.2	371.8	171
	MS	1.0	4.0	10.7	123.9	57
	<i>F</i> -statistic; $F_{0.5}(3,411)$	0.3	2.3	0.8	2.0	1
	Contribution (%)	2%	2%	1%	5%	1%
Foam	DF	3.0	3.0	3.0	3.0	3
	SSS	56.9	208.1	1049.2	2470.4	3870
	ASS	56.9	208.1	1049.2	2470.4	3870
	MS	19.0	69.4	349.7	823.5	1290
	<i>F</i> -statistic; $F_{0.5}(3,411)$	5.6	40.0	25.2	13.2	22
	Contribution (%)	32%	33%	36%	36%	31%

#### a. Effects of MIRHA Content

Generally, normal FC had lower compressive strength than the MIRHA-FC. At the early ages (3 days of age), control MIRHA-FC samples had superior compressive strength than the normal FC. It was due to the fact that the pozzolanicity of MIRHA started almost immediately when mixed with the concrete. Additionally, the increasing percentage of MIRHA in the concrete directly led to the declining percentage of Portland cement used in the proportion. This reduced the production of

Ca(OH)<sub>2</sub> and slowed down the reaction with SiO<sub>2</sub> presented in MIRHA. On the other hand, pozzolanic material supported in achieving more consistent distribution of air voids by providing uniform outside layer on each bubble and thereby prevented merging of bubbles. In addition, the replacement level 5-10% MIRHA was found optimum to contribute void distribution maximally and facilitate the strength. However, the trend of 5-10% level was different with 15% level. The 15% level showed the decrease in the strength due to the excessive water absorption. The character of its pore structure in MIRHA led to excessive water absorption and yielded disordered foam distribution. This decreased the strength of the concrete.

At the age of 28 days, the average normal strength of FC without MIRHA was found 92.3% of the required strength for structural lightweight concrete, which is 17 MPa. On the other hand, the FC concrete mixes containing 5% and 15% MIRHA achieved 113.8% and 109.3% of the strength of normal FC. However, the 10% MIRHA enhanced the strength above the normal FC by 138.9%. Even at the age of 90 days, the compressive strength of 10% MIRHA mixes was about 33.3% higher than the strength of normal FC. Beyond 90 days, the compressive strength of 10% MIRHA was increased by up to 49.9% at the age of 180 days.

The contribution of the MIRHA to improve the FC strength was obtained in the range of 15 to 28%. In addition, the contribution of MIRHA on early age compressive strength of FC was achieved of 20% still lower than foam content and w/c contribution (see Table 4.12). MIRHA content contribution did not affect on early age compressive strength. The compressive strength versus age of MIRHA FC with effect of MIRHA is illustrated in Figure 4.10.

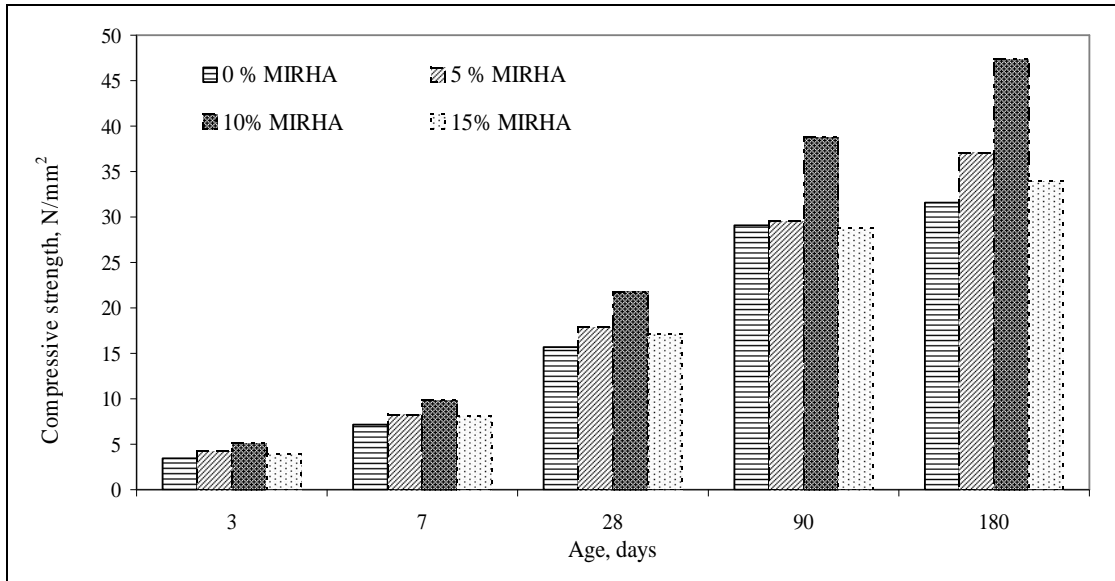


Figure 4.10 Compressive strength versus age of FC with effect of MIRHA

#### b. Effects of water cement ratio

The adequate amount of water and high pozzolanic reactivity were the main causes of the acceleration MIRHA react in the hydration process of concrete. When study the effect of w/c on compressive strength, similar found was observed up to 28 days. At w/c of 0.35 and 0.4 maximum compressive strength was found. This result was found in line with the water demand of cement and MIRHA as discussed in 4.2.5.

It was due to the optimum of amount water required to facilitate the hydration process using pozzolanic material with the  $\text{Ca(OH)}_2$  produced by OPC. However, when w/c exceeded 0.4, it retained the utilized water for the hydration reaction and contribute to the formation of capillary pores in foamed concrete that caused the decrease in the strength. Hakan's[123] suggested that decreasing w/c and increasing curing time would be able to reduce the pore width of the specimen which automatically enhances the strength. The contribution value of w/c factor to facilitate the strength of FC was in the range of 19 to 36%. The compressive strength versus age of MIRHA FC with respect to w/c is shown in Figure 4.11.



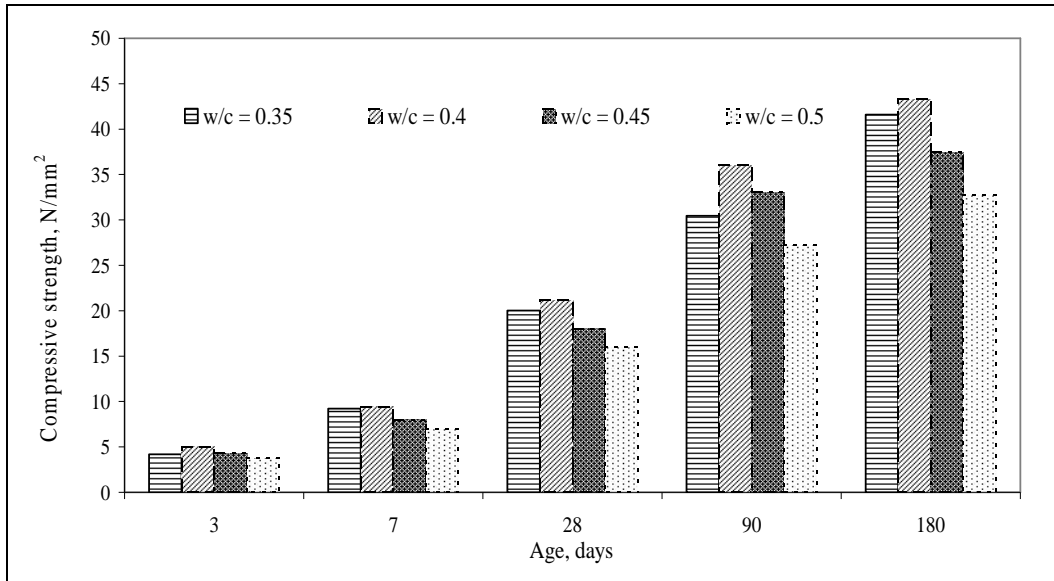


Figure 4.11 Compressive strength versus age of FC with various w/c

**c. Effects of sand cement ratio**

According to previous work [68], the compressive strength of FC was affected by the sand cement ratio (s/c). The high FC strength achieved for the mixes containing 0.25 s/c at the age of 7 days and 0.5 s/c at the age of 28 days and beyond. Figure 4.12 presents the compressive strength against age of MIRHA FC with various s/c values. The aggregate cement ratio indicated the amount of filler in the binder and the strength of the FC would decline if the amount of filler was raised.

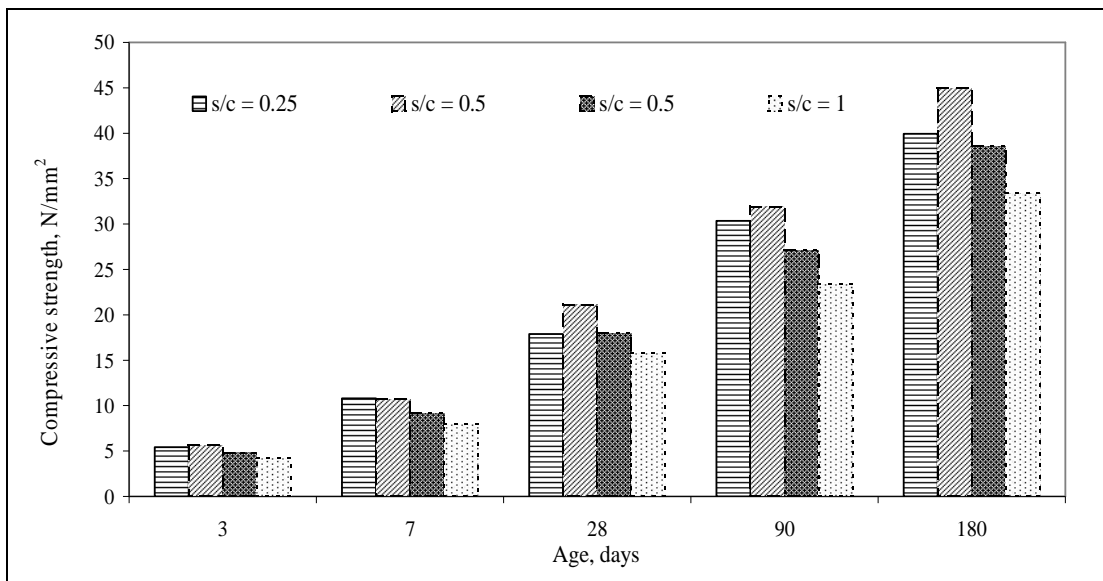


Figure 4.12 Compressive strength versus age of FC with various level of s/c

#### d. Effects of Superplasticizers

As shown in Figure 4.13, the strength of FC contains SP was higher than the strength of FC without SP. The highest strength was obtained when SP dosage was used as 1%. 1.5% dosage experienced the reduced strength which was due to disordered void distribution and the unsteadiness in the foam. Superplasticizers contributed value of SP to improve compressive strength in the range of 1 to 5%.

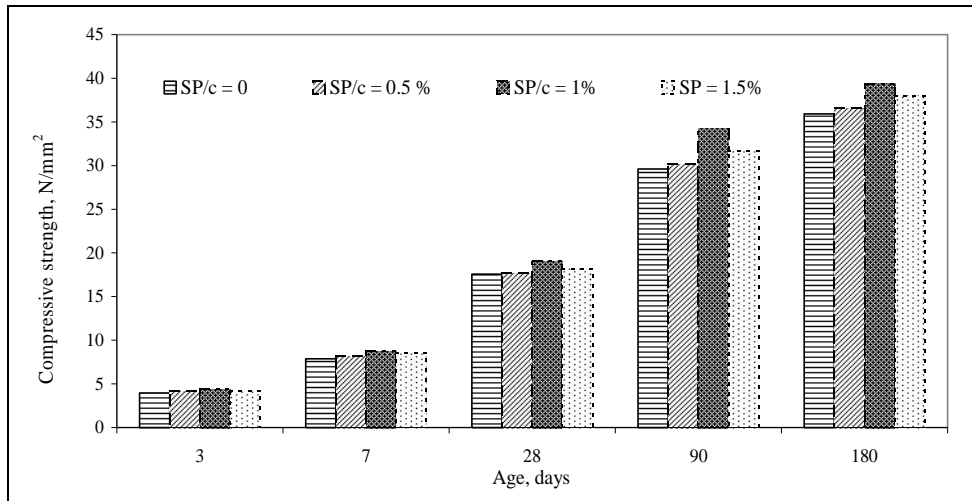


Figure 4.13 Compressive strength versus Age of FC with various level of SP

#### e. Effects of Foam Content

The presence of bubbles in the FC contributed significantly to the performance of FC. The strength of FC was significantly influenced by the volume of voids present. In addition, the volume of foam affects the interconnectivity of bubbles, so the void distribution and sizes are affected, and hence the spacing factor in the FC. The effects varied with different air contents but they affected the mechanical properties. However, as shown in Figure 4.14, the strength of FC which contains 20% foam did not demonstrate better compressive strength because the amount of foam was too small and the distribution was imperfect and uneven. So the bubble merger occurs in certain places [37]. This resulted in a fairly large space. This weakness reduced the compressive strength when tested. It was found that the optimum FC is 25% and higher compressive strength were obtained at all ages.

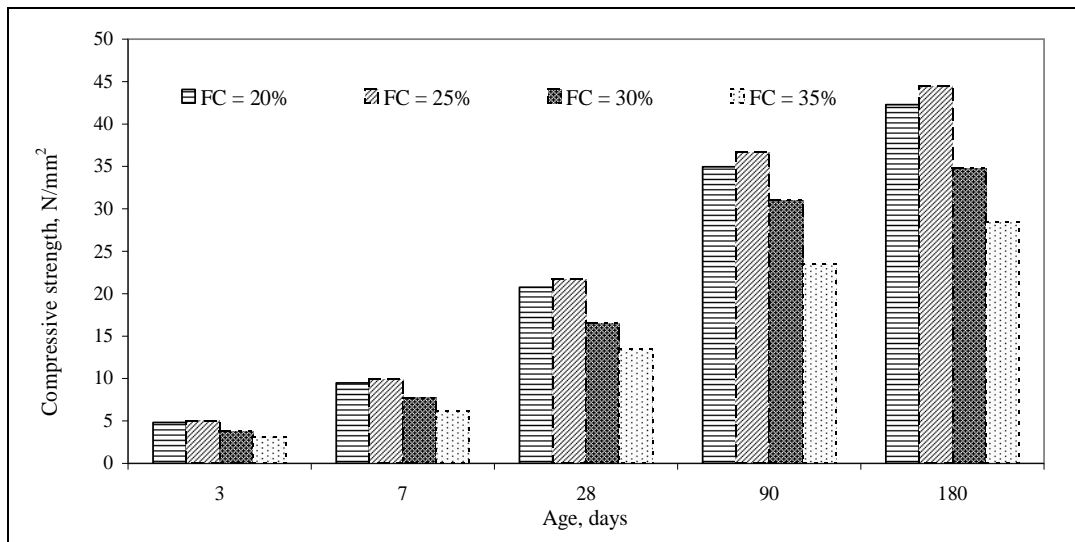


Figure 4.14 Compressive strength versus age of FC with various foam content

On the whole, the continuation of the effects of constituent of MIRHA FC on compressive strength is presented in Table 4.13. Table 4.14 shows that MIRHA, w/c and foam content are classified low level in the classification of the effect constituent on compressive strength. However, FC MIRHA compressive strength is dominated by these parameters. The reason of these parameters had significant contribution because of the reasons: (i) MIRHA facilitate the progress of hydration process and assist in the dissemination stage bubbles in fresh FC. (ii) w/c is a key parameter for the workability FC and hydration process of cement. (iii) Foam content determines the amount of voids in the concrete and the void space is a strong influence on the FC compressive strength.

Table 4.13 The summary of the effect of constituent on compressive strength

The Criteria	Effect of MIRHA	Effect of w/c	Effect of s/c	Effect of SP	Effect of fc
Desired level	10%	0.4	0.5	1%	25%
Characteristic	FC has located significantly the strength developments of normal FC lower than MIRHA FC	The water cement ratios with values 0.35 and 0.4 have similarity to achieve higher strength than the other w/c	The higher compressive strength FC is affected by the lower sand cement ratio (s/c)	The strength of FC which contains SP is higher than the strength of FC without MIRHA	Inserting more foams to the mixes will decrease strength
Contribution (%)	15-28	19-36	12-15	1-5	31-36
Explanation	It may be indicated that the pozzolanicity of MIRHA to accelerate the hydration process faster.	It may be affected by the optimum of amount water to facilitate the hydration process.	The aggregate cement ratio indicates the amount of filler in the binder.	For equal workability the addition of superplasticizer (SP) reduces the water/cement ratio	The presence of bubbles in the FC contributed the largest void in the mortar.

Table 4.14 Classification of the effect constituent on compressive strength

Constituent	Class designation	Contribution values (%)	Description
s/c and SP MIRHA, w/c and foam	VL	0-20	Very Low
	L	21-40	Low
	M	41- 60	Medium
	H	61-80	High
	VH	81-100	Very High

#### 4.5.4. Total Porosity of FC

Total porosity is the volume of voids in concrete that have an important impact on compressive strength of foamed concrete. In this study, porosity was measured for six cylinders of the size of 25.4 mm in diameter and 25.4 mm in height for each mix of foamed concrete, which were moist-cured for 180 days. The effect of MIRHA content, water cement ratio (w/c), sand cement ratio (s/c), superplasticizer content (SP), and foam content (fc) on FC are analyzed and discussed below.

Table 4.15 presents the 180 days porosity results of the sixteen mix proportions of FC. It was obtained in the range of 24.3% to 57.7%. The main effect plotted for 180 days porosity of FC is shown by Figure 4.15. The degree of contribution of the each significant factor for 180 days porosity of FC was calculated. The results are given in Table 4.16.

Table 4.15 180 days test results of Porosity for FC

Experiment number.	Porosity (%)
FC- 1	31.7
FC-2	24.3
FC-3	35.6
FC-4	57.7
FC-5	37.1
FC-6	34.0
FC-7	38.5
FC-8	37.8
FC-9	26.6
FC-10	25.7
FC-11	38.9
FC-12	32.6
FC-13	42.4
FC-14	38.7
FC-15	33.0
FC-16	36.6

Table 4.16 Analysis of variance results of porosity of FC

Parameter	Statistical parameters	180 days porosity
MIRHA	DoF	3
	SSS	735
	ASS	735
	MS	245
	<i>F</i> -statistic; $F_{0.5}(3.411)$	101
	Contribution	13.42%
w/c	DoF	3
	SSS	1379
	ASS	1379
	MS	460
	<i>F</i> -statistic; $F_{0.5}(3.411)$	190
	Contribution	25.17%
s/c	DF	3
	SSS	1088
	ASS	1088
	MS	363
	<i>F</i> -statistic; $F_{0.5}(3.411)$	150
	Contribution (%)	19.85%
SP	DF	3
	SSS	206
	ASS	206
	MS	69
	<i>F</i> -statistic; $F_{0.5}(3.411)$	28
	Contribution (%)	3.75%
FC	DF	3
	SSS	2071
	ASS	2071
	MS	690
	<i>F</i> -statistic; $F_{0.5}(3.411)$	285
	Contribution (%)	37.81%

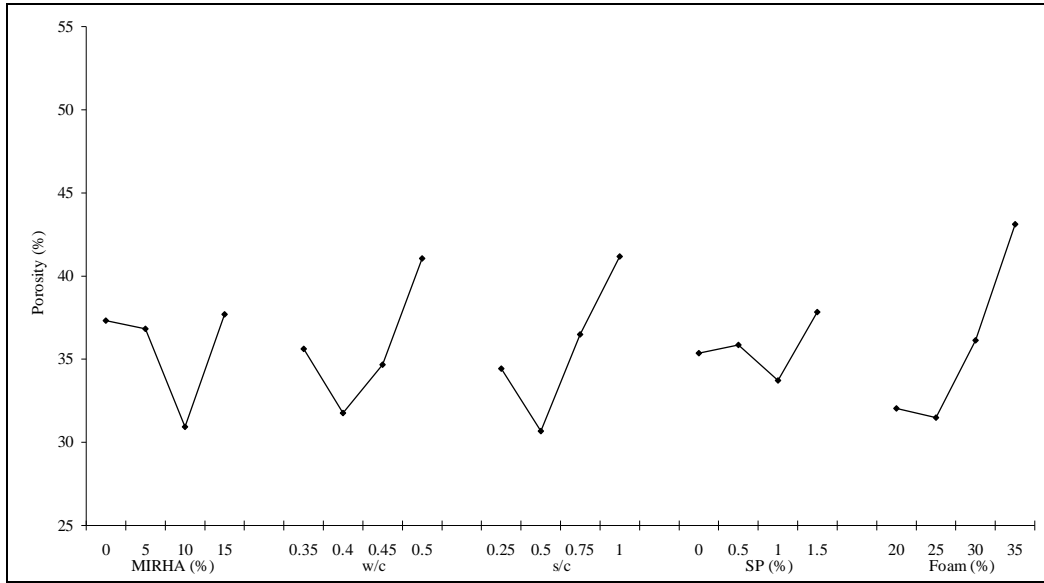


Figure 4.15 Main effect plot for porosity

In general, the parameters with each level have a similar effect on porosity of FC and depicted in Figure 4.15 (at 180 days). Various effects on porosity are discussed below.

#### a. Effect of MIRHA Content

In Figure 4.15, the porosity of normal FC was higher than MIRHA FC (except 15%). MIRHA with amorphous, silica content and the large surface area increased the hydration process and refined the pore structure of FC. The increase in hydration led to a reduction of calcium hydroxide (CH) in paste and increase in calcium silicate hydroxide (C-S-H) gels. 10% MIRHA showed lowest porosity in FC. The highest value of porosity 38% was achieved FC when incorporating 15% MIRHA. The contribution of MIRHA parameter to build the porosity of FC was attained 13.42%.

#### b. Effect of water cement ratio

It is a known fact that porosity increased as the water cement ratio increased. Figure 4.15 shows that except at the 0.35 level, the porosity against w/c follow the previous trend. Porosity decreased with the progress of hydration and 0.4w/c seemed to be optimum w/c level and the porosity increased as the w/c was increased beyond 0.4. At 0.35 w/c the moisture available for hydration process was insufficient and this

subsequently resulted in lack of C-S-H. As a consequence porosity of the concrete matrix increased. The contribution of w/c parameter to facilitate significantly the porosity of FC was in the value of 25.17%.

**c. Effect of sand cement ratio**

By and large high porosity occurred when the sand cement ratio was increased (see Figure 4.15). Sand had a larger diameter than the cement particles and when the sand grains were mixed with cement, physically and chemical interactions occurred. The sand cement ratio was large, meaning that the volume of cement to interact with when the aggregate decreased. Therefore it promoted space between aggregate. These spaces contributed to the increase in porosity of the concrete. The trend was not applicable to 0.25 s/c as the porosity increased when the s/c dropped below 0.5 s/c. Again this was attributed to the fact that 0.5 s/c was the optimum level below which the trend was not applicable affect holy. The contribution of s/c parameter to arrange the porosity of FC was in the value of 19.85%.

**d. Effect of Superplasticizer**

Figure 4.15 illustrates the effect of SP on FC porosity. The prime aim of the addition of SP was to reduce porosity. Even though SP was not part of hydration process but the mechanism of the SP was to increase the workability that ultimately would facilitate the hydration process. It is evident that 1% SP the optimum level as far as the porosity is concerned.

**e. Effect of Foam Content**

High foam content will cause porosity to rise as the foam content construct the main void space in the concrete matrix. As described in Figure 4.15, the optimum foam content is at 25% which also concurs with on compressive strength. Foam content is categorized low level in the classification of the effect constituent on porosity and also w/c. (see. Table 4.18). Table 4.17 presents the general observation of the effects of parameters of MIRHA FC on porosity. It can be concluded that foam content was the considerable parameter to accomplish a low porosity MIRHA FC. It

has an obvious reason that giving an amount of air through the foam into the mix is going to affect the porosity.

Table 4.17 The summary of the effect of constituent on porosity

The Criteria	Effect of MIRHA	Effect of w/c	Effect of s/c	Effect of SP	Effect of fc
Desired level	10%	0.4	0.5	1%	25%
Characteristic	The porosity of normal FC is higher than MIRHA FC	porosity increases because the water cement ratio was also raised. Except at the 0.35 level, those levels show does not follow the previous trend	High porosity was indicated by increasing sand cement ratio	Addition of SP is to reduce the porosity.	Enlarging foam content will cause porosity raised.
Contribution	13.4	25.17	19.85	3.75	37.81
Explanation	MIRHA with amorphousness, silica content and the large surface area increases the hydration and refines the pore structure of FC.	In the hydration process, water cement ratio has a very important role, especially the influence of chemical reaction of cement and CRM components.	The sand cement ratio is large, exactly the volume of cement to bind the aggregate decreases.	This indicates that the mechanism of the SP to work effectively to facilitate the hydration process.	It can be explained obviously foam content construct the main void space in the porosity property.

Table 4.18 Classification of the effect constituent on porosity

Constituent	Class designation	Contribution values (%)	Description
MIRHA, s/c and SP	VL	0-20	Very Low
w/c and foam	L	21-40	Low
-	M	41- 60	Medium
-	H	61-80	High
-	VH	81-100	Very High

#### 4.5 Optimum FC Mix Proportion

In order to confirm the optimum mix-design proportion obtained using the Taguchi's approach method, an experimental study was performed to check whether the compressive strength can be really maximized and dry density and porosity can be really minimized by the proposed optimum mixture proportions.



In order to acquire the significant results same materials and same conditions were used with the Taguchi analyses. Table 4.19 presents the optimal mix-design proportions in regards to the dry density, compressive strengths, and porosity.

Table 4.19 lists the optimal mix design verification test result and to be statistically completed. The results showed that the proposed optimum mix proportions satisfied the expected maximization for compressive strength and minimization for dry density and porosity.

As can be shown, the optimum dry densities obtained ranged from 1399 to 1505 kg/m<sup>3</sup>. The mean, standard deviation and coefficient of variance obtained were 1450 kg/m<sup>3</sup>, 40.59 and 2.8% respectively. The optimum dry density obtained in this research is to meet the standard for structural lightweight concrete application ASTM-C330 [26], i.e. less than 1680 kg/m<sup>3</sup>.

Similarly, the 3, 7, 28, 90 and 180 days measurements of 50 mm cube compressive strengths of the six mixes exhibited standard deviations and coefficients of variance between 0.7 and 1.01 N/mm<sup>2</sup> and between 1.55 and 15.47% respectively. As can be seen, the repeatability of 3, 7, 28, 90 and 180 day's strength values, in particular, were satisfactory, with coefficient of variance values of less than 10%. This analysis confirmed that compressive strength of MIRHA FC was more than 17 MPa at 28 days. This result is fulfilled as structural lightweight concrete requirement [26].

Table 4.19 Optimal mix-design proportions for properties of FC

Optimal mix Proportion	MIRHA (%)	w/c	s/c	SP (%)	fc (%)
Dry Density (kg/m <sup>3</sup> )	15	0.5	0.25	1	35
3d-compr. strength (N/mm <sup>2</sup> )	10	0.4	0.5	1	25
7d-compr. strength (N/mm <sup>2</sup> )	10	0.4	0.5	1	25
28d-compr. strength (N/mm <sup>2</sup> )	10	0.4	0.5	1	25
90d-compr. strength (N/mm <sup>2</sup> )	10	0.4	0.5	1	25
180d-compr. strength (N/mm <sup>2</sup> )	10	0.4	0.5	1	25
180d-porosity (%)	10	0.4	0.5	1	25

Table 4.20 Optimum mix-design verification test results

Data	180 days dry density (kg/cm <sup>3</sup> )	Compressive strength (N/mm <sup>2</sup> ) at different ages (days)					180 days porosity (%)
		3	7	28	90	180	
1	1472	12.7	15.5	27.3	41.5	50.6	32.7
2	1424	10.5	12.6	24.7	39.2	49.9	29.0
3	1478	13.2	13.6	26.4	39.7	50.5	32.2
4	1423	11.4	12.5	26.4	39.3	49.0	30.6
5	1505	12.7	15.3	27.7	41.0	52.1	34.2
6	1399	11.3	12.4	25.1	39.2	49.8	30.2
Mean	1450	12.0	13.7	26.3	40.0	50.3	31.48
Standard Deviation	40.59	1.06	1.42	1.18	1.00	1.07	1.90
Coefficient of Variation, %	2.80	8.88	10.43	4.50	2.51	2.12	6.03

#### 4.6 Summary

The following conclusions were drawn for effects of MIRHA on Mechanical Properties.

1. MIRHA as CRM in this study has the following characteristic i.e. partially-crystalline and high silica content, lower LOI, high specific surface area, APSAI has a value of nearly 1, high water demand. MIRHA was found to be an effective pozzolan as accelerator on early strength compared to silica fume and fly ash as described by APSAI obtained. Increasing amounts of MIRHA in the FC led to reduction in non-evaporable water contents ( $w_n$ ) as compared to the normal FC. The MIRHA FC mixes were found to use less water for hydration as compared to normal FC. The hydrate water content that indicated the chemically bound water in the C-S-H phase was highest for the MIRHA FC over at 3 days of hydration, while the normal FC showed the lowest value.
2. MIRHA-FC workability was strongly influenced by the w/c, because of the key factor to overcome the friction between solid particles and bubbles and to maintain the MIRHA had adsorptive characters.

3. On dry density, it can be summarized that foam content was the significant parameter to attain a low dry density MIRHA-FC. It has a very apparent reason that by entering the amount of air through the foam in the mix is going to affect the density of concrete.
4. The effects of constituent of MIRHA-FC on compressive strength was affected MIRHA, w/c and foam content which were classified low level in the classification of the effect constituent on compressive strength. MIRHA facilitate the progress of hydration process and assist in the dissemination stage bubbles in fresh FC. Water cement ratio was a key parameter for the workability FC and hydration process of cement. Foam content determines the amount of voids in the concrete and the void space is a strong influence on the FC compressive strength.
5. On porosity, it can be concluded that foam content was the considerable parameter to accomplish a low porosity MIRHA-FC. It has an obvious reason that giving an amount of air through the foam into the mix is going to affect the porosity.

## CHAPTER 5

### RESULT, ANALYSIS AND DISCUSSION ON HYDRATION CHARACTERISTIC

#### 5.1 Overview

This chapter discusses the result of experimental program namely (i) non-evaporable water by OD/FI and TGA experimental, (ii) change in non-evaporable water content due to the presence of MIRHA, (iii) FC degree of hydration with and without MIRHA, (iv) compressive strength correlations to non-evaporable water, porosity and gel-space ratio characteristic,

#### 5.2 The Non-Evaporable Water ( $w_n$ ) Analysis by OD/FI

Non-evaporable water content ( $w_n$ ) can be used to determine the degree of hydration. For normal FC with MIRHA, determining the degree of hydration using chemically bond water is complicated because it is difficult to separate the water associated with the reaction of the MIRHA in the hydrated cement. A previous study [106] showed that the effect of cement replacement material on the non-evaporable water per unit mass of binder was lower at all ages. It is due to the presence of lower cement content, the pozzolanic reaction of the CRM typically does not bind as much water as hydrated cement. However, an assumption that the CRM either does not react or contribute to chemically bound water is not totally true. Results of  $w_n$  obtained from OD/FI are shown in Table 5.1.

Table 5.1 Non-evaporable water content ( $w_n$ ) by OD/FI

MIRHA (%)	$w_{n/c}$ (g/g initial cement) at different ages (days)				
	3	7	28	90	180
0	0.101	0.116	0.131	0.147	0.153
5	0.1	0.115	0.129	0.145	0.15
10	0.096	0.111	0.126	0.14	0.145
15	0.089	0.102	0.116	0.129	0.134

The result of Table 5.1 is shown graphically in Figure 5.1. This figure includes  $w_n/c$  results versus time of all four mixtures. The  $w_n/c$  values of normal FC and MIRHA-FC had same similar develop according its age. This shows that MIRHA as CRM has similarities with properties of cement. However, the addition of MIRHA in mix proportion of FC to lead decline the  $w_n/c$  values than that of normal FC. It was due to the fact that to reduce amount of cement will cause the quantity of chemical water bound as  $w_n$  is reduced as well.

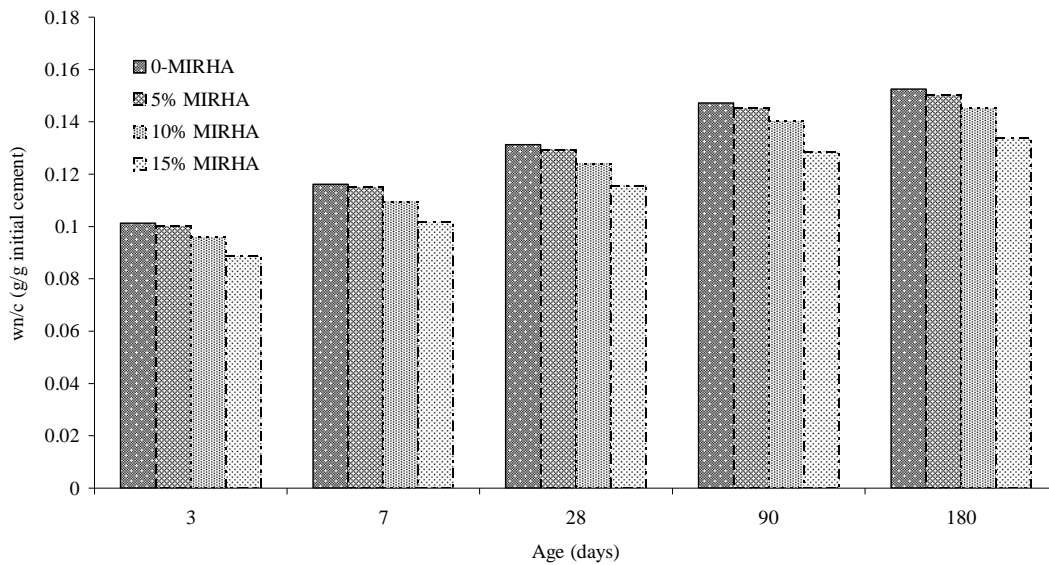


Figure 5.1 OD/FI Non-evaporable water content over time with MIRHA effect

### 5.3 The Non-Evaporable Water ( $w_n$ ) Analysis by TGA

TGA procedure was used to separate the chemically bound water attributed to CH, and to provide an indication of the  $w_n$  in the C-S-H stage. The non-evaporable water ( $w_n$ ) results from TGA measurements and analysis by Taguchi's method (section 4.4) is presented in Table 5.2. The table is divided into MIRHA percentage, specimen age

in day, C-S-H/AFm bound water (expressed as C-S-H/AFm), CH bound water (expressed as CH), and miscellaneous high temperature mass losses (expressed as Misc), as well as the total of mass loss from 105-900°C (expressed as  $w_n/c$ ).

Table 5.2 TGA results for FC

MIRHA (%)	Age (days)	Mass Loss (g/g initial cement)			
		C-S-H/AFm	CH	Misc	$w_n/c$
0	3	0.069	0.027	0.005	0.101
	28	0.091	0.036	0.005	0.132
	180	0.103	0.041	0.007	0.151
5	3	0.071	0.024	0.005	0.100
	28	0.093	0.031	0.006	0.130
	180	0.107	0.035	0.007	0.149
10	3	0.072	0.019	0.005	0.096
	28	0.095	0.025	0.006	0.126
	180	0.108	0.028	0.008	0.144
15	3	0.069	0.015	0.005	0.089
	28	0.091	0.019	0.006	0.116
	180	0.104	0.022	0.007	0.133

The same data in the table above are shown graphically in Figure 5.2. This figure is divided by  $w_n/c$  mass loss type and includes the results over time.

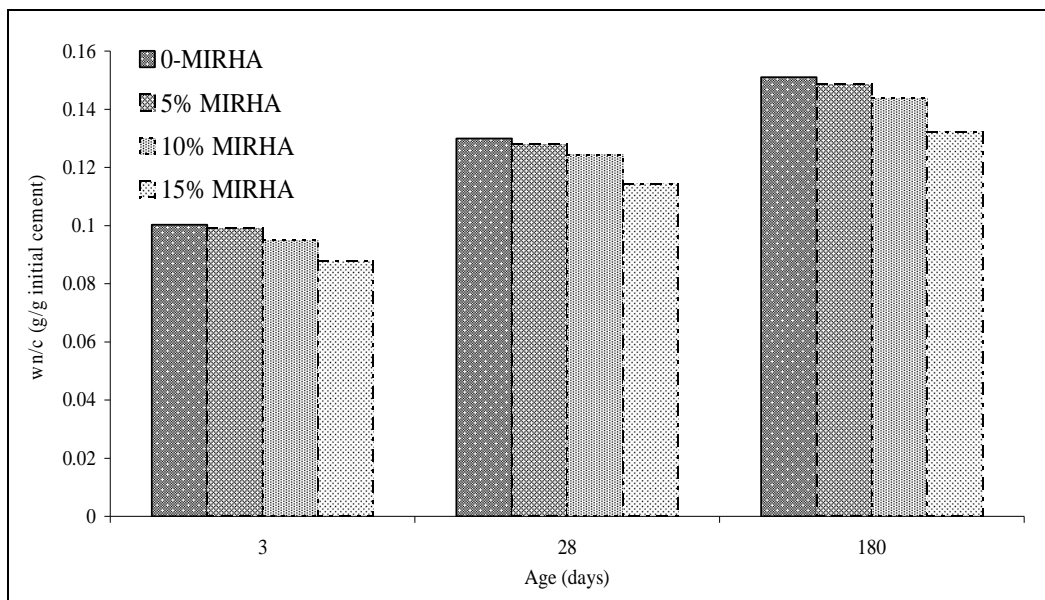


Figure 5.2 TGA Non-evaporable water contents over time

In general, the TGA non-evaporable water contents are matched with the OD/FI non-evaporable water contents. Based on the above discussion, the  $w_n$  that is incorporated with MIRHA has lower chemical water bound than the normal mix. This result was similar to that reported in previous work [80] that RHA inclusion in cement paste mix with water 30% of cement.

Reduction of  $w_n$  due to the addition of MIRHA on FC can be explained as follows:

- a. It was due to the fact that the increasing percentage of MIRHA in the FC mixes directly led declining percentage of OPC used in the proportion. To reduce amount of cement will cause the quantity of chemical water bound as  $w_n$  is reduced as well.
- b. MIRHA participates in three main reactions: (i) with unhydrated  $C_3S$  and water to form one type of C-S-H; (ii) with the CH to form a different C-S-H; and (iii) with existing C-S-H to yield a further modified hydrate. In incorporate the same quantity of  $C_3S$ , Adding MIRHA in system combines less water per gram of cement than does that for  $C_3S$  alone. Therefore, MIRHA serves to lower the amount of bound water in the system.
- c. MIRHA particles also serve to adsorb water, thus making the water unavailable for cement hydration. This adsorption thus increases the amount of evaporable water. In addition, the pozzolanic C-S-H is not only a different type of C-SH than that from cement hydration, but one that also adsorbs more water, thus decreasing the available hydration water further. Thus, MIRHA FC have lower  $w_n$  than normal FC.

From aforementioned discussion, it can be concluded that pozzolanic reaction of MIRHA alter the system hydration process, yielding lower non-evaporable water content FC.

#### 5.4 C-S-H and AFm Bound Water

CSH and AFM were the largest production in the cement hydration process. AFm is the shorthand notation for hydrated aluminate, ferrite and monosulfate phases. In the cement hydration equations, the C-S-H and CH are not the only hydration products formed in cement hydration. AS such, the Afm phases contain bound water which is removed during the TGA heating process,

The graphical representation of the C-S-H and AFm data over time (Table 5.2) is shown in Figure 5.3. For all mixtures, the over all trend is that the C-S-H and AFm bound water content increases over time.

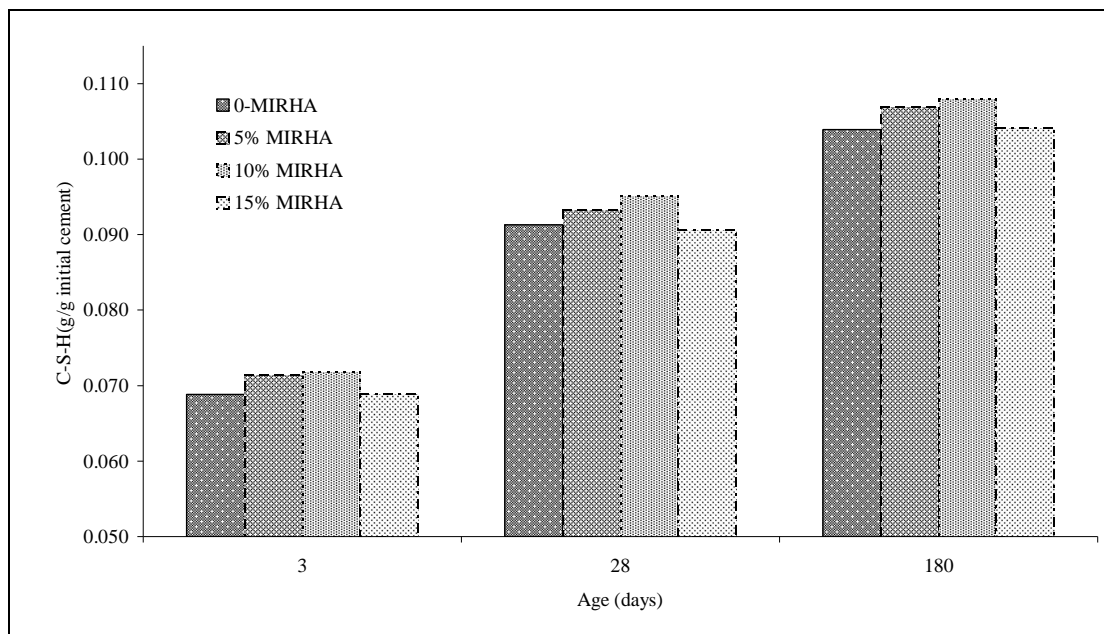


Figure 5.3 C-S-H and AFm bound water over time

The graphical representation of the C-S-H and AFm data over time (Table 5.2) is shown in Figure 5.3. For all mixtures, the over all a trend was that the C-S-H and AFm bound water content increases over time.

Since the majority of the  $w_n$  is result of C-S-H and AFm bound water, it was not surprising that the graph results for the C-S-H and AFm bound water (Figure 5.3) look very similar to those for the TGA non-evaporable water content (Figure 5.2).



The primary pozzolanic reaction, as described in section 2.3.3, is a conversion of CH to C-S-H. Other reactions, such as the modification of existing C-S-H can also occur. The most common type of C-S-H is created when pozzolanic material reacts with existing CH and converts to C-S-H. Another type of C-S-H can also be formed from the reaction of pozzolanic material with existing C-S-H thus creating a modified C-S-H. Nicole's study [124] mentioned that increasing the replacement level of RHA generally increased the amount of CaO in gel product. It may be the CaO content that enables the formation of C-S-H product.

## **5.5 CH Bound Water**

The calcium hydroxide (CH) contents of the chosen mixes at selected ages were verified using Thermogravimetry analysis. The mass loss corresponding to the temperature range of 420-520°C is taken as that associated with the decomposition of CH. CH content of normal FC can be used as a measure of the progress of hydration, but in FC modified with pozzolanic material, CH could be lower because of lower cement content or the pozzolanic reaction that consumes CH, or higher because of the enhancement in cement hydration in the presence of the pozzolana. Hence, in this study, normalized CH content ( $CH_{\text{normal}}$ ) is used which is defined in equation (2-26).

The results of the CH bound water contents that are collected from Table 5.2 over time are depicted in Figure 5.3.

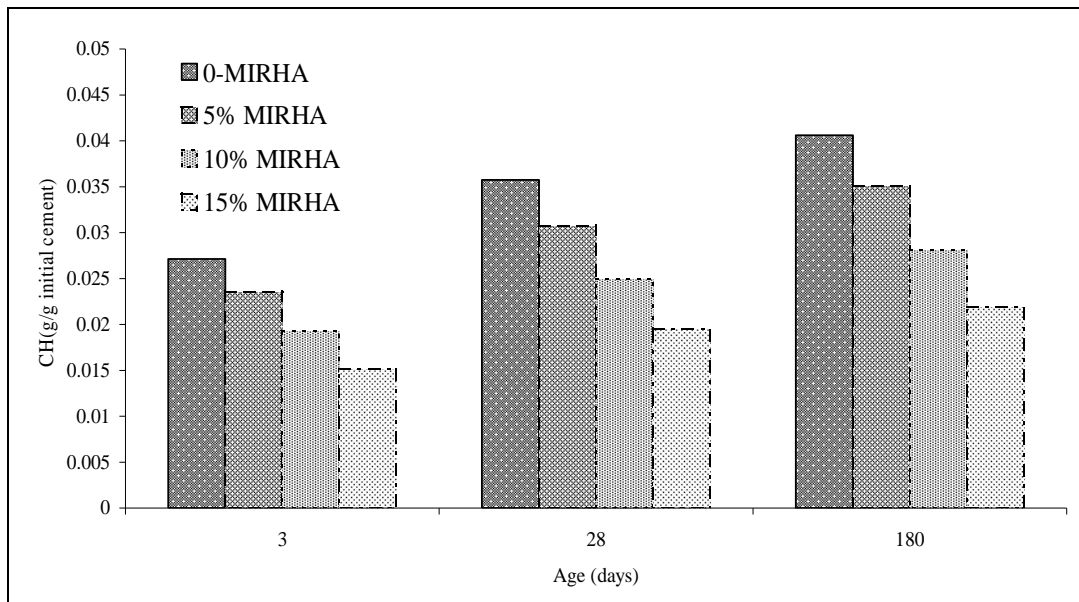


Figure 5.4 CH bound water over time

Since the amount of CH bound water is directly related to the quantity of CH, the most striking trend in these results is that for the MIRHA mixture CH bound water contents was lower than the control. MIRHA was consuming the CH to play bridging role in strength and durability by C-S-H product. As a reference [98, 99], addition of RHA possibly may be recognized to form C-S-H gel due to the reaction occurring between RHA and  $\text{Ca}^{2+}$ ,  $\text{OH}^-$  ion or  $\text{Ca}(\text{OH})_2$  in hydrating cement.

If the value of  $\text{CH}_{\text{normal}}$  is greater than 1.0, it indicates that the presence of the replacement material has resulted in more CH than normal mixes with the same amount of cement. In other words, this is a clear clue of enhancement in cement hydration especially when the CRM used is only pozzolanic as is the case with MIRHA. For cementitious material, a  $\text{CH}_{\text{normal}} > 1.0$  might indicate a combination of hydration enhancement as well as the hydration of the CRM. For  $\text{CH}_{\text{normal}}$  less than 1.0, the situation is less clear. The CH content of the modified paste can be lower than  $\text{CH}_{\text{pure (t).m}_c}$  because of one of the following reasons: (i) the pozzolanic material have a retarding effect. (ii) pozzolanic reaction of the CRM has depleted CH, or (iii) there is enrichment in cement hydration, but the secondary reaction is more dominant, resulting in reduced CH content.

Figure 5.5 show the  $CH_{normal}$  of MIRHA FC that has lower value than 1.0 at all ages because of the pozzolanic reaction of MIRHA consumes CH.  $CH_{normal}$  of MIRHA FC almost achieves 1.0 at 3 days, indicating the occurrence of pozzolanic reaction as early age,  $CH_{normal}$  can thus be used as in as an indicator of the onset of pozzolanic reaction.

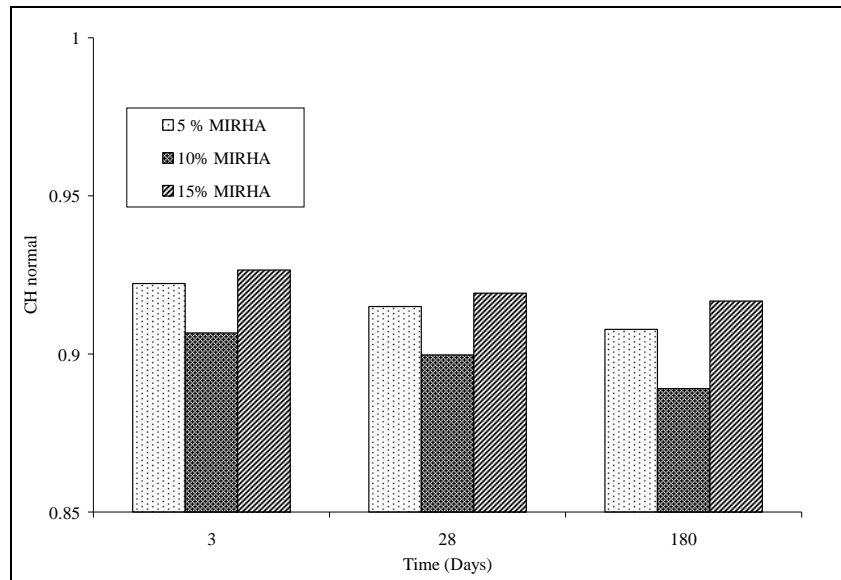


Figure 5.5  $CH_{normal}$  values of MIRHA

## 5.6 Comparing C-S-H/AFm and CH Bound Water Content

Another way to study the results presented in Figure 5.3 and Figure 5.4 is to compare directly CH and C-S-H/AFm bound water contents. This relationship is presented in Figure 5.6.

One clear result from this graph is the comparative difference between the quantities of bound water in CH and C-S-H/AFm. Indeed, the CH bound water contents range from 15-38% of the C-S-H/AFm bound water contents, with the higher ratios occurring at earlier ages. This finding reiterates the conclusion that C-S-H/AFm bound water is predominant quantity in bound water measurements at later ages.

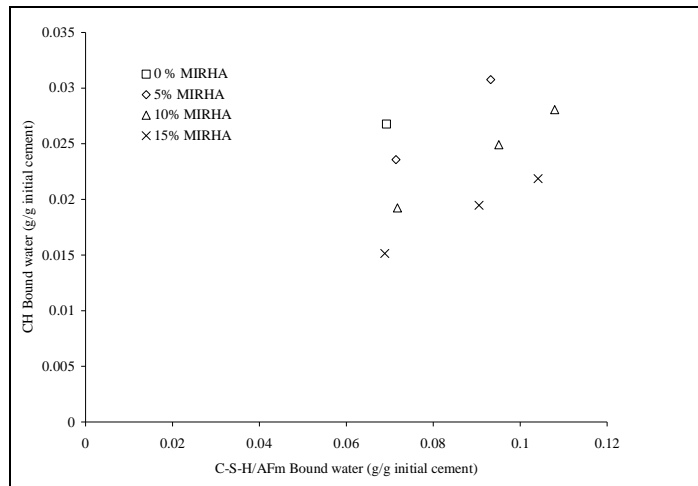


Figure 5.6 C-S-H/AFm versus CH bound water contents

Based on the chemical composition of the specific cement used, and the cement hydration equations (section 0, equation (2-13) through (2-16), the ratio of CH to C-S-H/AFm bound water can be calculated to be approximately 0.38. This value of 0.38 is somewhat various over time as the four hydration reactions are not simultaneous, but the ratio approaches this constant value with degree of hydration. The reference line shown is the same one (slope = 0.38, intercept = 0.00175) and shown in Figure 5.7. The normal FC and MIRHA FC seem to follow the same trends seen in Figure 5.7.

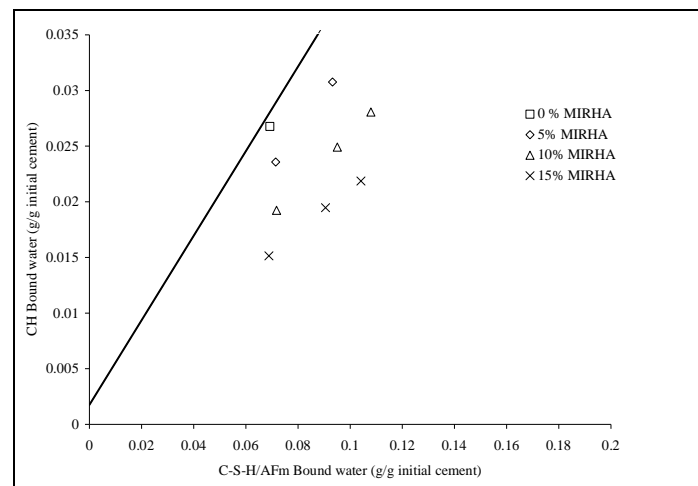


Figure 5.7 C-S-H/AFm versus CH bound water contents with reference line

This figure is of fundamental importance as the values obtained for water bound in CH have already been validated, and the slope of the line is a fundamental characteristic of the cement used in the experiment. This strongly suggests that the

data point falling to the right of the line indicate measured values of water bound in C-S-H/AFm that increasingly overestimate the true values. It is important to note that this theoretical line was derived for cement hydration only, and thus technically does not apply normal FC data. On the other hand, since there is reported evidence that pozzolanic reactions may not occur immediately, that fact that the other FC data follow the line at early age is not necessarily surprising.

### 5.7 Change in Non-Evaporable Water Content Due to the Presence of MIRHA

In this section, a procedure that developed by Nathan [106] to acquire the change in  $w_n$  content due to the incorporation of MIRHA or filler is detailed, and this information will be used to extract the total degrees of hydration of the FC incorporating MIRHA.

Table 5.3 shows the change in non-evaporable water contents due to the presence of MIRHA (as expressed  $\Delta w_n/c$ ) that is calculated by equations (2-32). A closer look at the data in Figure 5.1 it also shows that, for all the ages, the  $w_n$  of MIRHA FC are higher than the  $w_n$  of the normal FC multiplied the mass fraction of cement ( $m_c$ ) in the MIRHA FC. For instance the  $w_n$  10% MIRHA FC at 180 days is 0.145, which is greater than  $0.9 \cdot 0.153$ , where 0.153 is the  $w_n$  of normal FC. This shows that MIRHA contributes to  $w_n$  by facilitating an improvement in the hydration of available cement grains, and/or through its own pozzolanic reaction.

Table 5.3 Change in non-evaporable water contents due to the presence of MIRHA by OD/FI

MIRHA (%)	$\Delta(w_n/c)_r$ (g/g initial cement) at different ages (days)				
	3	7	28	90	180
5	0.0039	0.0046	0.0046	0.0054	0.0052
10	0.0048	0.0050	0.0058	0.0077	0.0078
15	0.0027	0.0030	0.0040	0.0035	0.0040

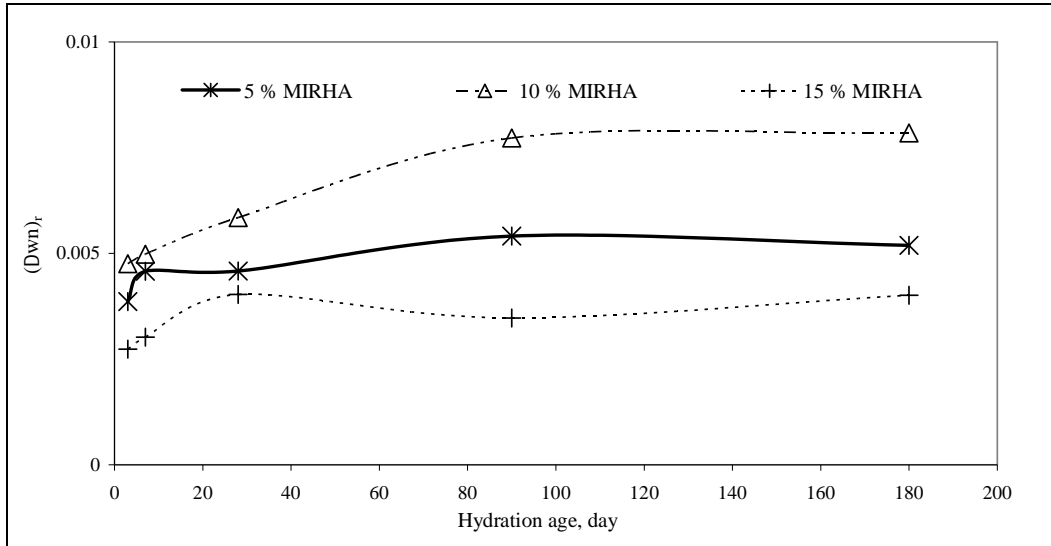


Figure 5.8 Change in  $w_n$  due to the presence of MIRHA using OD/FI technique

Table 5.4 Change in non-evaporable water contents due to the presence of MIRHA by TGA

MIRHA (%)	$\Delta(w_n/c)_r$ (g/g initial cement) at different ages (days)		
	3	28	180
5	0.0033	0.0042	0.0052
10	0.0042	0.0055	0.0079
15	0.0022	0.0037	0.0040

Figure 5.8 shows the values of  $\Delta(w_n/c)_r$  plotted against hydration age for the MIRHA FC by OD/FI. Until about 28 days, the  $\Delta(w_n/c)_r$  values of the FC with MIRHA powder increased, indicating increased hydration of the cement grains because of the higher effective w/c. Beyond 28 days, 15% MIRHA  $\Delta(w_n/c)_r$  is seen to decrease, showing that the secondary reaction of the replacement material is not compensating for the dilution effect. However, for the FC incorporating with 5% and 10% MIRHA powder,  $(\Delta w_n)_r$  increases consistently with time. This shows that a 5-10% replacement of cement with MIRHA powder has higher value for change non-evaporable water can be considered to be effective.

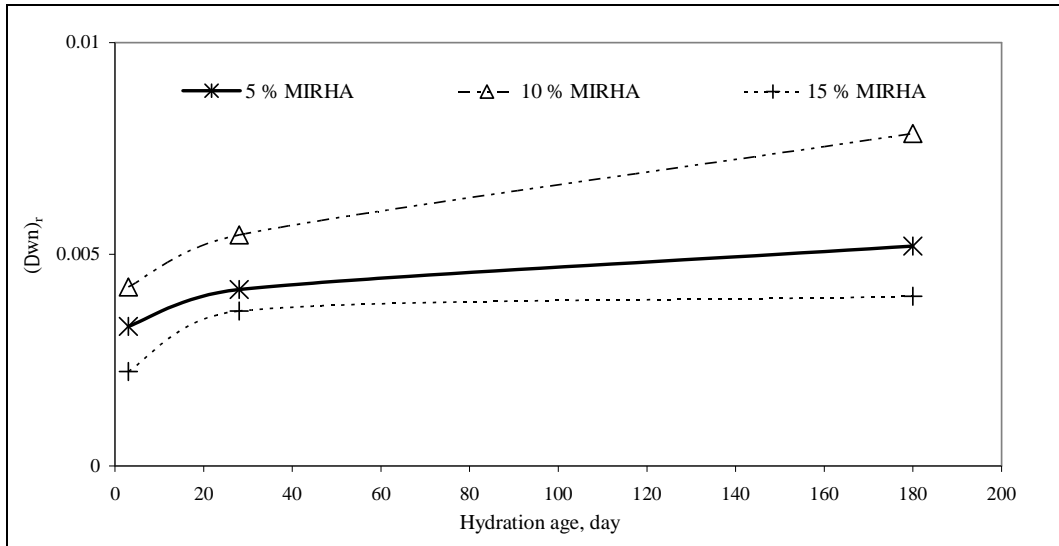


Figure 5.9 Change in Non-evaporable water contents results of replacement material hydration for FC by TGA

Figure 5.9 show the values of  $(\Delta w_n)_r$  by TGA is plotted against hydration age for the MIRHA FC. This result has similar phenomenon to indicate that MIRHA is effective to result calcium silicate hydrate.

## 5.8 Degree of Hydration of FC

Calculating degree of hydration (DoH) is one of the primary reasons for measuring non-evaporable water contents in cement-based mixtures. This section will consider degree of hydration based on the FC mixture data from all sixteen experiments from orthogonal array experiment, thus synthesizing the experimental work. Many researchers convert non-evaporable water measurements directly to degree of hydration values using the relationship:

$$\alpha = \frac{(w_n)_c}{(w_n)_{c-\infty}} \quad (5-1)$$

The Bogue composition of the cement calculated using the oxide contents, along with the reported chemically bound water contents of the compounds [30] were used to calculate the ultimate non-evaporable water content of cement  $(w_n)_{c-\infty}$ , which for the cement used in this study is 0.2386.

Figure 5.10 shows a plot of degree of hydration over time, where the degree of hydration values have been calculated with equation (5-1) for normal FC and equation (2-38) for MIRHA as cement replacement. Since the ultimate non-evaporable water contents  $(w_n)_{r-\infty}$  of MIRHA are much lower compared to that of the cement (In this work,  $(w_n)_{r-\infty} = 0.05$  [124]).

Further insight into this behavior can be obtained by using degree of hydration value to predict MIRHA FC properties, such as compressive strength and comparing these predicted values with measured ones. It can be observed from Figure 5.10 that the  $\alpha_T$  values of MIRHA-FC are higher than normal FC indicating the contribution from the pozzolanic reaction of MIRHA. Even though the results of non-evaporable water content by 15% MIRHA had the lowest value but did not give effect to the greatest degree of hydration. This may be due MIRHA particles also serve to adsorb water, thus making the water unavailable for cement hydration. This adsorption thus increases the amount of evaporable water. In addition, the pozzolanic C-S-H is not only a different type of C-SH than that from cement hydration, but one that also adsorbs more water, thus decreasing the available hydration water further.

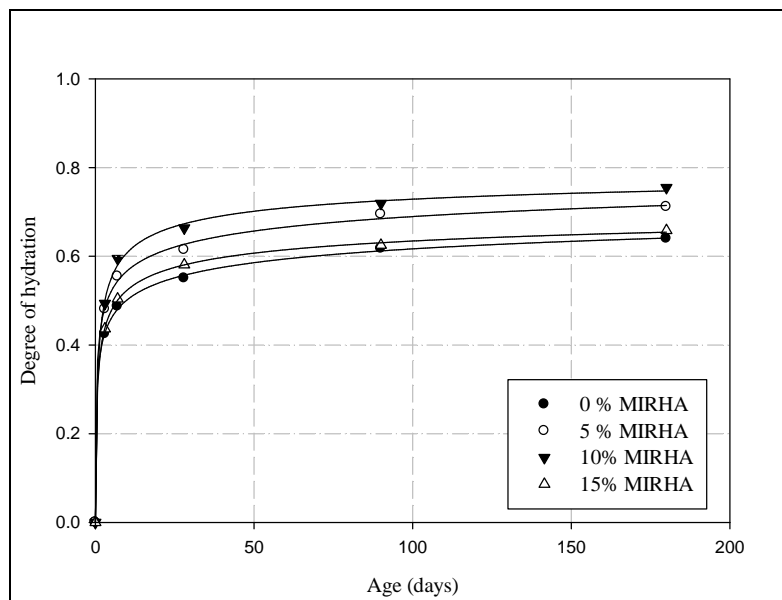


Figure 5.10 Degree of hydration of FC from  $w_n$  measured OD/FI



The correlation between total degree of hydration and time can be adequately expressed using a modified three-parameter hyperbolic expression of the form:

$$\alpha_T = a_1 \left[ 1 - \frac{1}{(1+a_2 t)^{\frac{1}{a_3}}} \right] \quad (5-2)$$

Where  $a_1$ ,  $a_2$  and  $a_3$  are fitting parameters (Table 5.5), the values of which are shown in respective figures. The continuous lines in Figure 5.10 represent the fits of equation (5-2) to the calculated total degrees of hydration. This equation is found to predict the total degrees of hydration of normal and MIRHA FC with an  $R^2$  value greater than 0.98 in all mixes. This model is compared with previous study [105] that investigating vitreous calcium aluminosilicate (VCAS) and silica fume (SF) as supplementary cement material in high-performance cementitious is listed in Table 5.6.

Table 5.5  $a_1$ ,  $a_2$  and  $a_3$  are fitting parameters for degree of hydration of FC

Mirha (%)	$a_1$	$a_2$	$a_3$
0	0.83	4.67	2.94
5	0.99	29.71	6.67
10	0.79	9.87	4.21
15	0.95	34.17	7.80

Table 5.6  $a_1$ ,  $a_2$  and  $a_3$  are fitting parameters for degree of hydration of VCAS and SF (Neithalath's study [105])

VCAS content (%)	$a_1$	$a_2$	$a_3$	SF content (%)	$a_1$	$a_2$	$a_3$
0	0.81	7.22	2.74	0	0.81	7.22	2.74
6	1.33	31.10	8.98	6	0.78	3.82	2.32
9	3.85	89.69	38.46	9	0.74	2.22	1.87
15	1.07	11.53	5.44				

## 5.9 Compressive Strength versus Non Evaporable Water Content Model

Even more interesting than individual trends of compressive strength and non-evaporable water contents over time is the relationship between two measured properties. This relationship (i.e. compressive strength versus non-evaporable water content) is shown graphically in Figure 5.11 and Figure 5.13 show the relationship between compressive strength and OD/FI non-evaporable water content (i.e. OD/FI  $w_{n/c}$ ) and the correlation for the compressive strength and TGA non-evaporable water content (i.e. TGA  $w_{n/c}$ ). The linear trends for the FC data points are depicted in Figure 5.12 and Figure 5.14. The increasing linear relationship between strength and the non-evaporable water content is clear. Moreover, there is no statistical difference between the trend lines for the FC by OD/FI and TGA procedure data in two figures. The  $R^2$  values for combined data are 0.796 and 0.801 for OD/FI and TGA procedure respectively. Hence the relationship between compressive strength and non-evaporable is consistent regardless of the method used to measure non-evaporable water content.

The effect of MIRHA on correlation of strength with non-evaporable add more evident that MIRHA as cement replacement material contribute C-S-H production that construct strength and durability. It can be seen in Figure 5.11 and Figure 5.13 that MIRHA  $w_n$  shown decreasing than normal FC due to the amount of cement to be replaced by MIRHA. Albeit the non-evaporable water was reduced, the strengths of MIRHA FC were presented higher result than normal mix.

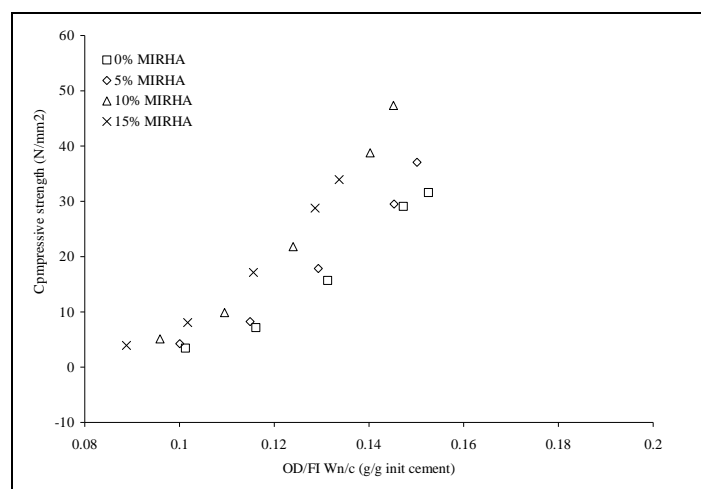


Figure 5.11 Compressive strength versus OD/FI Non-evaporable water content for FC

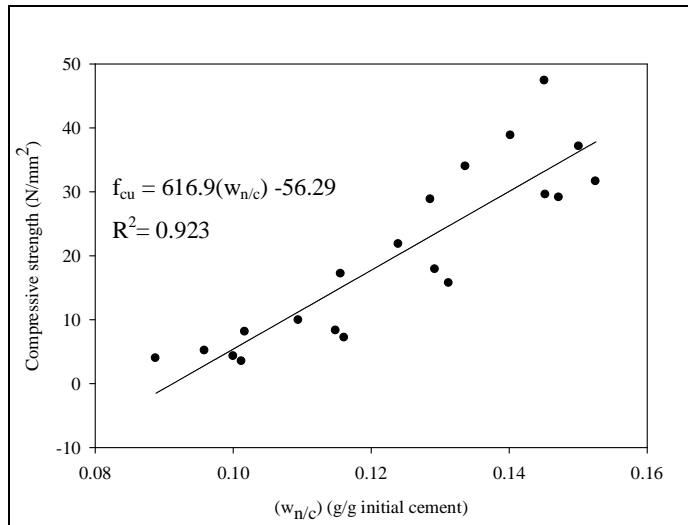


Figure 5.12 Compressive strength versus OD/FI Non-evaporable water content, with trend line for normal and MIRHA FC

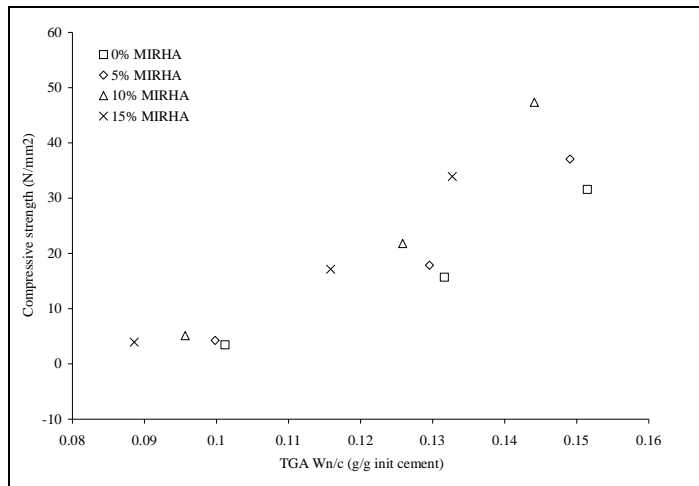


Figure 5.13 Compressive strength versus TGA Non-evaporable water content for FC

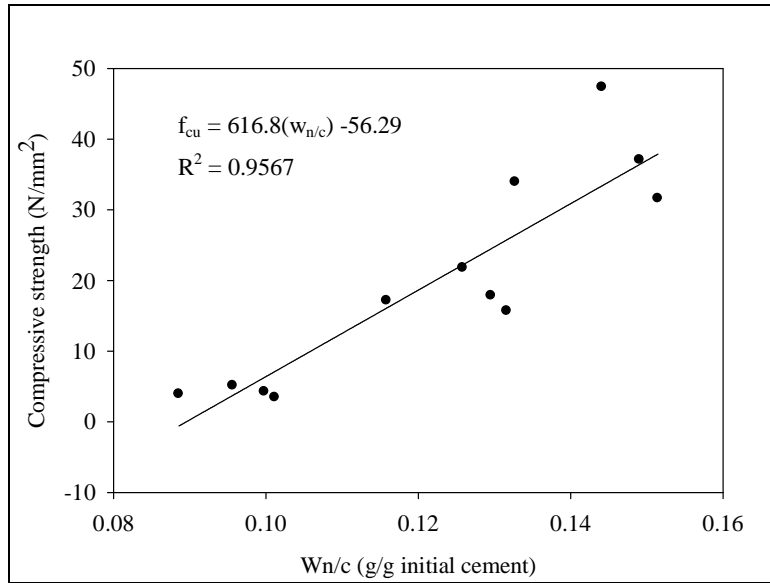


Figure 5.14 Compressive strength versus TGA Non-evaporable water content, with trend line for normal and MIRHA FC

This study has similar result with the previous study [102] that presented the correlation between compressive strength and non-evaporable water content for the silica fume mortar with equilibrium as following:

$$f_{cu} = 559 (w_{n/c}) - 14 \text{ N/mm}^2 \text{ per g/g initial cement} \quad (5-3)$$

Where:

$f_{cu}$  = compressive strength in  $\text{N/mm}^2$

$w_{n/c}$  = non evaporable water in  $\text{g/g}$  initial cement.

The relationship between compressive strength and non-evaporable water content for MIRHA was attained and form as  $f_{cu} = 616.8(w_{n/c}) - 56.29$  MPa per  $\text{g/g}$  initial cement. This correlation means that to gain high compressive strength, MIRHA FC uses less non-evaporable water content than normal FC. This suggests that MIRHA converts CH to C-S-H via pozzolanic reaction with little extra  $w_n$ .

## 5.10 Compressive Strength versus porosity model

Porosity is the major factor that is considered to have a major impact on compressive strength of FC. This section shows the correlation of strength versus porosity model for FC that is constructed by adopting the generalized by Balshin's model which can be expressed by formula (2-6). This correlation is drawn from Table 5.7 using the data of compressive strength and porosity collected in section 4.4.3 and 4.4.4. The same results are depicted in Figure 5.15 and Figure 5.16.

Table 5.7 The average data of 180 days Strength and porosity

Exp No	Strength (N/mm <sup>2</sup> )	Porosity	(1-Porosity)
FC-1	33.17	0.317	0.683
FC-2	50.40	0.243	0.757
FC-3	25.73	0.356	0.644
FC-4	10.26	0.577	0.423
FC-5	34.95	0.371	0.629
FC-6	40.63	0.340	0.66
FC-7	32.65	0.385	0.615
FC-8	32.99	0.378	0.622
FC-9	54.08	0.266	0.734
FC-10	56.13	0.257	0.743
FC-11	31.26	0.389	0.611
FC-12	40.89	0.326	0.674
FC-13	24.78	0.424	0.576
FC-14	30.17	0.387	0.613
FC-15	40.03	0.330	0.67
FC-16	33.69	0.366	0.634

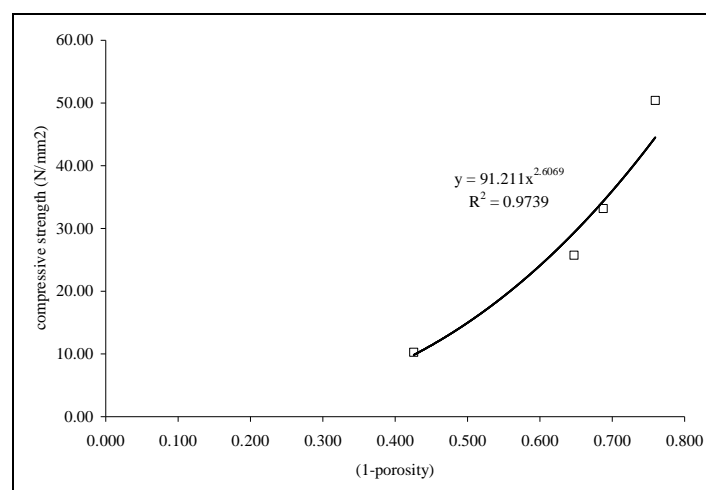


Figure 5.15 Strength versus porosity relation for normal FC (cement-sand)

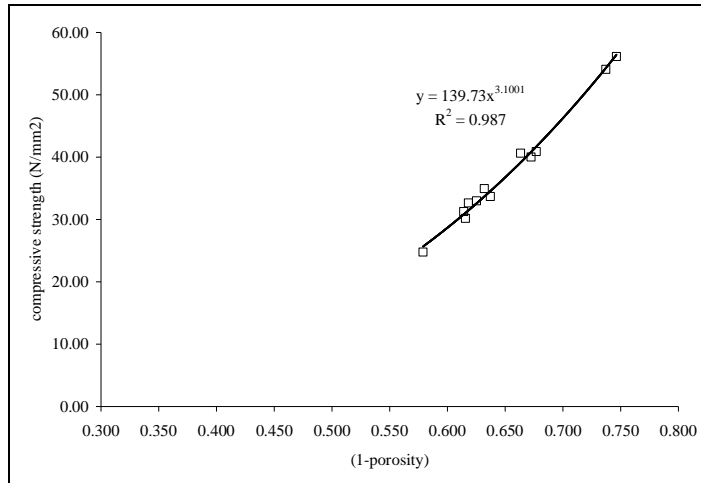


Figure 5.16 Strength versus porosity relation for FC with MIRHA

The porosity is computed theoretically by equation (2-5) by filling up the chemical bound water obtained in section 5.8 (in the previous study, the value of the non-evaporable water was always assumed in the range of 0.18 to 0.23). The main advantage of the proposed formula is that all the parameters in the equation are easily assessable. Furthermore, porosity is a property that is rarely to be measured outside the laboratory. The above formula helps to predict the required porosity of mix proportion. Subsequently, it can be correlated with strength. The correlation is beneficial to the user of FC. Figure 5.17 shows the comparison of theoretical porosity obtained and the measured porosity. The measured porosity is lower than theoretical one. The marginally lower values of measured porosity may be attributed to a few inaccessible pores as the vacuum saturation method can measure only accessible porosity (permeable porosity).

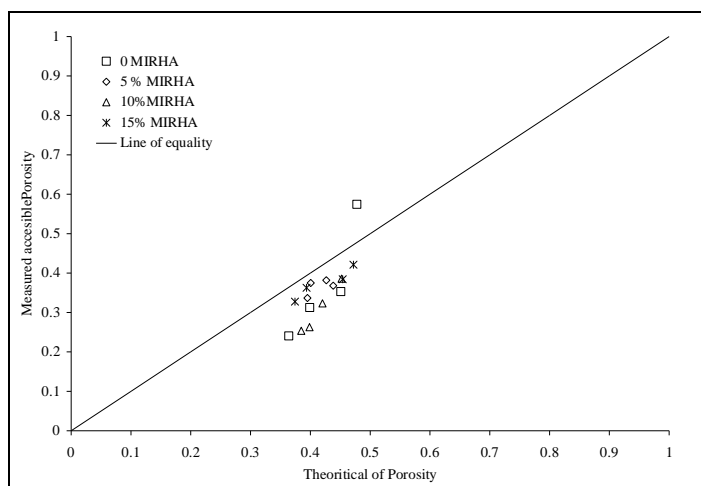


Figure 5.17 Measure accessible Porosity versus Theoretical of Porosity

From aforementioned discussion, it can be concluded that the correlation between compressive strength and porosity of normal FC and MIRHA FC was accomplished and form as follows:

$$f_{cu} = 91.211(1-p)^{2.6069} \quad (R^2 = 0.9739), \text{ for normal FC} \quad (5-4)$$

$$f_{cu} = 139.73(1-p)^{3.1001} \quad (R^2 = 0.987), \text{ for MIRHA FC} \quad (5-5)$$

Two model equations (5-4) and (5-5) show that the porosity of MIRHA FC has character which is lower than normal FC. Therefore, the compressive strength MIRHA FC will be greater than normal FC. This is because of pozolanic rection of MIRHA effectively the changing CH into CSH. It can affected diminishing the void space on FC.

### 5.11 Compressive Strength versus gel-space ratio model

The gel-space ratio is computed for control FC and MIRHA FC at different densities. Those are subsequently plotted against compressive strength obtained experimentally as shown in Figure 5.18 and Figure 5.19. As far as gel-space ratio is concerned, it correlates well with the compressive strength for normal FC as compared to MIRHA FC mixes. This may be attributed to the non-inclusion of the hydration products of MIRHA in the model. Comparing gel-space relationship shown in Figure 5.18 and Figure 5.19 , it is observed that the dependency of strength on gel-space ratio is relatively less for FC with MIRHA than control which can be observed from the reduction in power term from 2.801 for control to 2.76 for MIRHA. For comparison, the models proposed by Nambiar [72] are also listed in Table 5.8. For normal FC mix these models under estimate the strength and for MIRHA FC ash mix over estimate the strength. The deviation from author's model was found to be more at higher density range.

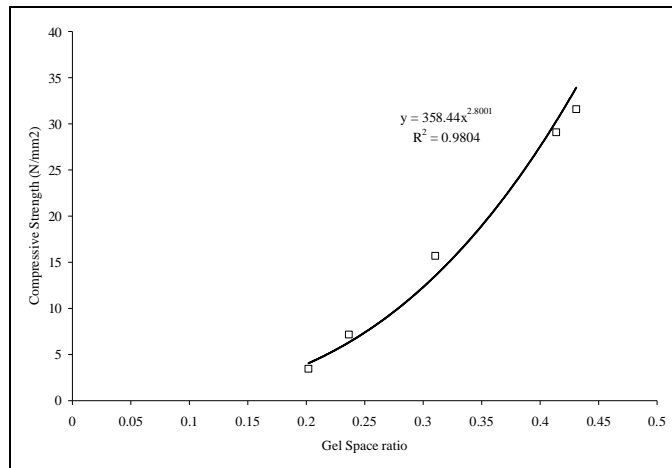


Figure 5.18 Relation between the strength of concrete and gel space ratio normal FC

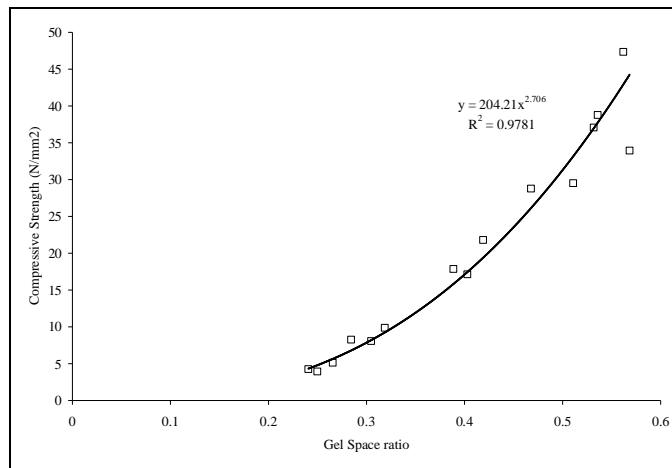


Figure 5.19 Relation between the strength of concrete and gel space ratio MIRHA FC

### 5.12 Comparison of Foamed Concrete Model of Porosity and Gel Space Ratio

A comparison of density and gel-space ranges in both studies are given in Table 5.8 and Table 5.9. Nambiar's study [72] considered a low density range and within this range the deviation is less, and this deviation can be attributed to the difference in material characteristics. The fact that the increase in strength by replacing sand with fly ash reported by Nambiar was lower than that observed in the present study points towards the effect of pozzolanicity that used in both the studies. Table 5.8 and Table 5.9 compares the above derived pore-specific and gel-specific models for strength of foam concrete made of cement-sand and cement-sand with different pozzolan mixes. From the  $R^2$  values, the model based on porosity correlates well with measured



strength and is considered as the best model. Also, the main advantage of this equation proposed is that all the parameters in the equation can easily be measured.

Table 5.8 Summarizing Nambiar's study for porosity and gel-space ratio to strength

Mix Type	Dry density range, kg/m <sup>3</sup>	Gel-ratio range	porosity (n)	R <sup>2</sup>	gel-space ratio (g)	R <sup>2</sup>
cement-sand	713-1460	0.15-0.48	strength = 155.66 (1-n) <sup>4.31</sup>	0.871	strength = 188.13 (g) <sup>2.73</sup>	0.864
cement-sand-fly ash	505-1306	0.12-0.42	strength = 105.14 (1-n) <sup>2.68</sup>	0.883	strength = 127.72 (1-n) <sup>1.74</sup>	0.798

Table 5.9 Summarizing this study for porosity and gel-space ratio to strength

Mix Type	Dry density range, kg/m <sup>3</sup>	Gel-ratio range	porosity (n)	R <sup>2</sup>	gel-space ratio (g)	R <sup>2</sup>
cement-sand	1295-1605	0.201-0.43	strength = 91.211 (1-n) <sup>2.6069</sup>	0.9739	strength = 358.44 (g) <sup>2.8001</sup>	0.9804
cement-sand-MIRHA	1239-1636	0.24-0.562	Strength = 139.73 (1-n) <sup>3.101</sup>	0.987	strength = 204.21 (1-n) <sup>2.706</sup>	0.9781

### 5.13 Summary

The following conclusions were drawn for effects of MIRHA on Hydration Characteristic.

1. At later ages, the non-evaporable water content in the MIRHA leveled off, achieving an ultimate value about 12% less than that of the normal FC. This concurs with the results reported Zhang et al [80] and the graph shown in Figure 2.17.
2. The CH bound water contents decreased slightly starting day 3 in all MIRHA FC as compared to the normal FC. This decreasing trend continued over time such that the ultimate CH bound water value for MIRHA was about 21% of

that in the normal FC. The behavior mark the consumption of CH by RHA pozzolanic reaction, and has also been reported by Qingge Feng, et al [100]; see Figure 2.18.

## CHAPTER 6

### CONCLUSIONS AND FUTURE WORK

#### 6.1 Conclusion

The following conclusions can be drawn from the experimental work effects of Microwave incinerated rice husk ash on hydration and mechanical properties of foamed concrete.

1. The optimum mix-design 28 days compressive strength were attained at the composition of FC having 10% MIRHA, 0.4 w/c, 0.5 s/c, 1% SP and 25% fc. The verification test for confirmation was performed and resulted at 26.3 MPa compressive strength with standard deviation and coefficient of variance of 1.18 and 4.5%, respectively. This clearly indicates that the strength is more than 17 MPa which is requirement (ASTM-C330, ACI 213R-87 and BS EN 206-1/BS 8500) for strength lightweight concrete. Confirmation on dry density was found to be  $1450 \text{ kg/m}^3$  with standard deviation and coefficient of variance of 40.59 and 2.8%, respectively. These finding fulfill the density requirement of lightweight concrete which is not more than  $1,680 \text{ kg/m}^3$ .
2. MIRHA-FC workability was strongly influenced by the w/c, because of the key factor to overcome the friction between solid particles and bubbles and to maintain the MIRHA had adsorptive characters. On dry density, it can be summarized that foam content was the significant parameter to attain a low dry density MIRHA-FC. It has a very apparent reason that by entering the amount of air through the foam in the mix is going to affect the density of concrete. The effects of constituent of MIRHA-FC on compressive strength was affected MIRHA, w/c and foam content which were classified low level in the classification of the effect constituent on compressive strength. MIRHA facilitate the progress of hydration process and assist in the dissemination stage

bubbles in fresh FC. Water cement ratio was a key parameter for the workability FC and hydration process of cement. Foam content determines the amount of voids in the concrete and the void space is a strong influence on the FC compressive strength. On porosity, it can be concluded that foam content was the considerable parameter to accomplish a low porosity MIRHA-FC. It has an obvious reason that giving an amount of air through the foam into the mix is going to affect the porosity.

3. The optimum FC properties were achieved at 10% MIRHA composition as proven from highest compressive strength and lowest porosity. This level corresponds to the highest values in change in non-evaporable water, calcium silicate hydrate and degree of hydration. Other attributes at the optimum level are :
  - a. partially-crystalline nature
  - b. high silica content
  - c. low LOI
  - d. high specific surface area
  - e. APSAI nearly equal to 1
  - f. High water demand
4. The correlation of compressive strength of FC has been established with respect to non-evaporable water is in the form as  $f_{cu} = 616.8(w_{n/c}) - 56.29$ .

## **6.2 Recommendation for Future Study**

Although a detailed research program was performed during this research study, however, there are many gaps identified for further research, some of them are described as below:

1. This study is a pilot project that the utilization of MIRHA in small percentage.. The challenge is to investigate the properties characteristic of FC with large MIRHA composition to replace cement content.

2. On the other hand, MIRHA has potential to reduce shrinkage in concrete that is a big problem in the FC; this is the opportunities to investigate more in order to use FC for structural application.
3. FC is a material which has significant flow ability. It is a practical to explore combining with MIRHA for the promotion of high performance concrete. That is self compacting FC in future.

## REFERENCE

1. R.C. Valore, "Cellular concrete Part 1 Composition and methods of production," *ACI Journal.*, vol. 50, pp. 773-96, 1954.
2. A. Kusbiantoro, "The Effect of Microwave Incinerated Rice Husk Ash (MIRHA) On Concrete Properties," M.Sc. thesis, Dept. Civil Eng., Univ. Tek. Petronas, Malaysia, 2007.
3. D.D. Bui, "Rice husk ash as a mineral admixture for high performance concrete," Ph.D. dissertation, Dept. Civil Eng., Delft University, Netherland, 2001.
4. P.K. Mehta, "Properties of blended cement made from rice husk ash," *ACI Journal.*, Vol.74, pp. 440-442, September 1977.
5. G.R. Sensale, A.B. Ribeiro and A. Gonçalves, "Effects of RHA on autogenous shrinkage of Portland cement pastes," *Cement & Concrete Composites*, vol. 30, pp. 892–897, 2008.
6. P.K. Mehta, "Rice Husk Ash-A Unique Supplementary Cement Material," in *Advances in Concrete Technology*, Malhotra, Ed. Ottawa, Canada: CANMET, 1992.
7. International Rice Research Institute. *Table 1. Paddy rice production (000 t), by country and geographical region, 1961-2007. (FAO)*. 2008, Available from: [http://beta.irri.org/solutions/index.php?option=com\\_content&task=view&id=250](http://beta.irri.org/solutions/index.php?option=com_content&task=view&id=250).
8. C.L. Hwang and S. Chandra, "The use of rice husk in concrete," in *Waste materials used in concrete manufacturing*, S. Chandra, Ed. William Andrew, 1997, pp. 184-234.
9. C.L. Hwang, C.L. and D.S. Wu, "Properties of Cement Paste Containing Rice Husk Ash," *ACZ SP-114*, V. M. Malhotra, Ed., pp. 733-765, 1989.
10. M.R. Jones and A. McCarthy, "Behaviour and assessment of foamed concrete for construction applications," in *Proceedings of the International Conference on the Use of Foamed Concrete in Construction*, London, 2005, pp. 61-88.

11. E.P. Kearsley and P.J. Wainwright, "The effect of high fly ash content on the compressive strength of foamed concrete," *Cement and Concrete Research*, vol. 31(1), pp. 105-112, 2001.
12. E.P. Kearsley and P.J. Wainwright, "Ash content for optimum strength of foamed concrete," *Cement and Concrete Research*, vol. 32(2), pp. 241-246, 2002.
13. T.H. Wee et al., "Air-Void System of Foamed Concrete and its Effect on Mechanical Properties," *ACI Materials Journal*, vol.103 (1), pp. 45-52, January-February 2006.
14. H.K.Lee, H.K. Kim and E.A. Hwang, "Utilization of power plant bottom ash as aggregates in fiber-reinforced cellular concrete," *Waste Management*, vol. 30(2),pp. 274-284, 2010.
15. K.S.Wang et al., "Lightweight properties and pore structure of foamed material made from sewage sludge ash," *Construction and Building Materials*, vol. 19(8), pp. 627-633, 2005.
16. Z.Pan, F. Hiromi and T. Wee, "Preparation of high performance foamed concrete from cement, sand and mineral admixtures," *Journal Wuhan Univ. of Tech. Materials Science*, vol 22(2), pp. 295-298, 2007.
17. *ASTM-Standard Test Method for Foaming Agents for use in producing cellular concrete using Preformed Foam*, ASTM-C796-97, 1997.
18. ACI committee 523, "Guide for cellular concretes above 50 pcf, and for aggregate concretes above 50 pcf with compressive strengths less than 2500 psi," *ACI Journal*, vol.72: p. 50-66, 1975.
19. Y.L.Lee and Y.T. Hung, "Exploitation of Solid wastes in Foamed Concrete Challenges A Head, in Use Foamed Concrete in Construction," in *Proceedings of the International Conference on the Use of Foamed Concrete in Construction*, London, 2005, pp. 15-27.
20. M. Nehdi, Y. Djebbar, and A. Khan, "Neural Network Model for preformed foam cellular concrete," *ACI Material Journal*, vol. 98, pp. 402-09, 2001.
21. D. Aldridge, "Introduction To Foamed Concrete: What, Why, How? in Use of Foamed Concrete in Construction," in *Proceedings of the International Conference on the Use of Foamed Concrete in Construction*, London, 2005, pp. 1-14.
22. M.R. Jones and A. McCarthy, "Preliminary views on the potential of foamed

- concrete as a structural material," *Magazine of Concrete Research*, vol. 57(1), pp. 21-31.
23. G. Augenbroe and A.R. Pearce, "Sustainable Construction in the United States of America, in A perspective to the year 2010", Georgia Institute of Technology, 2010.
  24. R.C.Valore, "Cellular concrete Part 2 Physical properties," *ACI Journal*, vol. 50, pp. 817-36, 1954.
  25. E.K.K. Nambiar and K. Ramamurthy, "Fresh State Characteristics of Foam Concrete," *Journal of Materials In Civil Engineering*, vol.20, pp. 111-17, February 2008.
  26. *ASTM-Specification for lightweight aggregates for structural concrete*, ASTM-C330-69, 2001.
  27. *ACI-Guide for Structural Lightweight Concrete*, ACI-213R-87, 1987.
  28. E.P. Kearsley, "Just foamed concrete – an overview," in *Specialist Techniques and Materials for Construction*, London, 1999, pp. 227-37.
  29. *ASTM-Standard specification for portland cement*”, in *Annual Book of ASTM Standards, Vol.04.01, American Society for Testing and Materials*, ASTM-C150, 2004.
  30. A.M.Neville, "Properties of Concrete," London, Longman, 2006.
  31. K. Ramamurthy, E.K.K. Nambiar and G.I.S. Ranjani, "A Classification of Studies on Properties of Foam Concrete," *Cement & Concrete Composites*, Vol. 31(6), pp. 388-396, 2009.
  32. D.P. Bentz, G. Sant and J. Weiss, "Early-Age Properties of Cement-Based Materials. I: Influence of Cement Fineness," *J. Mat. in Civ. Engrg*, vol. 20(7),pp. 502-308, 2008.
  33. *ASTM-Standard specification for coal fly ash and raw or calcined natural pozzolan for use as a mineral admixture in concrete*, ASTM-C618, 2004.
  34. *ASTM-Standard specification for ground granulated blast-furnace slag for use in concrete and mortars..* ASTM-C989, 2004.
  35. *ASTM-Standard specification for use of silica fume as mineral admixture in hydraulic cement concrete, mortar and grout*, ASTM-C1240, 2004:
  36. P. Aitcin, "Binders for durable and sustainable concrete," London, Taylor & Francis, 2008.



37. E.K.K. Nambiar and K. Ramamurthy, "Influence of filler type on the properties of foam concrete," *Cement & Concrete Composites*, vol. 28, pp. 475–480, 2006.
38. S. Karl and J.D. Worner, "Foamed concrete – mixing and workability., in Special Concrete – Workability and Mixing," In: Bartos PJM, Editor. 1993, E&FN Spon, : London, 1993, pp. 217-24.
39. E.P. Kearsley and H.F. Mostert, "Designing mix composition of foamed concrete with high fly ash contents," in *Proceedings of the International Conference on the Use of Foamed Concrete in Construction*, London, 2005, pp. 89-96.
40. A. Laukaitis, R. Zurauskas and J. Keriene, "The effect of foam polystyrene granules on cement composite properties," *Cement and Concrete Composites*, vol.27, pp. 41-47, 2005.
41. S.B. Park, E.S. Yoon and B.I. Lee, "Effects of processing and materials variations on mechanical properties of lightweight composites," *Cement Concrete Research*, vol. 29(2), pp. 193-200, 1998.
42. Y.M. Hunaiti, "Strength of Composite Sections with Foamed And Lightweight Aggregate Concrete," *Journal of materials In Civil Engineering*, vol. 17(1),pp. 111-13 May 1997.
43. Y.M. Hunaiti, "Composite action of foamed and lightweight aggregate concrete," *Journal of Materials in Civil Engineering*, vol.8(3),pp. 111-13, 1996.
44. F.C. McCormick, "Rational proportioning of preformed foam cellular concrete," *ACI Material Journal*, vol. 64, pp. 104-09, 1967.
45. T.G. Richard, "Low temperature behaviour of cellular concrete," *ACI Journal*, vol. 74, pp. 173-78, 1974.
46. T.G. Richard et al., "Cellular concrete- A potential loadbearing insulation for cryogenic applications," *IEEE Transactions on Magnetics*, vol. 11(2),pp. 500-03, 1975.
47. E.P. Kearsley and P.J. Wainwright, "Porosity and permeability of foamed concrete," *Cement and Concrete Research*, vol. 31(5),pp. 805-812, 2001.
48. E.P. Kearsley and P.J. Wainwright, "The effect of porosity on the strength of foamed concrete," *Cement and Concrete Research*, vol. 32(2), pp. 233-239, 2002.
49. K.J. Byun et al., "Development of structural lightweight foamed concrete using polymer foam agent," in *ICPIC-98*. 1998.

50. I.T. Koudriashoff, "Manufacture of reinforced foam concrete roof slabs," *Journal of the American Concrete Institute*, vol. 21(1),pp. 37-48, 1949.
51. R.J. Pugh, "Foaming, foam films, antifoaming and defoaming," *Advances in Colloid and Interface Science*, vol.64,pp. 67-72, 1996.
52. A.S. Jalmes et al., "Differences between protein and surfactant foams: Microscopic properties, stability and coarsening, " *Colloids and Surfaces: A Physico Chem.Eng.Aspects*, vol. 263, pp. 219-225, 2005.
53. D. Myers, "Surfactant Science and Technology," NewYork, VCH Publishers, 1998.
54. M.R. Jones and A. McCarthy, "Heat of hydration in foamed concrete: Effect of mix constituents and plastic density," *Cement and Concrete Research*, vol. 36(6),pp. 1032-1041, 2006.
55. R. Joana, S. Valls and R. Gettu, "Study of the influence of superplasticizers on the hydration of cement paste using nuclear magnetic resonance and X-ray diffraction techniques," *Cement and Concrete Research*, vol. 32, pp. 103–108, 2002.
56. S.A. Rizwan, "High Performance Mortars and Concretes Using Secondary Raw Material, in Maschinenbau," Ph.D. dissertation, Verfahrens-und Energietechnik, Technischen Universitat Bergakademic Freiberg, Freiberg, 2006.
57. F.C. McCormick, "Rational proportioning of preformed foam cellular concrete," *ACI Material Journal*, vol. 64, pp. 104-09, 1967.
58. E.K.K. Nambiar and K. Ramamurthy, "Models relating mixture composition to the density and strength of foam concrete using response surface methodology," *Cement and Concrete Composites*, vol. 28, pp. 752-60, 2006.
59. *ASTM-Standard Specification for Flow Table for Use in Tests of Hydraulic Cement*, ASTM-C230, 2003.
60. M.R. Jones, M.J. McCarthy and A. McCarthy, "Moving fly ash utilisation in concrete forward: a UK perspective". in *Proceedings of the 2003 International Ash Utilization Symposium*, University of Kentucky, paper #113, 2003.
61. C.T. Tam, T.Y. Lim, S.L. Lee, "Relationship between strength and volumetric composition of moist-cured cellular concrete," *Magazine of Concrete Research*, vol. 39,pp. 12-18, 1987.
62. *ACI-Guide for Cast-in-place low density concrete*, ACI5231R-1992, 1992.

63. E.P. Kearsley and P.J. Booyens, "Reinforced foamed concrete, can it be durable," *Concrete/Beton*, vol. 91, pp. 5-9, 1998.
64. M.Z.A.A. Rahman, A.M.A. Zaidi, and I.A. Rahman, "Physical Behaviour of Foamed Concrete under Uni-Axial Compressive Load: Confined Compressive Test," *Modern Applied Science*, Vol 4, No. 2, pp. 126-132, 2010.
65. P.J. Tikalsky, W. MacDonald, "A method for assessment of the freeze-thaw resistance of preformed foam cellular concrete," *Cement and Concrete Research*, vol. 34(5), pp. 889-9, 2004.
66. M.R. Jones and A. McCarthy, "Utilising unprocessed low-lime coal fly ash in foamed concrete, " *Fuel*, vol. 84(11), pp. 1398-1409, 2005.
67. E.P. Kearsley, "The use of foamed concrete for affordable development in third world countries," in *Appropriate Concrete Technology*, London, 1996, pp. 233-43.
68. M.S. Hamidah et al., "Optimisation of Foamed Concrete Mix of Different Sand-Cement ratio and Curing Conditions," in *Proceedings of the International Conference on the Use of Foamed Concrete in Construction*, London, 2005, pp. 61-88.
69. M. Visagie and E.P. Kearsely, "Properties of foamed concrete as influenced by air-void parameters," *Concrete/Beton*, vol. 101, pp. 8-14, 2002.
70. G.C. Hoff , "Porosity-strength considerations for cellular concrete," *Cement and Concrete Research*, vol. 2, pp. 91-100, 1972.
71. N. Shafiq, "Transport characteristics of fluids and ions in concrete performance criteria for concrete durability," Ph.D. dissertation, in *School of Civil Engineering*, The University of Leeds, 1999.
72. E.K.K. Nambiar and K. Ramamurthy, "Models for strength prediction of foam concrete," *Materials and Structures*, vol. 41, pp. 247-54, 2008.
73. V.S. Ramachandran (ed), "Concrete Admixtures," Handbook 2nd ed, USA, Noyes, 1995.
74. P. K. Mehta, P.J.M. Monteiro, "Concrete: microstructure, properties and materials," USA, McGraw-Hill, 2006.
75. V.M. Malhotra, "Fly Ash, Slag, Silica Fume, and Rice Husk Ash in Concrete: A Review," *Concrete International*, vol. 15(4), pp. 23-28, 1993.
76. K. Ankra, "Studies of Black Silica Produced Under Varying Conditions," Ph.D.

- dissertation, University of California, Berkeley, 1975.
77. M.S. Ismail and A.M. Waliuddin, "Effect of rice husk ash on high strength concrete," *Construction and Building Materials*, Vol.10, No.7, pp.521-526, 1996.
  78. M. Nehdi, J. Duquette and A. El-Damatty, "Performance of rice husk ash produced using a new technology as a mineral admixture in concrete," *Cement and Concrete Research*, Vol.33, No.8, pp. 1203-1210, 2003.
  79. P.K. Mehta, "Method for Producing a Blended Cementitious Composition," U.S. Patent 6 451 104 B2, September 17<sup>th</sup> 2002.
  80. Zhang, R. Lastra, and V.M. Malhotra, "Rice husk ash paste and concrete: Some aspect of hydration and the microstructure of the interfacial one between the aggregate and paste," *Cem Concr Res*, vol. 26 No. 6, pp. 963-977, 1996.
  81. R. Siddique, "Waste Materials and By-Products in Concrete," Verlag Berlin Heidelberg, Springer, 2008,
  82. D.D. Bui, J. Hu, and P. Stroeven, "Particle Size Effect on the Strength of Rice Husk Ash Blended Gap-Graded Portland Cement Concrete," *Cem Concr Res*, vol. 27, pp. 357-366, 2005.
  83. R. Jauberthiea, et al., "Origin of the Pozzolanic Effect of Rice Husks," *Construction and Building Materials*, vol. 14, pp. 419-423, 2000.
  84. *ASTM-Standard Specification for Coal Fly Ash and Raw or Calcined Natural Pozzolan for Use in Concrete*, ASTM-C618-03, 2003.
  85. P.K. Mehta, "Mineral Admixture for Concrete – An Overview of Recent Developments," in *Advance in Cement and Concrete. In : Proceedings of an Engineering Foundation Conference*, University of Newhampshire, Durham, 1994, pp. 243–256.
  86. M.H. Zhang and V.M. Malhotra, "High-performance concrete incorporating rice husk ash as a supplementary cementing material," *ACI Materials Journal*, Vol.93 No.6, pp.629-636, 1996.
  87. M. Safiuddin, "Development of Self-consolidating High Performance Concrete Incorporating Rice Husk Ash, " Ph.D dissertation, in *Civil Engineering*, University of Waterloo, Ontario, Canada, 2008.
  88. Hwang, C.L., T.F. Peng and L.G. Lin, " Effect of Burning Temperature on the Pozzolanic Reactivity of Rice Husk Ash," *Journal of the Chinese Institute of*

- Civil and Hydraulic Engineering*, Vol. 2, No. 3, pp. 263-272, 1990.
89. D.D. Bui, "Rice husk ash as a mineral admixture for high performance concrete," Ph.D dissertation, Delft University, 2001.
  90. P. Chindaprasirt , C. Jaturapitakkul , and U. Rattanasak, "Influence of fineness of rice husk ash and additives on the properties of lightweight aggregate," *Fuel*, vol. 88, pp. 158-162, 2009.
  91. Limnological R.C.C.F., *X-Ray Diffraction*. 2004.
  92. G. Arehart, G., "Introduction to X-Ray Diffraction," *Department of Geological Sciences MS 172*, ed. U.o. Nevada-Reno.
  93. P.K. Mehta, "Siliceous ashes and hydraulic cements prepared there from," U.S. Patent 4 105 459, August 8<sup>th</sup> 1978.
  94. D.G. Nair, K.S. Jagadish, and A. Fraaij, "Reactive pozzolanas from rice husk ash: An alternative to cement for rural housing," *Cement and Concrete Research*, vol. 36(6), pp.1062-1071, 2006.
  95. AmpTek. (2002). "X-Ray Fluorescence Spectroscopy," Bedford, MA., U.S.A. Available: <http://www.amptek.com/xrf.html>.
  96. A.E. Dakroury and M.S. Gasser, "Rice husk ash (RHA) as cement admixture for immobilization of liquid radioactive waste at different temperatures," *Journal of Nuclear Materials*, vol. 381(3), pp. 271–277, 2008.
  97. G.R.de Sensale, A.B. Ribeiro, and A. Gonçalves, "Effects of RHA on autogenous shrinkage of Portland cement pastes," *Cement and Concrete Composites*, vol. 30(10), pp. 892-897, 2008.
  98. V.S. Ramachandran, "Handbook of Thermal Analysis of Construction," Norwich, NY: William Andrew, 2002.
  99. K.S. Qijun Yu, S. Sugita, M. Shoya, Y. Isojima, "The reaction between rice husk ash and Ca(OH)<sub>2</sub> solution and the nature of its product," *Cement and Concrete Research*, vol. 29, pp. 37–43, 1999.
  100. Qingge Feng, et al., "Study on the pozzolanic properties of rice husk ash by hydrochloric acid pretreatment," *Cem Concr Res*, vol. 34, pp. 521-526, 2004.
  101. T.C. Powers and T.L. Brownyard, "Studies of the physical properties of hardened Portland cement paste," *J. Am. Concr. Inst. (Proc.)*, vol. 43, pp. 101–132, 249–336, 469–505, 549–602, 669–712, 845–880, 933–992, 1947.
  102. S.V. Hobbs, "A Study of Non-Evaporable Water Content in Cement-Based

- Mixtures With and Without Pozzalanic Materials," Ph.D. dissertation, Cornell University, 2000.
103. L.E. Copeland and J.C. Hayes, "Determination of Non-evaporable Water in Hardened Portland Cement Paste," in *A.S.T.M. Bulletin*, pp. 70-74, 1953.
  104. T.C. Powers, "Structure and Physical Properties of Hardened Portland Cement Paste," *J. Amer. Ceramic Soc.*, vol. 41, pp. 1-6, 1958.
  105. N. Neithalath, J. Persun, A. Hossain, "Hydration in high-performance cementitious systems containing vitreous calcium aluminosilicate or silica fume," *Cement and Concrete Research*, vol. 39(6), pp. 473-481, 2009.
  106. S. Nathan and N. Neithalath, "Influence of a fine glass powder on cement hydration: Comparison to fly ash and modeling the degree of hydration," *Cement and Concrete Research*, vol. 38, pp. 429-436, 2008.
  107. R. Roy, "A primer on the Taguchi method," New York, Van Nostrand Reinhold Company, 1990.
  108. Erdog˘an Ozbay, et al., "Investigating mix proportions of high strength self compacting concrete by using Taguchi method," *Construction and Building Materials*, vol. 23, pp. 694-702, 2009.
  109. Ibrahim Tu˘rkmen, Ru˘stem Gu˘llal, and C.C. elik, "A Taguchi approach for investigation of some physical properties of concrete produced from mineral admixtures," *Building and Environment*, vol. 43, pp. 1127-1137, 2008.
  110. Harun Tanyildizi and A. Coskun, "Performance of lightweight concrete with silica fume after high temperature," *Construction and Building Materials*, vol. 22, pp. 2124-2129, 2008.
  111. Jiju Antony, et al., "An application of Taguchi method of experimental design for new product design and development process," *Assembly Automation*, pp. 18-24, 2006.
  112. Genichi Taguchi, S. Chowdury, S. Taguchi, "Robust Engineering," USA, McGraw-Hill Professional, 2000.
  113. P. Chindaprasirt, S. Rukzon., "Strength, porosity and corrosion resistance of ternary blend Portland cement, rice husk ash and fly ash mortar," *Construction and Building Materials*, vol. 22, pp. 1601-1606, 2008.
  114. Bentech, "Operation & Maintenance manual for Microwave Incinerator," 2006.
  115. *ASTM- Standard Specification for Concrete Aggregates*, ASTM-C33, 2003.

116. *BS-Methods of test for water for making concrete*, BS3148, 1980
117. ASTM-C869-2006, *Standard Test Method for Foaming Agents for used in Making Preformed Foam for cellular concrete*. 2006.
118. L. D'Aloia Schwartzentruher, R. Le Roy , and J. Cordin, "Rheological behaviour of fresh cement pastes formulated from a Self Compacting Concrete (SCC)," *Cement and Concrete Research*, vol. 36, pp. 1203–1213, 2006.
119. BS1881–116, *Method for determination of compressive strength of concrete cubes*. 2000.
120. *ASTM-Determining Density of Structural Lightweight Concrete*, ASTM-C567-00, 2000.
121. *ASTM-Standard recommended practice for choice of sample size to estimate the average quality of a lot or process*, ASTM-E122, 1972.
122. H.N. Atahan, O.N. Oktar, and M.A.Tesdemir, "Effects of water–cement ratio and curing time on the critical pore width of hardened cement paste," *Construction and Building Materials*, vol. 23, pp. 1196–1200, 2009.
123. P.H. Nicole, J.M.M. Paolo. and C. Helena, "Effect of Silica Fume and Rice Husk Ash on Alkali-Silica Reaction," *ACI Materials Journal*, Vol. 97, No. 4, pp. 486-492, July-August 2000.
124. E. Garcia, "Non-evaporable water from neat OPC and replacement materials in composite cements hydrated at different temperatures," *Cem. Concr. Res*, Vol.33, page 1883–1888, 2003.
125. S.Yasushi and K.Norihiko, "Quantitative Analysis of Tridymite and Cristobalite Crystallized in Rice Husk Ash by Heating," *Industrial Health*, Vol.42, pp.277-28, 2004.

## APPENDICES

### APPENDIX A: RAW DATA OF THIS STUDY



## APPENDIX B: MICROWAVE INCINERATOR

## APPENDIX C: TGA DATA PROCESSING



## APPENDIX D: PUBLICATION

